

ABSTRACT

ROBINSON, WILLIAM RICHARD. Spherical Microwave Confinement and Ball Lightning.
(Under the direction of Dr. David Aspnes.)

This dissertation presents the results of research done on unconventional energy technologies from 1995 to 2009. The present civilization depends on an infrastructure that was constructed and is maintained almost entirely using concentrated fuels and ores, both of which will run out. Diffuse renewable energy sources rely on this same infrastructure, and hence face the same limitations. I first examined sonoluminescence directed toward fusion, but demonstrated theoretically that this is impossible. I next studied Low Energy Nuclear Reactions and developed methods for improving results, although these have not been implemented. In 2000 I began Spherical Microwave Confinement (SMC), which confines and heats plasma with microwaves in a spherical chamber. The reactor was designed and built to provide the data needed to investigate the possibility of achieving fusion conditions with microwave confinement. A second objective was to attempt to create ball lightning (BL). The reactor featured 20 magnetrons, which were driven by a capacitor bank and operated in a 0.2 s pulse mode at 2.45 GHz. These provided 20 kW to an icosahedral array of 20 antennas. Video of plasmas led to a redesign of the antennas to provide better coupling of the microwaves to the plasma. A second improvement was a grid at the base of the antennas, which provided corona electrons and an electric field to aid quick formation of plasmas. Although fusion conditions were never achieved and ball lightning not observed, experience gained from operating this basic, affordable system has been incorporated in a more sophisticated reactor design intended for future research. This would use magnets that were originally planned. The cusp geometry of the magnetic fields is suitable for electron cyclotron resonance in the same type of closed surface that in existing reactors has generated high-temperature plasmas. Should ball lightning be created, it could be a practical power source with nearly ideal characteristics that could solve many of our current energy-production problems.

Spherical Microwave Confinement and Ball Lightning

by
William Richard Robinson

A dissertation submitted to the Graduate Faculty of
North Carolina State University
in partial fulfillment of the
requirements for the degree of
Doctor of Philosophy

Physics

Raleigh, North Carolina

2010

APPROVED BY:

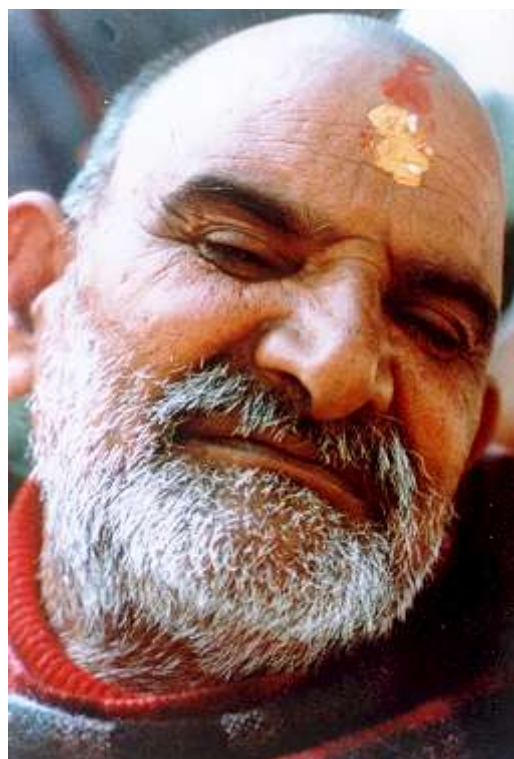
Dr. David Aspnes
Committee Chair

Dr. Stephen Reynolds

Dr. Dean Lee

Dr. Mohamed Bourham

DEDICATION



Neem Karoli Baba

BIOGRAPHY

Bill Robinson was born to a musical family in Denton, Texas in 1955. He started piano lessons at age three and violin at ten, and moved to Massachusetts in 1961. Composition started in 1972 while a student at Phillips Academy Andover. After that came a year at Eastman School of Music, then many years at NTSU in Denton (now UNT). Including a year as a physics major, he earned a BM in music composition there in 1984. After the Rainbow Gathering in the North Carolina mountains in 1987, Bill moved to the Charlotte area and has been in North Carolina ever since, except for two years on the road in the Southwest.

Bill came to Raleigh in 2001 to study physics at NCSU, and earned a BS in 2004. After that he continued on with graduate studies at NCSU. He is active in the study and practice of yoga, Hinduism, Dances of Universal Peace, and mystical practices of many kinds, and is a devotee of Neem Karoli Baba. This strongly influences his music, most of which is devotional in nature even if not explicitly indicated.

His compositions include woodwind, brass, string, piano, and synthesizer quintets; a recorder and a string quartet; songs, sacred and satirical; eleven sonatas for solo violin or viola; two pieces for jazz band; a piano sonata; sonatas for cello, flute, and violin with piano accompaniment; a duet for violin and cello; a trio for violin, oboe and piano, another for clarinet, cello and piano, and another for soprano, violin and piano; a quartet for violin, clarinet, cello and piano; concertos for violin, piano, and string quartet with orchestra; and a song for nonet or chamber orchestra and baritone. Recently completed are a *Mantra Cantata* for chorus and orchestra in Sanskrit and Hindi, and *Clarinet Sextet* for clarinet and strings.

Bill has a website at **billrobinsonmusic.com** that has all his work in physics and music, including extensive photo galleries of the research project from its early construction in 2006 to the present.

ACKNOWLEDGMENTS

I would like to thank Vocational Rehabilitation for their generous assistance during my undergraduate years, beginning in Texas at UNT in 1981, 1982, and 1984, and also at NCSU from 2001 through 2004. They not only helped pay tuition, but also bought expensive hearing aids and helped me purchase a minivan.

This research would not have been possible without the involvement of Dr. David Aspnes, who served as my remarkably patient faculty advisor after four semesters of teaching this old dog the new tricks of electromagnetism. Even as all my teachers from kindergarten through fifth grade retired after a year with me, so it appears I am likely Dr. Aspnes' final graduate student. (My sixth grade teacher fell and broke her neck, but was tough enough to stay on the following year...)

My first contact with a faculty member at NCSU was with Dr. Stephen Reynolds before I came here in 2001. I was much impressed by how flexible the department could be and saw that I could have a productive role to play here. Dr. Reynolds has since been a person I can talk to about matters physical and musical and is a person whose judgment I can trust.

Plasmas are not a focus of the physics department here; I am indebted to Dr. Mohamed Bourham for the two courses in plasmas I took from him in the Nuclear Engineering department.

I would also like to thank Dr. Michael Paesler, head of the Physics department, for appreciating eccentric research—not to mention eccentric researchers—and for helping to make this environment a friendly and accommodating one that is enjoyable to be part of.

TABLE OF CONTENTS

LIST OF TABLES.....	ix
LIST OF FIGURES.....	x
1.1 Chapter 1.....	1
1.1 Introduction.....	1
1.1.1 What was the research?.....	1
1.1.2 What was accomplished?.....	1
1.1.3 Why is this important?	1
1.1.4 Overview of the thesis	2
1.2 Requirement for a Concentrated Energy Source	3
2 Chapter 2: Early Research (1995 to 2004).....	6
2.1 Sonoluminescence.....	6
2.2 Fusion; Hot, Cold, and Warm	14
2.3 Ball Lightning	16
2.3.1 Back to school at NCSU	16
2.3.2 Existing Art of Ball Lightning	16
2.3.3 Example of a Bad but Well-Known BL Theory	19
2.3.4 Observations of Natural BL	21
3 Chapter 3.....	25
3.1 Middle History of the Research	25
3.2 Magnetic Spherical Microwave Confinement (2006).....	26
3.2.1 Introduction.....	26
3.2.2 Confinement Mechanisms	31
3.2.3 Existing Experimental Evidence.....	42
3.2.4 Test Reactor Design	44
3.3 Construction starts, August 2006.....	48
3.3.1 The history of the research continues	48
3.3.2 Pressure Chamber, Early Version	49
3.3.3 Magnetrons	50
3.3.4 Baffles	52
3.3.5 Coax Cable and Connecting Antennas to the Magnetrons	53
3.3.6 Video.....	55
3.4 Early Plasmas (2007 through summer 2008).....	57
3.4.1 Improvements to the Pressure Chamber	57
3.4.2 Sparker	59
3.4.3 Thoughts about BL Fuel	61
3.4.4 Glass globe and carbon veil (December 2007)	63
3.4.5 Grids and ceramic coatings.....	64
3.4.6 Solid Antennas; Mark I up to early Mark II	68
4 Chapter 4.....	70

4.1	Later History of the Research (fall 2008 to Summer 2009).....	70
4.2	Non-magnetic SMC as a kind of IEC	71
4.2.1	Confinement Mechanism.....	71
4.2.2	SMC Reactor Design	77
4.2.3	What this reactor can and cannot do	83
4.3	Trials at Duke (TUNL), first half of 2009	85
5	Chapter 5.....	90
5.1	Recent History of the Research (from Fall 2009).....	90
5.1.1	Return to NCSU.....	90
5.2	Reorientation to BL.....	93
5.2.1	Why a gridless IEC device can never be a fusion power reactor.....	93
5.2.2	Changing the reactor to BL for one last shot	95
6	Chapter 6: Results and Conclusions	97
6.1	Summary	97
6.2	What was accomplished.....	98
6.3	What is left to be done; Magnetic SMC.....	101
6.3.1	Generalities	101
6.3.2	Technical details	101
6.3.3	Next generation details	106
6.4	Reactor design should BL reaction occur	107
6.4.1	Design for BL	107
6.5	The need for Transcendental Physics	109
6.5.1	Historical overview	109
6.5.2	Characteristics of a general theory.....	110
6.5.3	Physical applications and experiments	113
6.5.4	Why BL needs Transcendental Physics	114
6.5.5	Problems in Transcendental Physics.....	117
6.5.6	The Oracle experiment and ITC	120
Appendices.....		128
7	Appendix A: Warm Fusion I (1998).....	129
7.1	Warm Fusion I: TiD ₂ and D ₂ Gas	129
7.2	Cold Fusion.....	130
7.2.1	Show me.....	130
7.2.2	Work to date.....	130
7.2.3	Why they wimp out.....	131
7.3	History of this Research.....	132
7.3.1	Beginnings	132
7.3.2	Turning point	133
7.3.3	D ₂ and Aerosol Catalyst; Warm Fusion	134
7.3.4	Reactor types.....	135
7.4	Overview of the Warm Fusion Reaction	136
7.4.1	Terminology.....	136

7.4.2	Chapman-Jouguet Detonation Shocks	138
7.4.3	Conditions required.....	139
7.4.4	WF Shock from Ambient to Final Equilibrium	140
7.4.5	Reaction products.....	143
7.5	Metal Hydride Powder.....	145
7.5.1	Powder type	145
7.5.2	Powder size	147
7.5.3	Powder density.....	147
7.6	Spark Plasma WF Initiation	149
7.6.1	Basic spark physics	149
7.6.2	Desired traits	150
7.6.3	Spark gaps.....	151
7.6.4	Plasma jet.....	151
7.6.5	Wire explosion	153
7.7	C-J Shock Analysis	153
7.7.1	Equations.....	153
7.7.2	Sequence of Calculations.....	163
7.7.3	Interpretation of Table of Shock Characteristics	165
	Table of Shock Characteristics (Columns 1-15)	168
7.8	Fusion Engine	169
7.8.1	Cycle	169
7.8.2	Cylinder Design	170
7.8.3	Advantages and Difficulties.....	170
7.9	Fusion Turbine	171
7.9.1	General Idea.....	171
7.9.2	Cycle	172
7.9.3	Advantages and Difficulties.....	173
7.9.4	Reaction Chamber Design	174
7.10	Figures.....	176
8	Appendix B: Warm Fusion II, Lithium Warm Fusion.....	180
8.1	Existing Evidence	180
8.1.1	Differences from Warm Fusion	181
8.2	Lithium Warm Fusion.....	183
8.2.1	Conditions Required	183
8.2.2	Reaction and Products.....	183
8.2.3	Application Differences from PRWF I	184
8.3	C-J Detonation Shock Equations	186
8.3.1	Equations Unchanged from PRWF I	186
8.3.2	Equations Changed from PRWF I	186
8.4	Interpretation of Table of Shock Characteristics	191
8.4.1	LHWF	191
8.4.2	LNWF	192

8.4.3	LTFW.....	193
Table 8.4	Shock Characteristics (columns 16-31)	194
9	Appendix C: Magnet Calculations.....	195

LIST OF TABLES

Table 7.7 Shock Characteristics (columns 1-15)..... 157

Table 8.4 Shock Characteristics (columns 16-31)..... 183

LIST OF FIGURES

Figure 2.1	Reaction Chamber.....	9
Figure 2.2	Pool Reactor.....	10
Figure 2.3	General Schematic Pool Reactor.....	11
Figure 2.4	Reactor Vessel.....	12
Figure 2.5	General Schematic Power Reactor.....	13
Figure 2.6	A welding spark as a lame but prominent BL candidate.....	21
Figure 2.7	Melbourne BL.....	24
Figure 3.1	Section B field.....	28
Figure 3.2	Contours of B isosurfaces.....	29
Figure 3.3	Sample B magnitude, half-section.....	30
Figure 3.4	Sample B magnitude from center to pressure wall.....	30
Figure 3.5	Coil windings in amp-turns.....	30
Figure 3.6	B _{rot}	32
Figure 3.7	Fill pressure vs. temperature, argon.....	36
Figure 3.8	Argon confined by ponderomotive forces.....	41
Figure 3.9	Argon and deuterium density profile.....	41
Figure 3.10	Deuterium confined by B _{rot}	42
Figure 3.11	Deuterium confined by ponderomotive force.....	42
Figure 3.12	Lisitano coil.....	43
Figure 3.13	Early antenna design.....	45
Figure 3.14	Acrylic magnet spindles.....	48
Figure 3.15	Initial mounting of hemispheres.....	49
Figure 3.16	Group of five magnetrons, HV relay.....	52
Figure 3.17	The Baffled Bill.....	52
Figure 3.18	Mounting baffles and early antennas.....	53
Figure 3.19	Inner and outer cones.....	54
Figure 3.20	Feedthrough connector.....	55
Figure 3.21	First camera mount.....	56
Figure 3.22	Mounting for sparker.....	60
Figure 3.23	Sparker in action.....	61
Figure 3.24	First thin wire grid.....	65
Figure 3.25	Thin wire in operation: replacement.....	66
Figure 3.26	Water-based ceramic: final grid installed.....	67
Figure 3.27	Polyclay-filled antennas.....	69
Figure 4.1	The two basic spherical convergent focus fusion methods.....	72
Figure 4.2	Double potential well structure.....	73
Figure 4.3	Tests from Oct. and Nov. 2008.....	80
Figure 4.4	South hemisphere, assembled reactor, and target room at TUNL.....	85
Figure 4.5	Stripping off ceramic: casting: finished antenna.....	87
Figure 4.6	Scintillator detector with camera, and mounted.....	90
Figure 5..1	O-ring seal: painting the antennas: mounted on SH.....	96

Figure 5.2	Diodes on capacitor: top of SH: bottom of NH.....	97
Figure 6.1	Loss cone in velocity space (Geller 1996).....	103
Figure 6.2	Oracle experiment, control room.....	121
Figure 6.3	Assembling the antenna in its dome.....	121
Figure 7.1	Plasma Jet Plug.....	176
Figure 7.2	Fusion Engine Cycle Schematic.....	177
Figure 7.3	Fusion Turbine Cycle Schematic.....	178
Figure 7.4	Can Reaction Chamber.....	179

1 Chapter 1

1.1 *Introduction*

1.1.1 *What was the research?*

From 1995 to 2000 I investigated various unconventional approaches to energy production. From 2000 to 2006 I developed the theory behind microwave confinement in a spherical chamber with a cusp magnetic field using electron cyclotron resonance, for both low pressure plasma confinement with fusion in mind, or at higher pressures for ball lightning (BL). From 2006 to 2009 all my time went to reactor construction, development, and operation.

1.1.2 *What was accomplished?*

The reactor is a practical design that held a vacuum, generated plasmas, demonstrated the viability of multiple magnetron operation, and could be scaled up for further experiments. It includes HV power supplies, capacitor banks, plasma jets, elaborate control circuitry, video gear, vacuum pumps and associated systems, magnetrons and microwave cables with custom fittings, and near-field conical antennas specifically developed for this reactor. The work done over the last few years is essential in laying the way for any future efforts in this direction; I now know the engineering requirements in materials, fabrication and design that could only be learned in this manner. Finances and working alone made making magnets impossible, so this had to be left to some later date.

There was ambiguous evidence for confinement in the low pressure regime; there was no evidence of BL formation. One conclusion is that SMC, or any similar geometry, cannot work without magnetic fields as a type of gridless IEC reactor. Future reactors for either SMC or BL will definitely include pulsed, hemispherical magnets.

1.1.3 *Why is this important?*

Our civilization depends on finding a concentrated energy source that will last for the rest of our stay on the planet. BL clearly generates microwave energy, which if produced in a reactor could be converted to electrical power with 90% efficiency and no moving parts or

thermal cycle. There is the potential to solve the terminal problem of the Industrial Revolution, and the promise from observing natural BL that it can and will happen.

1.1.4 Overview of the thesis

This dissertation describes research and experimentation from 1995 to 2009 in a wide range of unconventional approaches to energy technology, beginning with sonoluminescence, followed by aerosol-based cold fusion, low-pressure plasma confinement for thermonuclear reactions using electron cyclotron resonance (ECR), confinement with just microwaves and an electrostatic grid, and attempts to make ball lightning.

The research was, while ambitious, scaled to the energy and resources of a single investigator without external funding. Direct spending was limited to the \$3000 a year in student loans. The reactor would have been impossible to construct without using equipment borrowed from the laboratory in Research II at Centennial Campus. Also I had many vital parts constructed by the Instrument Shop of the physics department. The Triangle Universities Nuclear Laboratory was quite generous in allowing me to site the reactor there for six months in 2009. Nothing could have been done without the generous attention of my advisor Dr. David Aspnes.

Everything was theoretical until August of 2006 when I started construction of a trial reactor; after that, almost all the work was by necessity devoted to design, fabrication, assembly and operation of the reactor, and recording of the resulting data. This documentation of the research reflects the dichotomy of activity. Theoretical work of any specificity dates from before construction, including the large computational effort to design complex hemispherical magnets for magnetic SMC. After construction began, the theory turned to a much more generalized mode, suited to interpretation of results and speculations on future developments. Multi-mode microwave fields with plasmas are intractable for analysis anyway, so a more rigorous analytical approach was not possible, nor would it be particularly informative. Numerical data acquisition was limited to the critical record of voltages on the capacitor banks, which gave indications of magnetron operation and grid power. The main information from operating the reactor was from a video camera. More

sophisticated plasma diagnosis would require far greater resources than was possible. As a result, sometimes there are equations in evidence, while at other times pictures of plasmas and equipment predominate. The emphasis throughout was on the most practical aspects of constructing and operating a reactor in an efficient, cost-effective, and functional manner, that would have some promise of industrial use at some future time.

The early years were those of a mostly self-taught researcher; I had only three semesters of physics training (from 1981 and 1982) before coming to NCSU in 2001. As the subject matter of the years prior to 2001 was always very speculative and could not lead to a viable reactor, I mention the work briefly in the body of the text and leave the details to appendices A and B. Appendix C is the Mathematica code used to compute the magnet geometry and windings for magnetic SMC.

While none of the experiments showed unambiguous evidence of confinement or anomaly, there were some videos that might have shown both. The research has shown a practical way of putting together a reactor of this type. Progress in the field requires more resources and manpower for a much more sophisticated device and diagnostics. I conclude the paper with a plea for an expansion of physical theory that would make ball lightning much more comprehensible and may lead to laboratory synthesis and reactor utilization.

1.2 Requirement for a Concentrated Energy Source

Many in the sciences and industry have been trying to find ways of replacing our current use of fossil fuels with renewable sources, which would make possible an indefinite continuation of our industrialized society. There is a fundamental problem relating to entropy; that is, our way of life since the Industrial Revolution is based on the one-time extraction of concentrated energy sources which are then dispersed to the environment. Also, it is based on the one-time mining of concentrated ores, some of which might then be recycled a few times. However the loss rate each cycle for even the most diligently conserved materials ensures that everything that comes from a mine or a well will disperse within a century or two, and most materials do so much more quickly at current rates of use.

Our present technology for gathering dispersed energy sources such as solar and wind relies on concentrated energy sources and materials. Once these are dissipated, much energy is required to recover critical materials from soil, sea water, air, and other difficult sources. It then becomes impossible to get more energy out of the collection, distribution, and utilization infrastructure for dispersed energy sources than that required to construct, maintain, and replace it. Thus the resource stream cannot be a closed loop using only renewable energy, and the entire system must collapse.

In some areas this process is within sight. At the Suwa sewage processing facility in Nagao prefecture, Japan, there are 1890 grams of gold per tonne of incinerated sludge. This compares to 20 to 40 grams per tonne of ore in Japan's Hishikari Mine¹, and is due to nearby manufacturers using gold. This illustrates the general idea is that all mined materials, even those carefully recycled, end up distributed over the environment and will be recoverable only by ever-increasing expenditures of energy.

Nuclear fission technology, which relies on finite mined fuels, is highly unlikely to solve the problem. We do not know how to make practical breeder reactors, using either uranium or thorium, with an acceptable degree of safety; and without breeding, there is insufficient fuel for more than a century. The amount of energy required is so large that fission power plants cannot be made quickly enough or in large enough numbers in all the places that would need them; if they could be made, they would exacerbate the waste and proliferation problems by many times. And then, we would be facing the same problems several decades from now as we do now, only with the dead hulks of huge concrete reactors and waste depositories as untouchable monuments for the indefinite future.

The only known fuel that never runs out is deuterium. Whether fusion power plants can be a practical energy source is an open question. There are reasons to believe that any technology, based on the physics that we know now, cannot solve the problem. It is very probable that the only reactors within reach for a very long time would be deuterium-tritium (D-T). We can get by burning lithium for D-T reactors for some thousands of years by which time we would know how to burn D-D. With D-T, 80% of the energy is in 14 MeV neutrons.

This, along with the minimum size requirements of the plasma, mean that the power plant would be several times the volume of a fission plant for the same amount of energy, and inevitably far more complex. As the infrastructure cost is a function of volume of engineered space and complexity, fusion plants must be much more expensive than current fission plants per unit power. This disparity would increase dramatically when materials and energy become more expensive after fossil fuel and ore depletion. With neutron damage, the plant would have to be torn apart and reconstructed periodically, which takes more energy in the future without concentrated material sources. There are problems in any thermonuclear plasma that transcend design that may not be solvable, such as design of a first wall, instabilities, contamination, and so forth. There are no proposed solutions that would result in a power plant that could compete economically with wind or solar even if they worked perfectly, or that could be built and run on the scale required without an infrastructure based on fossil fuels and concentrated ores.

As a result, we do not know of any solutions to the fundamental problems that would lead to the end of industrialized civilization as we know it. The agriculture now prevalent is entirely based on fossil fuels for fertilizer, cultivation, irrigation, pesticides and herbicides, food processing and transportation. Soil erosion and degradation, water depletion, climate change, and other factors only increase this reliance. As the system is not cyclical, it must eventually collapse. We are already close to fossil fuels becoming too expensive for agricultural use for much of the world; no known substitute exists capable of filling its role. Any remedy, which would have to include a reduction in population levels, requires a concentrated energy source that can continue for the rest of our stay on the planet. Only this can close the circle of the resource stream.

There appears to be no solution given the known limitations of physics. However there do appear to be anomalies that show promise. The rest of this thesis is a search for such anomalies and the means to utilize them to allow a continuation of a technological society. The alternative is an eventual regression to subsistence agriculture, or even hunter-gatherer, in the next several hundred years. (Given the degradation of the environment and thus the

low carrying capacity of the land compared to earlier times, as well as today's increased susceptibility to epidemic diseases and war, such a regression is likely to be catastrophic, with a drastic and sudden reduction in population to levels below those before the Industrial Revolution.)

While the inevitable regression without concentrated energy must occur eventually (one or two centuries), other factors can accelerate such a change to a much closer future; the stresses currently present would allow a sudden population crash with minor causes at any time. Such stresses will not decrease, and most will only increase with time. Thus, the magnitude of causes required to create a collapse decreases until normal fluctuations suffice. This pattern is replicated in any simple biological system where a species is free from predation and increases its numbers without restraint while reliant on some finite factor, be it food, water, or living space; there is exponential growth followed by almost all the population dying off².

2 Chapter 2: Early Research (1995 to 2004)

2.1 Sonoluminescence

In early 1995 I read an article by Seth Puterman in *Scientific American*³ about his experiments with single-bubble sonoluminescence. In 1934, H. Frenzel and H. Schultes discovered many bubbles generated by loud ultrasound in photographic developer fluid would glow with a faint light. Puterman and colleagues at UCLA worked on single-bubble sonoluminescence (SBSL) which allows easier measurements and systematic study.

They concluded that the bubbles cavitate, then implode with spherical shock waves that heat and compress the center to an extreme degree. The flash of light lasts a few hundred picoseconds, and its spectrum is consistent with temperatures of 20,000 K or more (the fluid cuts off shorter wavelength light). Subsequent studies have greatly increased our knowledge of SBSL since this 1995 article^{4,5}, but at this time Puterman contended that the temperature and pressure in the bubble reached conditions suitable for fusion ($\sim 10^8$ K).

As I had a bit of training in physics, but not enough to keep me from going in directions unlikely to bear fruit, I spent the next fourteen months (under conditions of severe isolation and without access to information or dialog) considering various ways to make a reactor that might maximize many-bubble SL sufficient for a fusion reactor. It was only after this time that I calculated the available sonic energy in the volume of the bubbles at their greatest size, and saw that even if this were concentrated without loss to the minimum possible number of atoms, only a few fusion reactions could result. Break-even, or even useful neutron production, was impossible.

Below are five drawings from about the middle of this research, reflecting my approach. I proposed operating the reactor under intense pressures up to 4000 psi; only later did I learn that SBSL studies show optimal glow at pressures less than atmospheric, and a steady decline above that. The transducers for generating ultrasound were, at this stage, using quartz crystals. However I saw shortly after making these drawings that quartz was unsuitable for several reasons, and in fact any piezoelectric crystal would not function well under these conditions. The only transducer that would work at the proposed 20 kHz frequency, ambient pressure, and enormous power, would be made from magnetostrictive materials. My design of such transducers is somewhat similar to those shown and is not included here. Further study showed that increasing the power to this extent, even with increased ambient pressure, will destroy any symmetry in the bubbles and ruin the hopes of extreme conditions on implosion.

While this design uses a needle for introducing pressurized gas to the liquid, I also tried underwater sparks, using a make-and-break circuit similar to a doorbell, but with similar end results.

Current understanding of SL shows that glowing bubbles contain almost exclusively noble gases, which are responsible for the light; other gas constituents dissolve out of the bubble within a few hundred cycles. In addition, maximum temperature estimates cluster around 10^4 K. As such, there is no hope of any meaningful “sonofusion”, and subsequent experiments when positive have not been replicated⁶.

Figure 1 shows a section, approximately full size, of the proposed reaction chamber, made of thick steel with 20 transducers screwed in symmetrically. A gas needle comes from below to introduce gas. **Figure 2** shows the reactor from the outside as it could be submerged in a pool. One of the fittings shown, with a cable coming out of it, is a viewing port with fiber optics. **Figure 3** is a schematic of an entire pool reactor to test the concept. **Figure 4** is a proposed cluster of these small chambers within a boiling water tank suited for a fusion reactor (very wishful thinking). **Figure 5** is a schematic of a power plant.

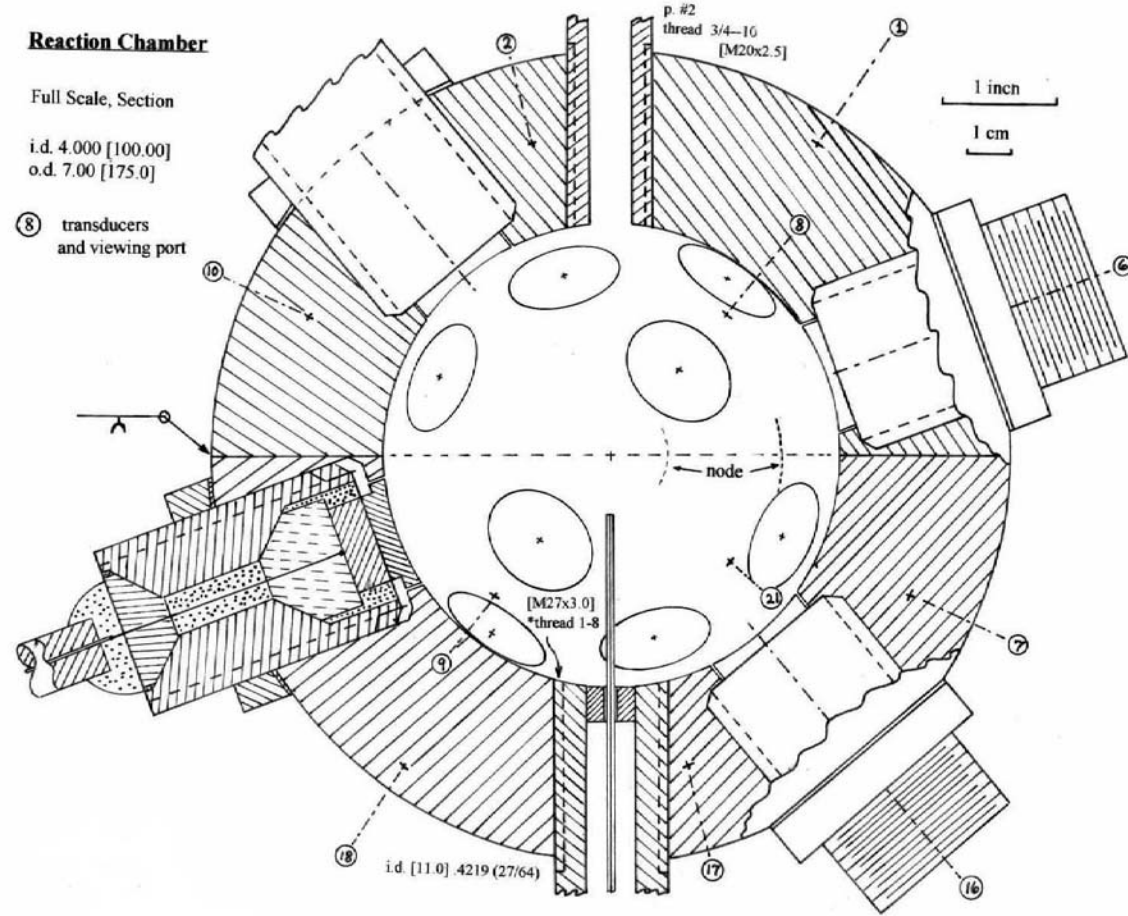


Figure 2.1: Reaction Chamber

Pool Reactor

Scale 1:2

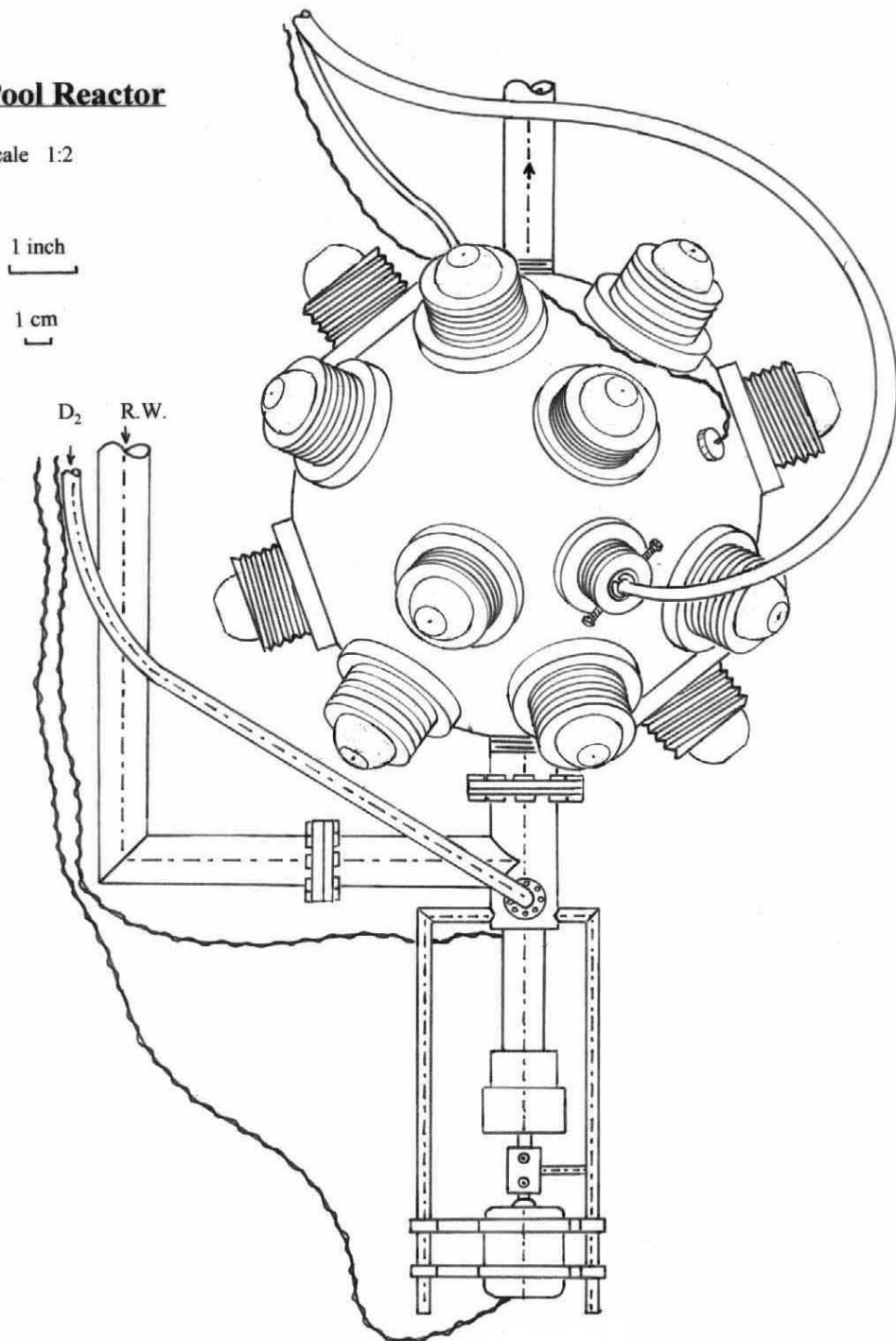


Figure 2.2: Pool Reactor

II

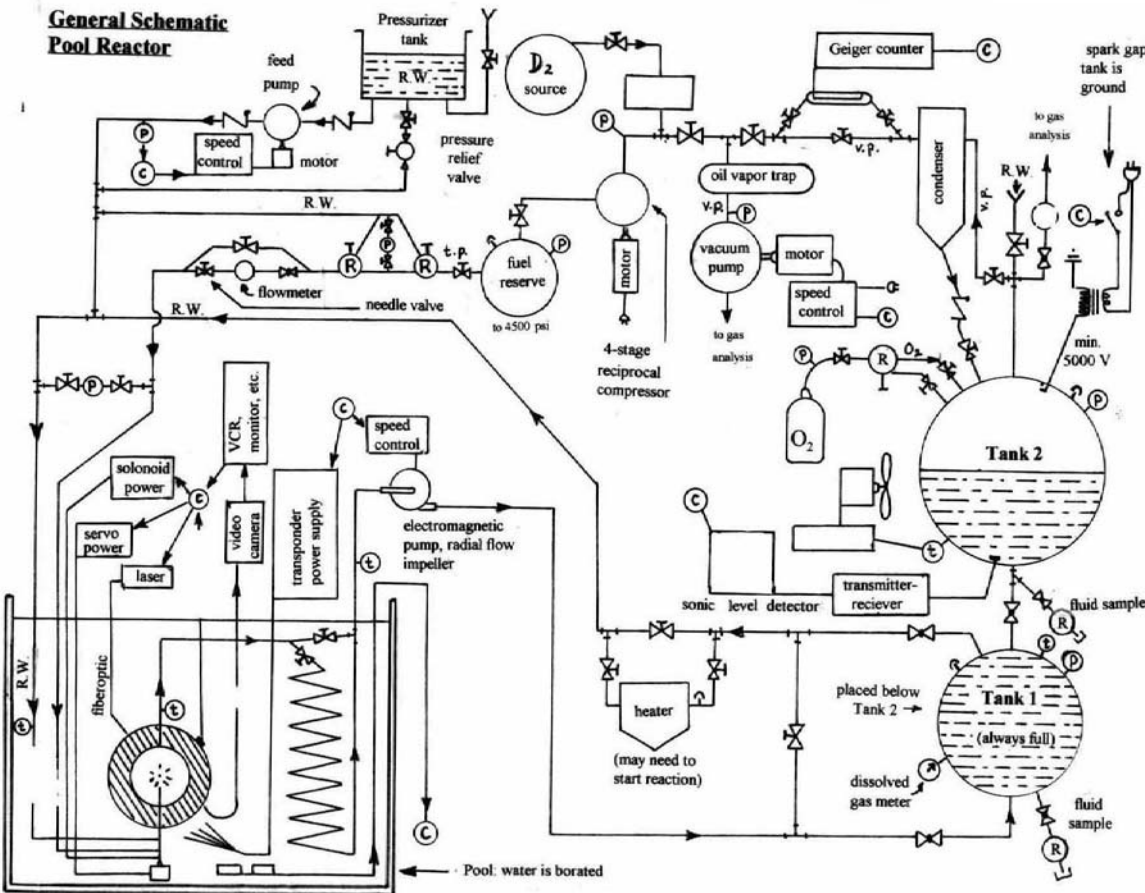


Figure 2.3: General Schematic, Pool Reactor

Reactor Vessel

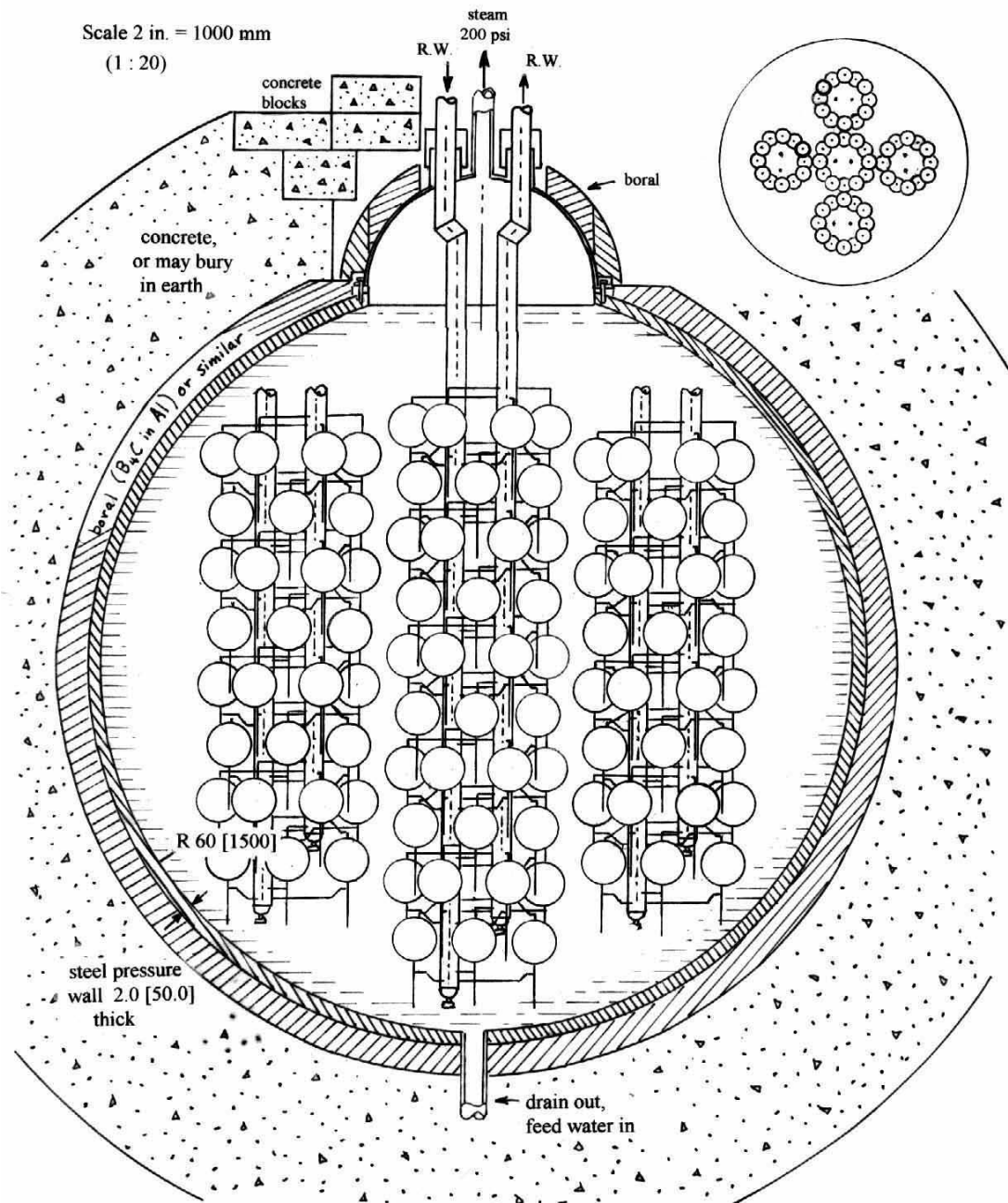


Figure 2.4: Reactor Vessel

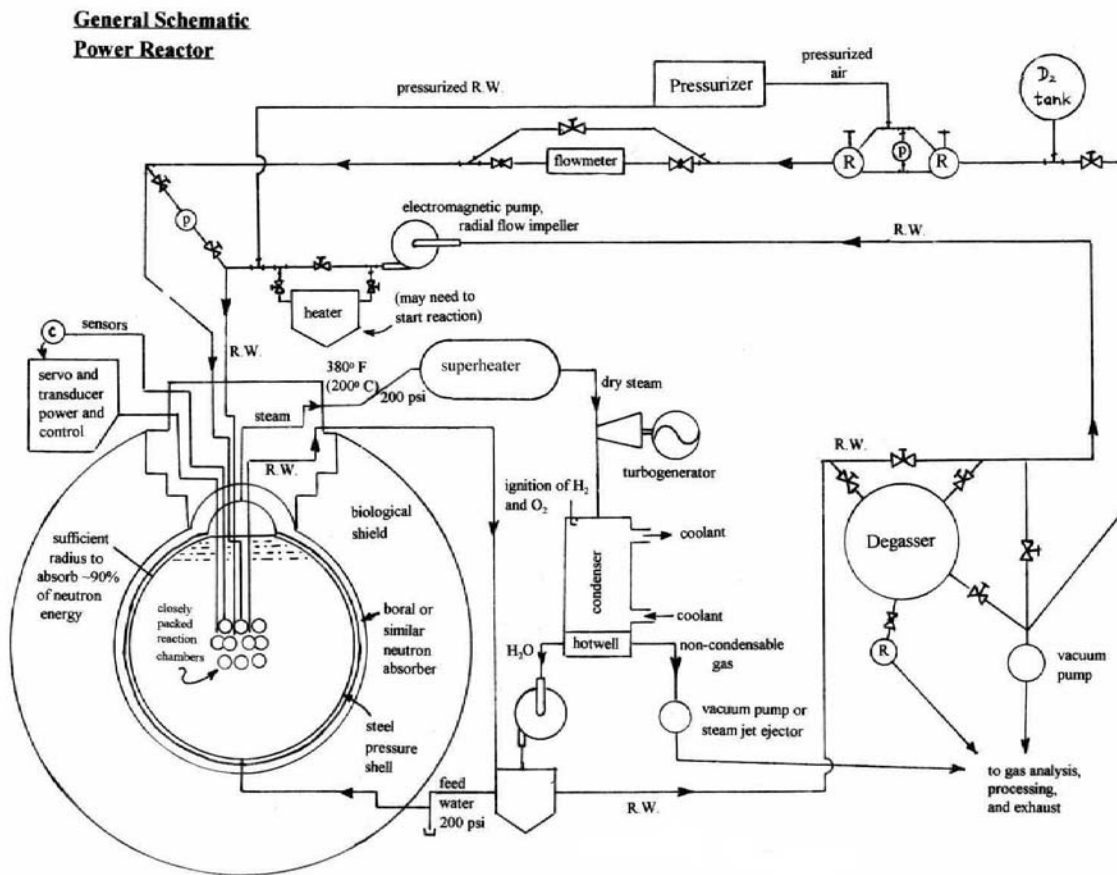


Figure 2.5: General Schematic, Power Reactor

2.2 Fusion; Hot, Cold, and Warm

After this initial effort proved fruitless, I started investigating all manner of approaches to fusion technology, especially exotic ones. The SL studies were assuming normal thermonuclear fusion as the goal, but I also investigated cold fusion (also called Low Energy Nuclear Reactions or LENR). This is a confusing and frustrating field of low repute in most physics institutions, and the pool of investigators includes people who do very dubious science. However there are some who are doing good work and who have results that are of legitimate interest to the open-minded researcher.⁷

The main problem for cold fusion in its standard form is the lack of a naturally-occurring example of anomalous energy production. The usual approach is to load hydrogen or deuterium in a number of metals to form hydrides, the idea being that somehow the distances between nuclei can be reduced, the Coulomb barriers mitigated, and there can be a variety of nuclear reactions. These reactions are not limited to just the hydrogen and often are claimed to involve a large number of transmutations; there is some evidence to back this up, but it is also very easy to be totally skeptical that anything like this can occur. None of the characteristic by-products expected in high-energy nuclear reactions are detected. Part of this can be understood since these are not high-energy reactions, so such products should not be produced; but there is little in the way of evidence or theory that lets us know what is actually happening. One would hope to find something outside the lab that pointed to just this kind of anomaly, but this has proven to be rarely claimed or measured, and when it is, usually in a way that is very difficult to believe.

This is why I eventually gravitated to ball lighting, since it is an example of anomalous energy production that *does* exist in nature. The wrinkle is that it does not exist in the lab—quite the opposite problem of LENR research.

My frustration with cold fusion was that the power density in the large majority of experiments is so low, and takes so long to occur, that the results are far from ambiguous; nothing works reliably enough or strongly enough to actually make a device that cannot be

denied, and which could lead to something useful. Thus, I investigated a huge variety of possible reactor types that would attempt to produce a much higher power density. In general I proposed a fine division of metal hydrides, usually titanium but also lithium and nickel, in the most extreme conditions of heat and pressure that the hydrides can withstand. The most promising method used shock waves in hopes of generating a LENR in each aerosol particle quickly enough to sustain the shock as a detonation. (Ultimately this was wishful thinking since if such hydrides were high explosives, we would certainly know this by now!) In time and after much labor, I calculated the parameters that would apply to such CF detonation shocks, keeping in mind the various qualities of hydrides, the kind of energy that would be required to sustain the shock, ambient pressures, and so forth. As this was as hot as cold fusion can get, but is still vastly colder than thermonuclear fusion, I called it “warm fusion” (a name used by others for other methods to achieve the same goals). The final two papers I wrote on this subject in 1998 are in **Appendices A** and **B**.

After the fact, I found that several other researchers have also considered rapid heating of hydrides to trigger reactions. As referenced in Storms (1998)⁸, Yamaguchi and Nishiokai (NTT, Japan)⁹ experimented with 1mm thick sheets of Pd coated with gold on one side and MnO_x on the other. When exposed to vacuum, one sample showed neutron emission of 0.1-0.2 mSv/hr for 2-3 seconds, and evidence for temporary heating to 1000 C at the Pd-Au surface. However, other samples did not show activity. Other work that showed initial positive results by means of rapid decomposition of palladium hydrides were by Iwamura et al. (Mitsubishi, Japan)¹⁰ and Lipson et al. (Russian Academy of Sciences)¹¹, but neither have been replicated successfully, and the individual samples during the initial positive runs showed radically different effects. These researchers used sheet palladium and not small particles as I proposed; however as noted above, my method could not function without some major modification as the basic materials are not high explosives.

2.3 Ball Lightning

2.3.1 Back to school at NCSU

In 1998, after recovery from a total hip replacement, I bought a dilapidated 1973 Winnebago motor home and left North Carolina for two years of exploration of the Southwest. I was looking for a new home base, while continuing my explorations into novel reactor designs. It seemed best to find a harmonious physics department and go back to school. After two years in the desert, I returned to North Carolina in the spring of 2000 and applied to NCSU. At this time I settled on a very interesting reactor concept; a sphere with many helical antennas pointing inwards, with plasma. Exactly how this would work eluded me, and I saw that many years of study, as well as construction, would be mandatory.

I started working on a BS in physics at NCSU in the fall of 2001. By about 2003, I realized that ball lightning was of great interest as an unsolved natural anomaly that could lead to the kind of reactor I had in mind.

2.3.2 Existing Art of Ball Lightning

It is beyond the scope of this thesis to catalog the thousands of sightings of ball lightning (BL); these are easily found online¹² and in book compilations. I will deal only with conclusions drawn from many observations, which tends to eliminate outliers and increase plausibility, and to look closely at a few illustrative cases.

There are several websites^{13,14} and some journal articles¹⁵ describing fireballs in 2.45 GHz microwave chambers (usually ovens) formed with aerosols. These are frequently described as ball lightning (BL), although there are many differences between natural BL and these fireballs. The most obvious is that nature does not require an external power source or reflective chamber. All the fireballs extinguish within microseconds of turning off the microwaves, and some only last milliseconds even with continuous external power. Also, the fireballs are buoyant, while BL does not typically float up. Recently there are reports of underwater discharges forming non-microwave-related fireballs, which have anomalous durations of up to half a second instead of the anticipated millisecond. However these are

buoyant in air, unlike BL, and do not have the same shape, power density, color range, or other characteristics usually found in natural BL. Thus there is progress and demonstrated anomaly, but not yet synthesis.

It is impossible to design a BL reactor directly from theory as nothing is known of BL physics—not its confinement mechanism, temperature, formation, or even its constituents, and certainly not optimal conditions. There is no reason to suppose that atmospheric conditions are best for BL. All proposed theories are fatally flawed when matched to the full range of reliable observations. It is known through damage reports that high-energy BL, and probably all BL, broadcasts microwaves at wavelengths roughly corresponding to its size; a mechanism for this is entirely unknown. High-energy BL produces energy at densities far beyond the range of chemical reactions or thermal energy storage, although no conventional nuclear reactions are possible.¹⁶ (Only a very few observations record radiation effects from BL; for example, there was a catastrophic event at a village near Maracaibo in Venezuela in 1886¹⁷.)

There are many unsolved mysteries with BL. One is that neutrals are confined as well as charged particles. This is evident from several factors repeated in observations; BL doesn't cool, at least over several seconds, but if hot neutral gas could convect out it would do so in far less than a second. BL can fizz, but also typically pops or even explodes violently on its demise, implying internal neutral particle pressure. The ionized component is parts per million, hence the partial pressure of charged particles is insufficient to explode at all. Also, BL doesn't rise, so it's as dense as the surrounding air, despite its temperature—requiring internal pressures of the order of 15 atmospheres if the temperature is several thousand K, as the color suggests.

The most severe anomaly in BL is its frequent ability to pass through solid barriers, including dielectrics (closed windows and ceramic walls), conductors (metal skin of airplanes), and solid earth. Sometimes damage results but much more frequently there is no effect on either the objects or to the BL. Any theory must answer this fundamental observation, and none so far passes the test.

There cannot be sustained magnetic fields without sustained currents, which are impossible in a free-standing plasmoid without superconductivity in loop currents—and the plasma is clearly not superconducting. Also, there cannot be sustained electric fields from separation of charges in the conducting plasma; electrostatic fields cannot confine any plasma, and charges are free to move and thus cannot remain separated beyond the plasma frequency, typically nanoseconds. Thus all the methods we have to confine BL simply do not apply. Even if there were a way to confine the tiny fraction of charged particles with electric or magnetic fields, there is no known way to confine neutral gas molecules or atoms except by solid or liquid surfaces.

Consider this: the only known confinement mechanisms for non-transient plasmas require external fixed magnets, as the thermal plasma pressure ($P = nkT$) exerts equal and opposite forces on the magnets. Since that is not applicable here, there is a basic Newtonian problem of force balancing in lieu of tension, which is only possible in solids. In addition, all magnetic confinement requires that the collision rate be lower than the gyrofrequency, so that the collisions don't bounce the particles out of the field lines. Otherwise there is little or no difference in diffusion rates parallel or across field lines, as is the case in atmospheric cool plasmas like flames. So even if there are magnetic fields they would make no more difference than they do to a candle flame.

There are also BL and BL-like reports over fault zones during seismic events, although there is a much wider range of phenomena than with storm-related BL. This includes long-lasting lights of odd shape, aurora-like events, and diffuse forms. This may be why Japan BL sightings are unrelated to storms at least 80% of the time, while in the rest of the world something like 90% of reports include storms in some way. Even stranger, there are BL sightings from underwater volcanic eruptions.

BL typically sustains roughly the same size, color, and luminosity throughout its lifetime, with some rare exceptions. As energy leaves the BL, if through no other means than by emission of light and RF radiation, the inevitable conclusion is that there must be a power source that sustains the plasmoid. The upper bound for energy density is in the range of 10^9 J

m^{-3} ; this is roughly the equivalent of molten iron. As noted above, this is far beyond the possibility of either thermal energy storage or chemical reactions, given the number of molecules present. The power output of high-energy BL is largely in the form of microwaves, which can be determined by the kind of damage left behind. Sometimes BL has an explosive end. The goal for a BL-based reactor would not be necessarily to recreate natural BL, but rather to host the mysterious reaction that sustains BL. This would make an ideal power reactor with no radioactivity, direct energy conversion from the microwave outputs, light weight, and (evidently) abundant fuel. With no understanding of why some BL explodes and some does not, there is a hazard that some configurations may lead to significant detonations.

2.3.3 *Example of a Bad but Well-Known BL Theory*

There are many theories about BL¹⁸, several of which claim to answer the enigma in all its particulars. One of the leading contenders from recent times is the proposal from John Abrahamson and James Dinniss¹⁹ which has had favorable press in several publications. *Nature* has been the leading journal for BL research since the early 20th century, and I use the Abrahamson and Dinniss article in *Nature* for a detailed critique, not only of their idea but of most serious efforts at BL theory.

A. and D. contend that “when normal lightning strikes soil, chemical energy is stored in nanoparticles of Si, SiO or SiC, which are ejected into the air as a filamentary network. As the particles are slowly oxidized in air, the stored energy is released as heat and light.” However, BL does not always require normal lightning to form, nor does it always form at the ground. Frequently it falls from clouds.

For confinement and definition of its shape, this is their explanation; “Ball lightning is commonly spherical, and shows elastic behavior. This is consistent with observed elastic properties of nanoparticle chains²⁰. Also, the repulsion of like particle charges will keep the net from collapsing in on itself, with those at the ball surface giving a surface-tension effect to the ball¹, restoring the spherical shape after deformation against solid boundaries. The ball

will generally follow the wind but electrical forces (caused by interactions with, for example, nearby conductors) may also be important.” However, as noted above, there cannot be confinement of the object by electrostatic forces; there can be no surface tension in a plasma or gas or in these hypothetical chains of burning silicon; and BL so frequently goes against the wind that this must be considered fundamental.

Even if the burning silicon somehow was available up in the clouds when BL forms there, the energy density of high energy BL can never be approached. They say, “The total chemical energy density is 3.3 MJ m^{-3} , lying within the very approximate observational estimates of $1.5\text{--}15 \text{ MJ m}^{-3}$ for average ball lightning²¹. A cool outer surface and lack of impression of (radian) heat are natural outcomes of this model, corresponding to generally observed properties^{22,23}.” But the actual value for high energy BL is more like 10^9 J m^{-3} , or about 1 kJ cm^{-3} . It is not enough to explain only the easy low energy phenomena that are similar in almost every respect to the high energy ones.

The most obvious fatal flaw in this, as in all theories I have seen or heard of, is the extraordinarily anomalous behavior of BL passing through barriers noted above. Clearly, no nanoparticle structure can pass unhindered through a closed window or a wall.

This theory also completely ignores the evidence of damage caused to animals, people, and trees, radio interference, and to the heating of water, all of which points to microwaves produced with extraordinary power density. How microwaves could be generated at all remains entirely unexplained.

By way of experimental evidence, A. and D. cite several experiments in this paper and in subsequent ones, none of which create an analog to natural BL. One notable one, with a dramatic video seen widely on the internet, is by G. S. Paiva et al.²⁴ in Brazil. They took a 50 V, 45 A DC power supply, not dissimilar to those used in arc welding, to power a graphite electrode applied to silicon wafers. Just as in any welding shop, the expected sparks of burning silicon burst forth, fell to the floor, bounced about, until they burned up. Somehow this was taken to be evidence of BL produced in the lab. This would imply that steel mills abound in BL, or that fireworks displays likewise share this phenomenon. The picture is from

a repeat of this experiment by M. Goossens, P. de Graaf and R. Dekker at NXP Semiconductors & Philips Research in Eindhoven, Holland.²⁵



Figure 2.6: A welding spark as a lame but prominent BL candidate

2.3.4 *Observations of Natural BL*

Given the complete lack of viable theory, the only guidelines for design of a reactor are from the thousands of BL sightings that have been recorded in sufficient detail. I will review those most of interest, especially concerning high-energy BL, variations in shape and color, how it forms, different environments, evidence for aerosols, damage reports (especially those indicating microwaves as the only possible means), and smell. The conventional approach has been to ignore or modify the observations to make some physical theory plausible. My approach is to assume that multiple observations are valid regardless of how impossible they may appear, and if that means not being able to apply a known physical theory, so be it.

The vast majority of observers do not record their experiences. I have met several people who have had personal encounters with BL but who have never told any investigator, and have been told of many others. (For instance, Dr. Hans Hallen of the NCSU physics

faculty says his mother saw BL come through a metal screen door into her home when she was a teenager.) As interest grows and the internet informs people of the importance of recording and reporting, the available literature is expanding and is available on-line on many sites. Books and publications are not the only, or even the best, source of information on BL. This is because the lack of theoretical work of any validity leads to difficulties in peer review and conventional publication. The important materials to access are the raw data from the field.

2.3.4.1 Susan Fontaine's experience

It is helpful to look closely at a single sighting of BL from a trained and objective observer. Susan Fontaine came within a few months of a doctorate in engineering, so she has familiarity with technical matters, and is a skilled musician familiar with the analysis of sound. She and her partner Michael spent summers in a cabin in Nova Scotia. Here is her minimally edited account:²⁶

There was a fast moving storm in progress. What we definitely saw, with two witnesses, was that the ball appearance was simultaneous with a very close lightning strike. The ball appeared as intense blue light, about a foot above floor, floating smoothly toward north wall (definitely not bouncing around, more of a smooth wandering). Size about 3-4" across, spherical shape. Lasted about 3 seconds. It made a popping sound as it disappeared - like the sort of pop used in cartoons. It was a downright silly sound. Volume was that of a loud speaking voice - very clear but not uncomfortably loud.

Less definite, with just me as the observer; it seemed that the ball appeared before I heard the thunder, simultaneous with the lightning (maybe even an instant before, which is weird). We both missed its initial appearance, but had the impression it entered through the wall beneath a window (vinyl frame, closed I believe). That wall faces the direction from which the storm was approaching (windward side). The ball had a brighter center, pea to marble sized, (with a pinkish tinge?). It is hard to say how large the ball was because it had no defined surface. The ball gave an impression of a fast sizzle surrounded by light, rather like a sparkler but at a much, much faster rate of sizzle. I had the impression it followed a smoothly curved (parabolic), horizontal path. The closest I can recreate the pop is the sound made when you stick finger into the corner of your mouth and pull it out but higher pitched (Michael says more snap). My vague guess is lowest pitch in octave above middle C, with higher overtones. Lower pitches ending first or pitch rose as sound ended. Neither sine nor sawtooth, but closer to sine. Closest instrument a clarinet? I found no marks on the wall

where I thought it may have entered and no marks along the path of the ball. I noticed no change of air quality or smell. No marks of a lightning strike outside the house. We are 400' above the ocean on a cliff. It may be possible that the lightning hit the water nearby but below us.

One other point. The house is clad with cedar shingles and has no interior walls yet so the wall from which I guessed ball appeared is plywood studded with nails projecting 1/2" to 3/4", in horizontal rows about 6" apart. (Not a cozy wall covering!) There is no wiring in that section of wall.

This is a valuable account since it includes carefully recorded phenomena frequently encountered by others. Not only was the BL only feet away from the two witnesses, it lasted long enough to observe clearly. There is no chance of it being an optical illusion, a product of persistence of vision, swamp gas, burning silicon dust, Venus, mass hallucination, or any of the many ways of explaining away BL frequently seen in the literature.

While the BL could have approached the house in a downwind direction, it did not evidently rely on a breeze inside the house to define its path (and could not have followed a breeze through the wall). Generally, BL does not go downwind, but rather seems indifferent to the wind direction. This is a principle puzzle of the phenomenon, since air passing through the BL does not cool it off, nor exert any pressure that would overcome whatever is making it move in the direction it chooses.

The entry of the BL into the house is another, amplified, aspect of the same puzzle. Any material object, plasmoids very much included, would collide with a closed window or wall, and show evidence of passage through the barrier. BL frequently passes through walls, closed windows, even the metal skin of airplanes, without apparent change to either it or the barrier. Sometimes, it does collide with barriers, burning holes, breaking windows, or exploding and leaving soot. In this case, though, there was no trace of its passage. This is a most important aspect of BL that I will discuss below at greater length.

In the absence of spectrometer measurements or any other direct detection of temperature, much of the clues about BL temperature come from the color and brightness of the glow. However, given the abnormally low interaction of the plasmoid with material barriers, it is a matter of conjecture as to how well coupled to electromagnetic radiation the

BL is and if we are seeing an attenuated and possibly color-shifted remnant of what is actually generated. Generally, BL tends to have about the same color as an incandescent light bulb and roughly the same luminosity; this one seems hotter and brighter than most. The upper limit, rarely seen, resembles a welding arc in brightness and results in UV-generated eye pain.

Notice the popping sound on the end of the BL. Once again, any conventional approach to this runs into serious trouble. With any plasma in equilibrium in atmospheric conditions (which would extinguish in microseconds), the proportion of charged particles would be parts per million; and only these would be confined by any known mechanism, relying on electric and magnetic fields—which as explained above, cannot apply here. Given no known mechanism for confinement of the neutral gas molecules, a sudden release of the partial pressure of the charged particles alone could never generate an audible sound. High energy BL can result in explosions so severe that towns can go on alert from fear of terrorist bombs detonating. (This occurred in the Melbourne sighting noted below.) Thus BL seems to go from a state where it has minimal interaction with the surroundings and inexplicable behavior, to one where it suddenly goes into a “normal physics” phase. All the confinement suddenly ceases and what one would expect from normal plasma collapse, cooling, and recombination happens in a normal time scale—with supersonic velocity, just as with linear lightning. However it is not clear whether the pop is from an explosion or implosion. It would be difficult if not impossible to replicate the explosive damage from high energy BL from implosions since the size of the BL is far too small in such cases.



Figure 2.7: Melbourne BL, 2002, including path behind hills

Figure 2.7 was photographed by Ern Mainka outside Melbourne Australia in 2002. He describes his remarkable sighting in detail on his website²⁷. The approximate diameter of this fireball was 45 m and the initial velocity on its downward path was about 720 kph, but it slowed to almost motionless before continuing. While the BL went behind hills and was out of view of the camera for most of its duration, it passed over populated areas and thus had multiple witnesses. This BL split into smaller plasmoids, each of which exploded with considerable force. The total duration was about 35 to 45 seconds. One interesting observation here is the distinct corona surrounding the gold-yellow core. It appears that the corona was at the start of the BL with the core forming later. Some BL reports include corona-like surroundings, while others have very well-defined boundaries.

3 Chapter 3

3.1 *Middle History of the Research*

I completed my BS in 2004 and continued on at NCSU in the physics graduate school. It seemed that the helical antennas in my idea from 2000 would have to be for microwaves, and so I studied everything applicable about microwaves to design a reactor. By early 2006 I had an elaborate scheme for what I termed Spherical Microwave Confinement (SMC), intended to aim at severe enough conditions for hot fusion. The idea was that if this could be used for BL as well, that would be serendipitous, but it would be better to start off with as conventional a proposal as possible.

The early formulation was an aluminum sphere, constructed from two joined hemispheres. Each hemisphere would be covered by a hemispherical electromagnet with a winding designed to create a cylindrical cusp field. The magnitude of the magnetic field would be the same on closed surfaces as described below. This magnet would be quite complex, costly, and challenging to construct, and would have to be in conjunction with a well-engineered microwave system. This would be quite possible given funding and multiple workers, but not possible working alone funded by student loans. As the latter was the case, the magnetic design was never constructed, and the microwave circuit was very simple.

There follows a description of magnetic SMC as it was in early 2006, just before construction started. At the time, I thought that this technique could result in confinement good enough for fusion reactors; later, especially after building a prototype, I realized that this was unrealistic, despite the tidy mathematics. Magnetic SMC is of interest to me now, in an updated version, as a practical plasma heating and confinement technique, as well as a possible method for initiating ball lightning or similar plasmoids.

One thing to note; section 3.2 does not use the magnetic field from the external magnets as the mechanism for confinement, as this cusp field would be far too weak for thermonuclear conditions. Instead it relies on putative self-generated fields of much greater local intensity at the skin surface of the plasmoid. (I no longer think this is possible.) As such this article does not delve into the magnetic mirror and associated topics like the mirror angle and various drifts. At the concluding section of this dissertation, I offer a more advanced and plausible suggestion for magnetic SMC. It remains to be seen how much can be salvaged from this 2006 concept. Section 3.3 reverts to the historical survey of the experiment.

3.2 Magnetic Spherical Microwave Confinement (2006)

3.2.1 Introduction

The first ideas for fusion reactors half a century ago used open magnetic confinement. There were several intrinsic advantages, chief among them the MHD stability of negative curvature fields; the curvature drift and “ \mathbf{B} ” drift are in opposite directions, vital in suppressing microinstabilities. Also, open fields allow beams of fusion products for direct energy conversion or space propulsion. However, the appeal of favorable curvature found in cusps has been tempered by the inability to plug the open ends to particle loss in fusion regimes. As a result the bulk of fusion research goes to closed magnetic geometries like tokamaks. These suffer from intrinsic instabilities and large areas of unfavorable curvature, and cannot operate without extreme expense and complexity. It is unlikely that an economic reactor can ever result from an engineering tour de force of such magnitude.

Spherical Magnetic Confinement blocks particle loss in an axial cusp arrangement by using currents formed by the surface of a spheroidal plasma responding to circularly polarized microwaves at the electron cyclotron resonance (ECR) frequency. In addition, the ponderomotive force presses inwards on the same surface away from cusps ^a. By ensuring the **B** field is at gyroresonance on that shell and nowhere else, SMC defines stable plasma location and size. Thus stability problems that have frustrated fusion designs could be overcome; if SMC is valid, it could make possible an economical, relatively simple fusion reactor with modest magnets and strong, easily built and maintained, simply-connected geometry.

In the initial test device, a spherical metal chamber holds 20 inward-directed helical antennas that radiate circularly polarized 2.45 GHz microwaves. A slightly larger concentric sphere holds magnetic coils that run along latitudes; on one hemisphere they rotate in one direction, and counter-rotate on the other. Carefully adjusting the current density tunes the **B** field so that the microwave frequency is $\Omega_e = eB/m_e$ at the intended plasma surface. This magnitude is called B_c . To initiate plasma (except in ball lightning experiments), the microwaves cause breakdown at the resonant surface.²⁸ On that surface SMC causes stable confinement within a spheroidal shell, and effectively plugs the cusps.

Steady-state operation requires very large or superconducting magnets and is not the focus of this research. For pulsed operation, rapidly increasing **B** causes an imploding plasma shell, which can result in hot dense conditions on reaching a small radius. Using a single current for the magnet coil, the B_c surface can only be spherical at one radius, which is best chosen at the pressure wall. (This is because outside that spherical surface the surfaces of equal magnitude become disturbed and do not allow closure.) Further in, the isometric surfaces will be oblate spheroids. To have spherical B_c surfaces during the entire implosion

^a Later research (2008) showed chaotic electron trajectories under these conditions, instead of large orbits which would result in very high ponderomotive forces; this chaos could be very useful for ball lightning experiments.

would require multiple coils with intricate current controls, and is probably not worth the expense and complication.

The plasmoid is opaque to the microwaves and so there is reverberation between the plasmoid surface and the metal pressure wall. Anticipated Q is no more than 50 due to efficient coupling with the plasma, and probably significantly less.

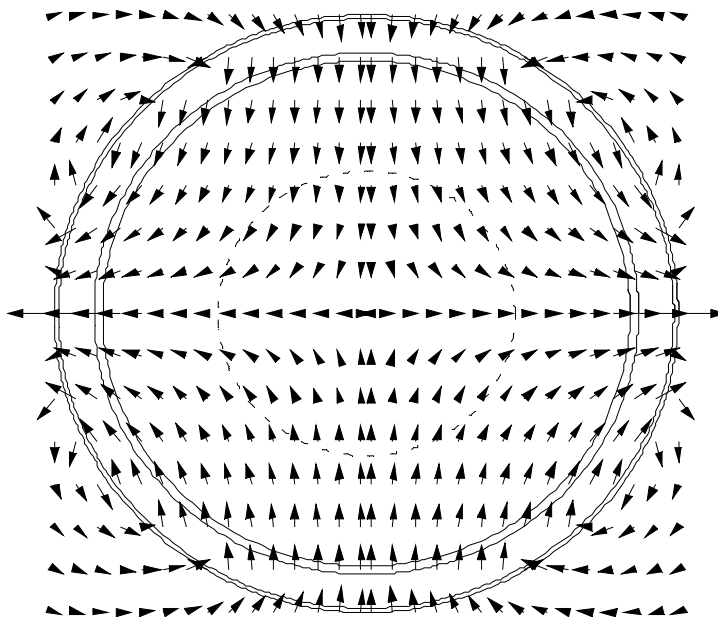


Figure 3.1: Section along polar axis showing the outer sphere holding the magnet coils, the ground sphere (pressure wall, double circle), distance of the antennas' tips from the center (dotted circle), **B** field cusp section (in vacuum). Rotation around the vertical axis gives 3-D.

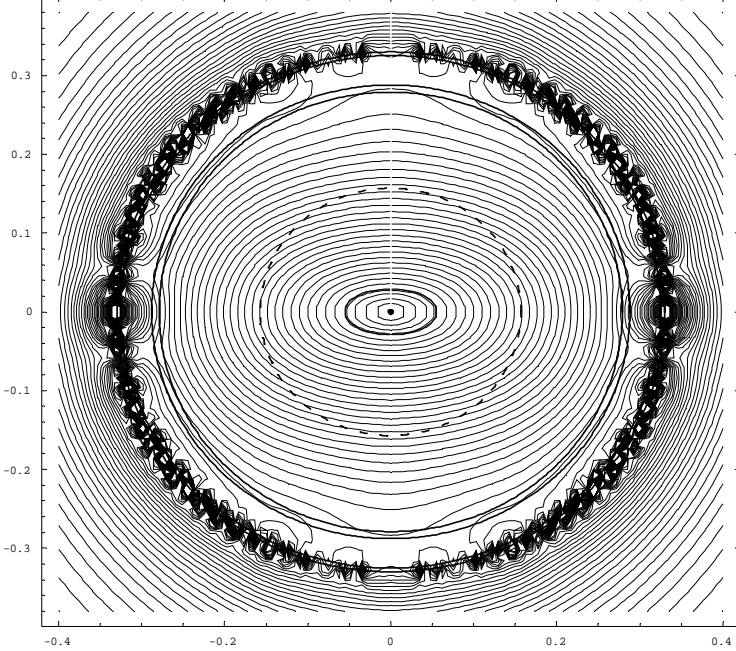


Figure 3.2: Contours show a section of B isosurfaces (constant magnitudes). Superimposed sections are the outer coil sphere (upper hemisphere current in one direction and lower hemisphere the other); pressure wall, and antenna tip and baffle distance as before. (See Green et. al.²⁹ for an analytic method for finding fields and current densities in spherical geometries.) Rotation around the vertical axis gives 3-D. Axis ticks in meters.

Figure 3.2 displays much that is critical to SMC. Each of the contour lines is a section of an isosurface for the \mathbf{B} field magnitude. The outer sphere on which the coil rests is the outer two solid circles. Openings at the poles (above and below) and a missing coil on either side of the equator allow access to the pressure vessel, shown by the next two circles. The gap between the two spheres gives room for coax cables, air cooling, and for the magnetic field to smooth out irregularities before entering the chamber. Helical antennas point inwards mounted on the pressure wall; their inner tips reach as far as the dotted circle.

I calculated the magnetic field strength with Mathematica by off-axis dipole formulas for loop currents, and added up individual contributions from an array of loops arranged as shown. **Appendix C** is the code. Adjusting the current to each loop leads to the desired surfaces and the required current distribution for the magnets.

Pulsed power to the coil causes the \mathbf{B} field magnitude to increase rapidly, so that each contour line will indicate a progressively larger value while the shape of all lines remains

constant. The contour that equals B_c travels inwards from the pressure wall in towards the center faster than the cold gas sound speed, changing shape from spherical to oblate spheroid and carrying the plasmoid surface with it. The extra-thick contour near the center is the target for the first experiment for the minimum B_c surface, and is the basis for the amp-turn calculations and **B** field cross-section plots (Figs. 3, 4 and 5). The center is indicated by a dot.

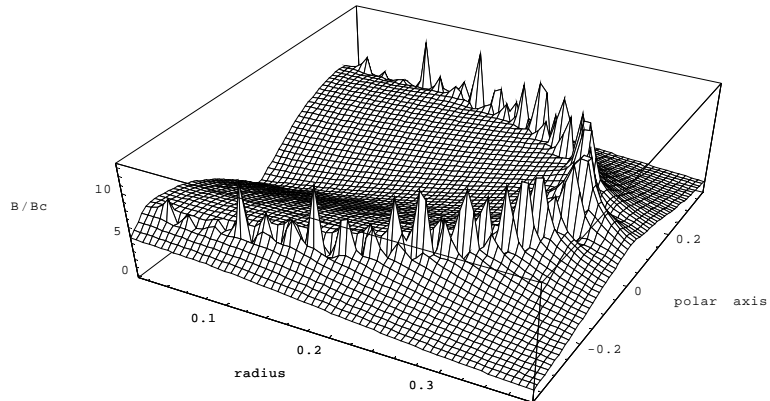


Figure 3.3: Sample B magnitude in vacuum in units of B_c for test reactor, half-section along polar axis (left edge)

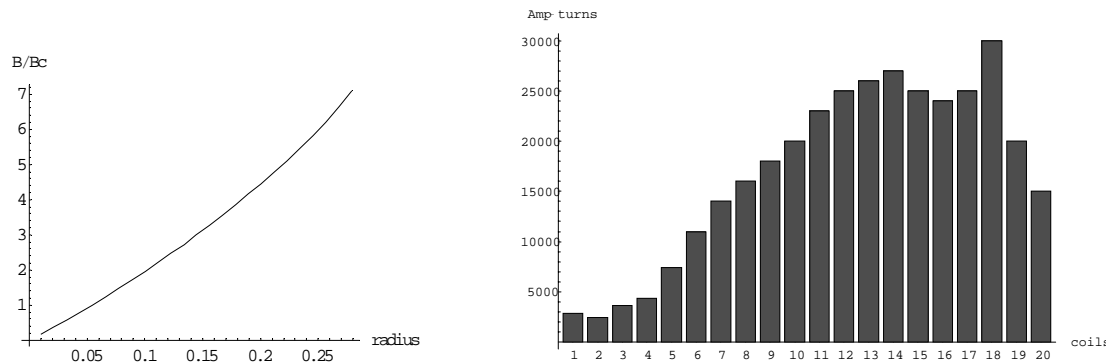


Figure 3.4: Sample B magnitude in vacuum from center to pressure wall along equatorial radius

Figure 3.5: Coil windings in amp-turns for test reactor, one hemisphere (other hemisphere is negative of this)

The magnetrons will be pulsed at about the same time as the magnet, which allows for high power radiation to be applied only when needed with small duty cycles ($\sim 10^{-3}$). Also, breakdown should be limited to the B_c surface, without plasma forming in the central region before the magnetic field gains sufficient strength. Thus the microwave energy density must reach high enough levels for plasma initiation at the pressure wall when, but not much before, the B_c surface gets there. ECR heating will increase as the microwave power goes up, as well as the SMC confinement, so that the temperature and pressure increase greatly exceed pure adiabatic compression. Inward shocks can continue after the plasma surface stops imploding (although oblate symmetry will not make a very small focus). As a result, extreme conditions can result at maximum compression.

3.2.2 Confinement Mechanisms

There are two methods for confining electrons in SMC; ions are confined secondarily by attraction to the electrons. Each method depends on the angle that the external \mathbf{B} makes with the plasmoid surface. B_{rot} works with the radial component of \mathbf{B} , and the ponderomotive force works with the tangential component of \mathbf{B} . Combined, the entire surface is contained at pressures that can far exceed the magnetic pressure from \mathbf{B} .^b

3.2.2.1 B_{rot} confinement

The circularly polarized microwaves rotate in two different directions, matching the gyrorotation of electrons in each cusp. For the inward-flowing cusp, the rotation is counterclockwise looking out (using the sense of rotation looking into the source of radiation); for the outward cusp, it will be clockwise. The electrons drift in response to the \mathbf{E} field in two different ways. Without gyroresonance, when $B = B_c$, the orbital radius and velocity are inertia-limited and small.³⁰ As a result, both heating and current effects are

^b Later analysis raised questions as to where, or if, the confinement force can transfer to the reactor--a fundamental Newtonian concern.

negligible. In gyroresonance, the \mathbf{E} field and velocity are in the same direction for about a third of the electrons at any given time, so the electrons accelerate until disturbed by a collision. This cyclotron behavior results in considerable current and heating. (The SMC confinement will apply to the large majority of the electron population even with only 1/3 in actual full gyrorotation.)

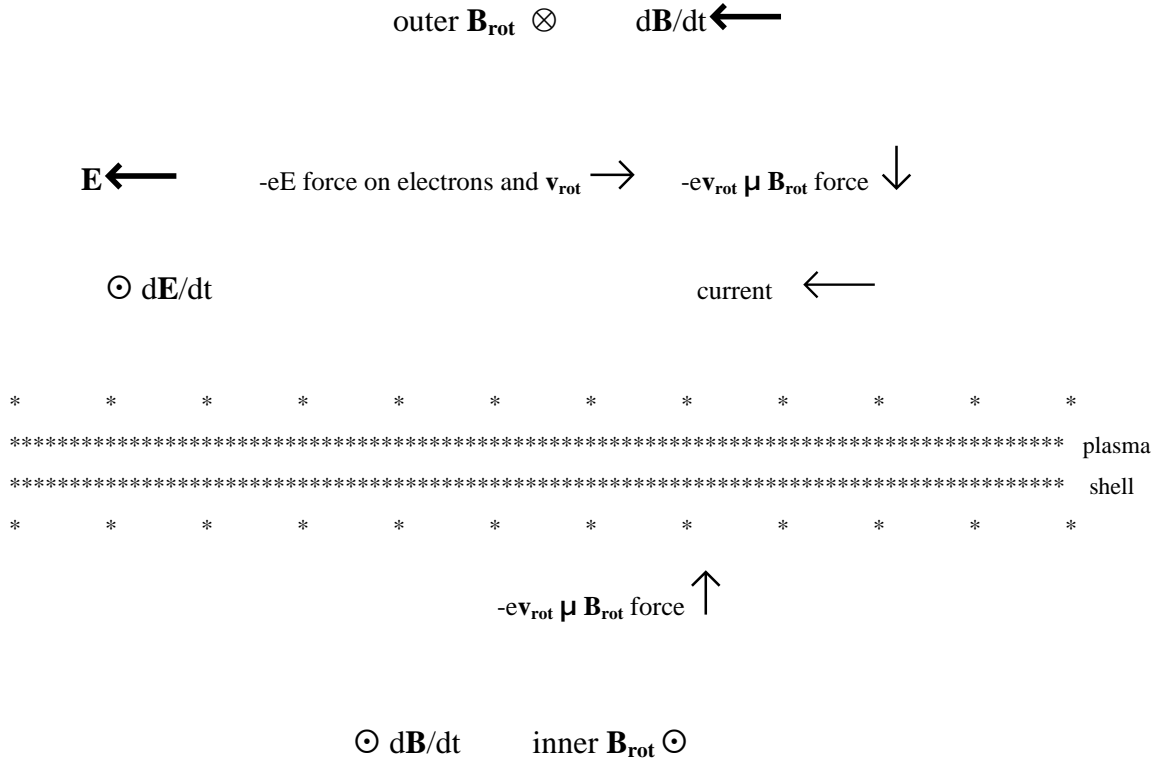


Figure 3.6: \mathbf{E} fields from microwaves, \mathbf{B}_{rot} rotating fields, electron drift and current both inside and outside the plasma shell rotate clockwise seen from below. (This is for near the magnetic poles where B_c is close to perpendicular and pointing into the plasmoid; rotation is clockwise looking out for B_c going out of the plasmoid, always in same direction as electron circulation.) The inner fields and drifts will not occur for a plasmoid of near constant density within the shell, such as at high temperatures.

The antennas are coordinated in phase, so that the \mathbf{E} fields each generate are approximately in the same direction within the scales appropriate (distances larger than instabilities) near the surface. The resulting current is in the form of a sheet; the \mathbf{E} fields have

negligible curl, so the electrons in any fairly small area move in unison at any given time in one direction and do *not* generate a radial **B**. The **B_{rot}** field generated by such motion is what would be generated by a thin sheet of current; tangential to the current, and in one perpendicular direction inside and the other direction outside. The sense of the **B_{rot}** field is such that the Lorentz force from the drift velocity is always into the sheet (current pinch effect). As long as the collision rate is sufficiently less than the microwave frequency, the B_{rot} thus generated can grow until its magnitude far exceeds B_c . Electrons will circulate rapidly and tightly around the strong **B_{rot}** lines which move quickly; they also will retain their slower orbit around the external, stable **B** lines. The following section leads up to a calculation of B_{rot} to ensure that it can become strong enough for confinement under the desired conditions.

The circularly polarized microwaves have a tangential electric field both outside the shell and exponentially decaying within the shell. To find the fields, we start with an idealized vacuum with strictly spherical symmetry and then modify for the actual condition. The phases of the microwaves, the multiplicity of magnetrons, and the variability of the geometry due to the plasmoid ensure that distinct resonant modes will not form in any dominant manner. To a first approximation, the microwave energy will distribute evenly through the central portion of the sphere where it is not by antennas.³¹

The quality factor Q is defined as 2π (energy in the system) / (energy lost per cycle). Q for this geometry is very difficult to calculate in detail, but a minimum, not counting losses to the antennas, is $Q_{min} \approx \frac{2\pi V}{\lambda S}$ with λ as the microwave wavelength, V the volume of the chamber, and S the plasma surface area. For the first reactor this is about 50, but the antennas and cancellation will lessen this quite a bit. (There are some experiments somewhat like this indicating of about 10, despite theory predicting 100³².) The total microwave power input, times the conversion to radiation efficiency (~90%) and Q, divided by ω and the chamber volume equals the energy density;

$$\frac{\epsilon_0}{2} E_{\max}^2 = \frac{(0.9) Q \text{Power}}{\omega \text{Volume}} \quad (3.1)$$

From this can come an estimate of the electric field magnitude E_{\max} . For the test reactor it will be about $4.3\sqrt{Q \text{Power}}$. (The actual magnitude at the plasma surface and into the skin depth, E_o , is difficult to estimate due to unknown reflections and resulting interferences. The two confinement mechanisms use radial E_r (B_{rot}) and tangential E_t (ponderomotive), which will probably differ somewhat. For this first approximation, I will use E_{\max} and adjust the theory after further research.) The flux from 4 kW should be more than sufficient for proof of concept, both for keeping the plasma hot and also for confinement. The first reactor will have at least 20 kW; more advanced reactors could have much more powerful microwave sources. The frequency might be lower, suited to larger reactors, but would be unlikely to be above about 8 GHz, the approximate limit for helical antennas. In addition, higher frequencies require proportionally higher B_c , which is a disadvantage; and there are always advantages to size in fusion reactors when such is possible.

To calculate the skin depth for reflective plasmoid densities we need the plasma frequency. Plasmas have an index of refraction that goes down from 1 as the density goes up, for a given frequency. The index reaches zero at the critical density (n_c) at which transmission into the plasma stops, when the plasma frequency ω_p equals the microwave frequency ω :

$$\omega_p = (n_c e^2 / \epsilon_0 m_e)^{1/2} \quad 18 \pi n_c^{1/2} = \omega \quad (3.2)$$

which for $\omega = 15.4 \times 10^9$ (2.45 GHz) means $n_c = 7.4 \times 10^{16}$, a practical level easily exceeded in the test reactor. All densities for reflective SMC must be substantially above the critical density so that the microwaves will bounce in a skin depth corresponding to the region of B_c . In reality there will be a complicated density gradient, but for this initial approximation the plasmoid has a hard edge and a skin depth of

$$\delta = \frac{c_o}{\sqrt{\omega_p^2 - \omega^2}} \quad (3.3)$$

As long as $\omega_p \gg \omega$, δ is taken as c_o / ω_p . With this approximation, $\delta = 5.3 \times 10^6 n_e^{-1/2}$. Even when this is inaccurate, for the purposes of computing B_{rot} it is sufficient for estimating the total number of electrons or ions rotating in the sheet current; approximately the same number of charged particles will respond to the radiation, found by multiplying n_e by the volume of the skin.

The test reactor will start by using argon, as there is a lower collision frequency at moderate vacuums and temperatures due to the Ramsauer-Townsend minimum. The only collision rate of consequence in the conditions first investigated is between electrons and neutrals ν_{en} . For ν_{en} at temperatures less than 14,000 K, with n_n the neutral density and T_e in Kelvin:³³

$$\nu_{en} = n_n (2.58 \times 10^{-6} T_e^{-0.96} + 2.25 \times 10^{-17} T_e^{2.29}) \quad (3.4)$$

For higher temperatures this matches the slope for an argon cross-section of 1.52×10^{-19} m, so for the high temperature case with T in eV,³⁴

$$\nu_{en} = (4.2 \times 10^5) n_n (1.52 \times 10^{-19}) T^{1/2} \quad (3.5)$$

The other gases of interest are hydrogenic, which can use well-known formulas for finding ν_e . Now we can estimate B_{rot} . In gyroresonance, the electron velocity is in the direction of the electric field and continues to increase until stopped by collision. For a third of the electrons, with ν_e being the total electron collision frequency (sum of all species in the general case),

$$\mathbf{v}_{\text{rot}} = -\frac{e}{m v_e} \mathbf{E} \quad (3.6)$$

Deriving B_{rot} from the sheet current density requires a factor of $\cos \psi$ with ψ the angle between \mathbf{B} and \mathbf{r} , since the mechanism depends on alignment. With $\rho = e \delta n_e / 3$,

$$B_{\text{rot}} = \frac{\mu}{2} \rho \delta |\mathbf{v}_{\text{rot}}| \cos \psi = \frac{\mu e^2 \delta E_o n_e}{6 m_e v_e} \cos \psi \quad (3.7)$$

Considering that opaque plasmas have a minimal n_e , and given achievable and practical E_{max} and E_o levels, B_{rot} easily exceeds B_c in low-collision plasmas. This would be especially appropriate in fusion reactors where B_{rot} can reach a few hundred Teslas, tightly restricted to the region around the skin. Higher temperatures and lower densities work in favor of increased field strength. In the test reactor, using argon, B_{rot} can reach B_c at 4000 W anywhere below about 200 mTorr. (Note that the limited spatial extent of B_{rot} and the small magnitude of \mathbf{B} might allow advanced fuels such as p-¹¹B without excessive cyclotron losses.)

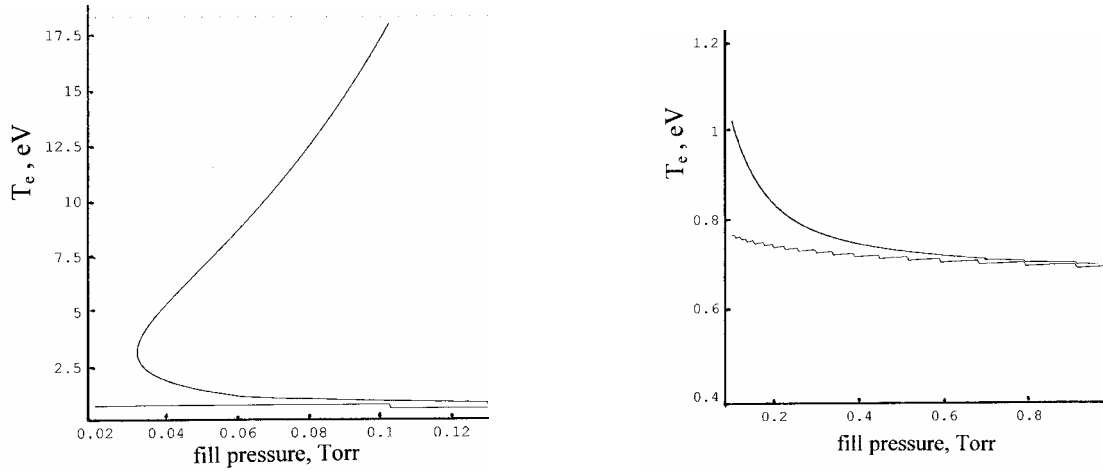


Figure 3.7: (All figures assume 4 kW power in test reactor, $Q = 50$, $\beta = 0.7$ and use E_{max} instead of an attenuated E_o .) Argon confined by B_{rot} below and to left of the upper contour. Single ionization.

The maximum temperature and density confined at a given β (the ratio of magnetic to plasma pressure) comes simply enough from equating the magnetic pressure times β to the plasma pressure and assuming Maxwellian electron distribution. The figures show results for modest conditions in argon anticipated for the test reactor. Confinement improves without intrinsic upper limit as T increases, as these equations do not include factors that come into play at high temperatures.

3.2.2.2 Radiation pressure

[Note; as indicated in the footnote to the introduction for magnetic SMC, later research (2008) shows that electrons under conditions of ECR and with microwaves at the resonant frequency are chaotic and do not have the large orbits that would result in extremely large ponderomotive forces. This could be advantageous in ball lightning experiments.]

The ponderomotive force per particle \mathbf{f}_{nl} (nl from “non-linear”) applies to both electrons and ions, but here we consider only its effect on the mobile electrons, and approximate for the moment no charge separation. This force is a result of the gradient in the spatial part of the microwave electric field, which is only appreciable in the radial direction at the surface of the plasmoid. Due to grazing incidence of some microwaves moving along the longitudinal direction of the \mathbf{B} field, there is a radial component to \mathbf{E} causing cyclotron motion and thus enlarged orbits of electrons just as for B_{rot} . The ponderomotive force is against the gradient of \mathbf{E} , and thus always inwards towards the center since \mathbf{E} attenuates exponentially into the plasma. For regions away from B_c , and thus out of cyclotron resonance (and away from appreciable $\nabla\mathbf{E}_s$),³⁵

$$\mathbf{f}_{NL} = -\frac{e^2 |\nabla\mathbf{E}_s|^2}{4m_e(\omega^2 + \nu_e^2)} \quad (3.8)$$

where \mathbf{E}_s is the spatial part of the electric field, ω is the microwave frequency, and ν_e is the sum of electron collision frequencies. For anticipated reactor conditions, this force is negligible without ECR. This is because the ponderomotive force is proportional to

$1/(\omega^2 - \Omega^2)$ where \mathbf{W} is the cyclotron frequency. [Later research showed that at ECR, cyclic behavior of the electron disrupts and becomes chaotic, and so the ponderomotive force does not reach extreme values at ECR.]³⁶

In the early 1970's, Donald Ensley³⁷ proposed two reactors using extremely intense microwaves (without ECR) for fusion reactors. One was spherical and heated a cryogenic fuel pellet in the manner of ICF; this could not work due to pre-heating of the pellet center as a result of the long wavelength and migrating electrons. The other was a low pressure, toroidal reactor relying entirely on radiation pressure without any external magnetic field applied. This was possible in his reactor only with a quality factor Q of 10^{11} , which required all reflecting surfaces to be cryogenic and superconducting, something not possible in a fusion reactor. The interest in his voluminous labors lies in the sophisticated mathematical treatment of the interaction between microwaves and plasmas in spherical geometries, some of which can be applied to SMC; he showed how plasmas confined by radiation pressure in spherical symmetry would be stable due to plasma instability waves having shorter wavelengths than the confining microwave radiation.

To see how high Q would have to be for any fusion reactor, we can see from Eq. (3.1) that the energy density of the radiation is a function of antenna efficiency, Q , input power, microwave frequency, and the volume of the plasma. To confine a fusion-relevant plasma requires countering the plasma pressure of nkT . The ratio of the plasma pressure to the confining force is \mathbf{b} , which must be less than unity. Different reactors need different maximum \mathbf{b} ; for cusp magnets, the curvature is always favorable, thus \mathbf{b} can be significantly more than for a tokamak, where \mathbf{b} is roughly 1%. With $n \sim 10^{20} \text{ m}^{-3}$ and T at a minimum of 10 keV for DT, the plasma pressure is about 1.6 atmospheres. Using a plasma volume of 1 m^{-3} and a frequency of 2.5 GHz, with a trial power of 1 MW and antenna efficiency of 0.9,

$$Q = \frac{n k T \omega Volume}{\beta Power(0.9)} = 2.7 \times 10^9 \beta^{-1} \quad (3.9)$$

Since practical \mathbf{b} levels are a few percent at most, Q has to be on the order of 10^{11} , far beyond any practical level. No chamber could be tuned with such precision, no first surface could reflect that well, and any plasma would disrupt the resonance at once.

In SMC, the ponderomotive force is greatly enhanced at the plasmoid surface where there is both cyclotron resonance and maximum $\nabla \mathbf{E}_s$. The gradient is radial and inwards at the skin. If the \mathbf{B} field is tangential, with a re-derivation, ω disappears after much algebra and only the total collision frequency remains. Taking the decay of \mathbf{E}_s to be exponential into the plasmoid in a hard-edge approximation, with ψ the angle between \mathbf{B} and \mathbf{r} , δ the skin depth, E_o the magnitude of the radial component of \mathbf{E}_s at the plasmoid edge, and z the radial distance into the shell,

$$\mathbf{f}_{\text{NL}} = -\frac{e^2 E_o^2 \exp(-2z/\delta)}{2m_e v_e^2 \delta} \sin \psi \hat{\mathbf{r}} \quad (3.10)$$

Note that $\omega > v_e$ when the fill pressure drops below a few Torr; high temperatures and lower densities dramatically decrease v_e , and thus increase \mathbf{f}_{nl} . Even in this approximate form, it is evident that cyclotron resonance can enhance the ponderomotive force greatly as the collision rate decreases. In fusion conditions, which have very low collision rates and high E_o , the force would be extremely effective at confinement of electrons exactly in those regions where B_{rot} confinement is weakest.

There is a typical density profile from ponderomotive pressure against a plasma surface (“profile modification”, usually in the context of high-power lasers)³⁸ which is derived using techniques of statistical mechanics. The microwave wavelength λ_o is much greater than λ_D , the Debye shielding distance; if extreme conditions result in $\lambda_o \sim \lambda_D$, then the reactor can use longer wavelengths. As a result, charge separation will probably be negligible until the generation of fusion reaction products, which have much higher energies and will cause complications which will alter the equation below. These products must be confined

enough to transfer energy to the plasma and cause ignition, so this is an important matter for future research.

In the simpler quasi-neutral case, taking z to be the radial distance inwards from the plasmoid edge, E_o the magnitude of the radial **E** component at the surface, n_{eo} the electron density inside the plasmoid beyond the skin, T the electron temperature in eV, and $\sin \psi = 1$,³⁹

$$n_e(z) = n_{eo} \exp\left(-\frac{e E_o^2 \exp(-2z/\delta)}{2m_e v_e^2 T}\right) \quad (3.11)$$

Note that if $n_{eo} < n_c = \omega^2 \varepsilon_o m_e / e^2$, the critical density, then **f_{nl}** will cause the surface to go a small distance inwards until **B** drops enough below B_c to weaken the force to equilibrium. If $n_{eo} > n_c$, then the radiation is reflected before $z = 0$ and the surface moves outwards and is not confined. Thus, the limits of confinement for a given T and n_{eo} are derived by setting $n_e(0) = n_c$. As the figures show, the confinement defined by this equation improves dramatically with increased T , without an upper limit intrinsic to the equation. This is due to decreasing v_e and δ as T goes up.

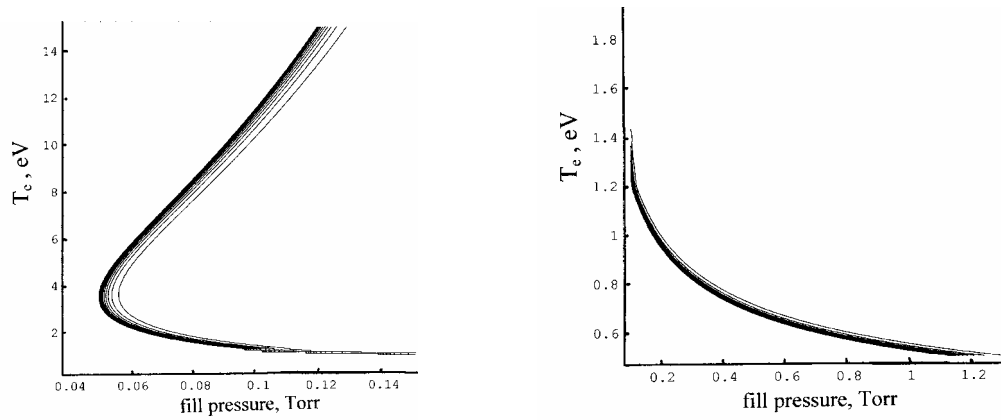


Figure 3.8: Argon confined by ponderomotive force. Contours are density confined, from 10^{21} to 10^{17} from left to right. Area to left of lines is confined for densities above 10^{21} ; area to right and above lines is below the critical density required to reflect microwaves at 2.45 GHz. Vertical axes, T in eV; horizontal, fill pressure in Torr.

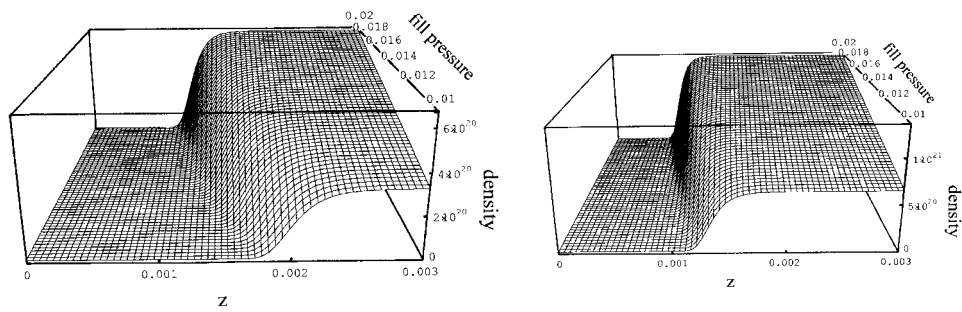


Figure 3.9: Argon and deuterium density profile due to ponderomotive force (**B** tangent to surface) well within confined T and n_e , with plasmoid surface at $z = 0$ (at least for mathematical purposes!). Argon at 20 eV, D at 20,000 eV (profiles change slowly with temperature).

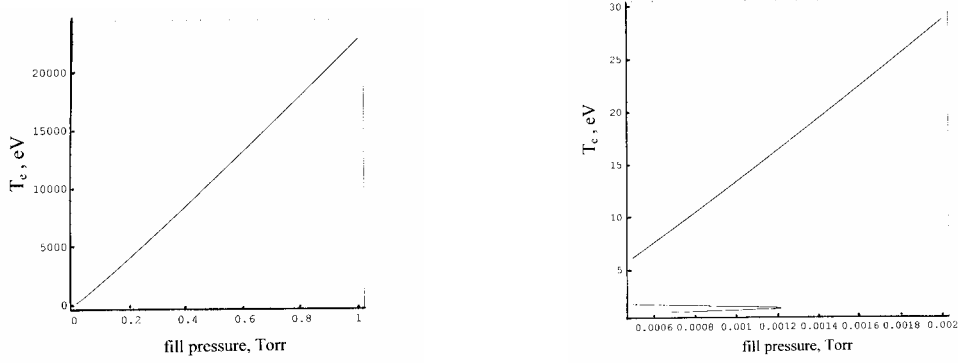


Figure 3.10. Deuterium confined by B_{rot} to left of line. Note very high temperatures required compared to argon.

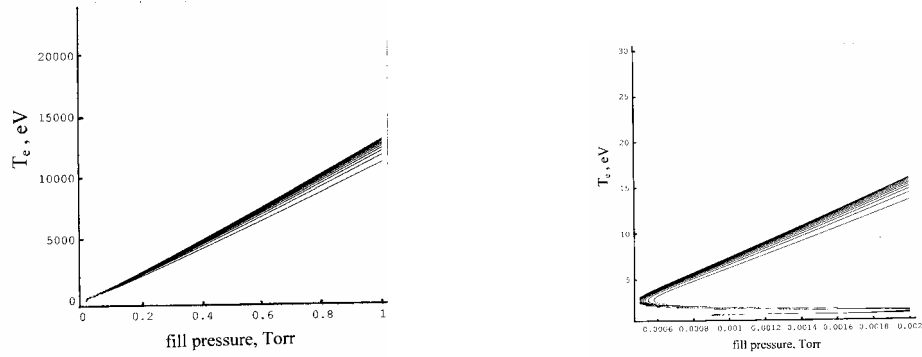


Figure 3.11: Deuterium confined by ponderomotive force, to same scale as Figs. 5 and 6. Densities above 10^{21} are left of lines as with argon; densities sub-critical are right of lines. Note the similarities in shape to the B_{rot} curves.

3.2.3 Existing Experimental Evidence

There was an experiment by Komori et al⁴⁰ in 1990 that was far from ideal for SMC but which showed the effects of \mathbf{B}_{rot} and f_{nl} confinement, although this was unrecognized. They used a Lisitano coil, which is an antenna made from slots cut in a pipe and was originally designed to create a plasma within the coil. Lisitano coils are not helical antennas as used in SMC as the turns are much too close together for an end-fire axial antenna. Their Lisitano coil was transverse to a cylindrical vacuum chamber with a 0.46 m diameter and 1.70 m length that was surrounded by a magnetic coil as shown in the schematic. The magnetic field was a simple mirror with the antenna inside the pinches and which could apply the 875 gauss B_c in large volumes of the cylinder. They used the same frequency and

power as for the SMC test reactor (2.54 GHz and 1.2 kW) and made their plasmas in argon. Their gas pressure was between 3×10^{-5} and 3×10^{-4} Torr.

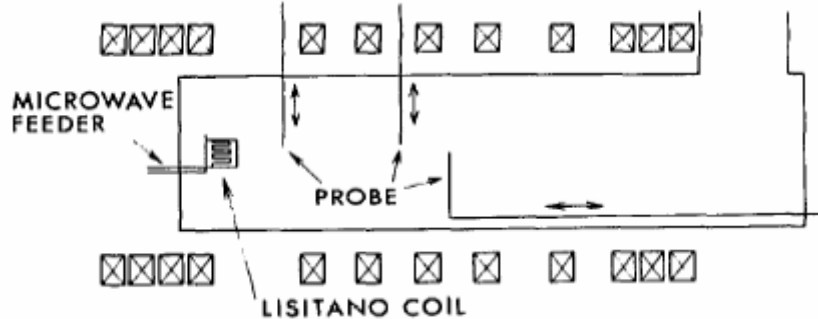


Figure 3.12: (from Komori et al.) Schematic of experimental apparatus.

The resulting **E** field was not circularly polarized but was azimuthal in TE_{0j} modes, which was sufficient for ECR interactions. (Coupling would be much better with circular polarization in the correct handedness to match the **B** field, and without the radial nodes and antinodes of the cylindrical modes.) The area of ECR varied and was of most interest to SMC when it was more than 8 cm. away from the Lisitano coil. In those cases, the plasma was well beyond critical density at ECR, and the space between the coil and the plasma was transparent. There was no tendency for the confined plasma to diffuse towards the region of low density near the coil, which since the coil was between the mirror pinch and the plasma, certainly appears favorable for \mathbf{B}_{rot} confinement at the open field lines.

Along the axis of the plasma they measured the profile modification and E_ϕ attenuation characteristic of either \mathbf{B}_{rot} or \mathbf{f}_{nl} confinement at the coil end of the plasma. They realized the characteristics of ponderomotive profile modification, but when they applied the conventional equation (10), the force was insufficient to explain the density profile. As a result they assumed that the confinement was due to the magnetic field, despite the data indicating otherwise. Had they applied eq. (11), which is appropriate in ECR conditions, they would have found sufficient \mathbf{f}_{nl} to account for the measurements. However the orientation of

the \mathbf{B} field along the axis is more appropriate for \mathbf{B}_{rot} . This is good news since that is more speculative than \mathbf{f}_{nl} .

The plasma was relatively uniform in density within its boundaries and T_e was about 10 eV, with temperature dropping with increased fill pressure. The absorption of the microwave energy occurred well before B_c in the region $0.85 \lesssim (B / B_c) \lesssim 1$, which is very favorable for SMC. Electrons escaping from the plasma surface will have ample opportunity to be confined before colliding with antennas or the wall, even though the B gradient is large enough for a well-defined B_c surface.

3.2.4 Test Reactor Design

3.2.4.1 Antennas

[Note: these early ideas were before any experiment, and relied on information dealing with helical microwave antennas designed for use in air without breakdown, and in far-field. After actual construction, it was clear none of these ideas were appropriate since everything is near-field; also, in low pressure gas in the range of interest, the space inside the helix breaks down first and absorbs most of the energy. Later antennas described after this section addressed these problems via major modifications.]

The antennas are arrayed symmetrically inside, pointing inwards, tapered radially to present the smallest possible shadow on the ground sphere. The proportions of the coil depend on the frequency, number of turns, radius of the outer sphere, and the radiation directionality and gain desired.⁴¹ The circumference of the helix at the center should be one wavelength. The coil length needs to be at least one wavelength long for sufficient gain. One-wavelength antennas will have 4 ½ turns evenly spaced. The thickness of the copper wire is 10 gauge (0.102 inch), which is thick enough for good structural integrity and below the 5% of wavelength limit. The wire is coated with ITC 296A ceramic⁴². This prevents direct interaction with the plasma shell as it implodes past the antennas.^c

^c Experience showed that this particular ceramic was quite unsuited to the purpose, and that any wire so coated must be low-expansion metal, such as Invar.

The distribution of the antennas is icosahedral, at the centers of each of the twenty triangular faces. Future reactors of larger size can use a soccer-ball symmetry, or similar.

The phases of each antenna must be controlled and the microwave source must be protected from reflections. In addition, power must be evenly distributed to each antenna.

The antennas produce primarily an end-fire radiation pattern; the circumference, number of turns, and turn spacing determine how tightly focused the energy is. Antennas of similar helicity will have a phase relationship to ensure as nearly a common direction for \mathbf{E} at the plasmoid in polar and equatorial regions respectively as possible. Tangential radiation for f_{nl} prefers phase coordination between polar and equatorial antennas.

The half-power beamwidth for a helical antenna is, approximately,

$$\text{HPBW} = 52 / [C_\lambda (N S_\lambda)^{1/2}] \quad \text{in degrees} \quad (3.12)$$

with N = number of turns, C_λ = circumference in wavelengths, S_λ = turn spacing in wavelengths. This is for cylindrical and not conical antennas. For the proposed reactor, HPBW will be about 50° , measured from the middle of the antenna. When the plasmoid becomes quite small, direct radiation will be a small fraction of what it receives, but will be a large fraction during most of the implosion.

All the antennas are center-feed with a short tangential stub from the center wire to the beginning of the coil.



Figure 3.13: Early antenna design, before and after mounting in hemisphere (2006)

3.2.4.2 Magnets

The magnets are wound on 3/16" acrylic hemispheres of 26 inch o.d. that are each cut in two sections and mounted on the inner hemispheres. The windings shown in figures above allow for a one inch gap two inches from the equator on each hemisphere. While a smoother winding would have slightly better performance, the gap is essential for access to the inner sphere, and the disturbance is small to the **B** field inside the pressure wall. In practice the windings will be smoother than that in the figures, which assume no width to the coils. The distance between the two spheres is the minimum required to allow organization of the B field into smooth isometric surfaces on entrance into the pressure chamber. The wire will have heat-resistant coatings up to 180° or 200° C. The coils may be air-cooled with compressed air introduced between the two spheres at each pole. Present rough estimates are for several coils powered in parallel at between 5 and 8 kV, but this is subject to considerable change before construction.

The isometric surfaces can only be spherical at one radius. This is chosen to be just within the pressure wall. If the spherical surface were further in, then isometric surfaces further out would be disrupted and not closed, and would be worthless for confinement during the beginning of the implosion. The oblate spheroids formed inside the spherical surface are acceptable for SMC confinement despite irregular reverberation.

Figure 2 shows the target size for the smallest B_c surface. Progressively smaller surfaces require much increased magnet strength since fields cancel more and more towards the center. This reactor relies on supersonic compression and heating to reach maximum density and temperatures; given the efficiency of the geometry, if loss mechanisms are moderate and the confinement is good, quite extreme conditions could be within reach.

Due to the cusp geometry and the shape of the B_c surface, it is important to have coil windings around the equatorial seal of the two hemispheres; thus, each hemisphere's four mountings are two inches away from the equator, made of four flat bars of 3/8" thick aluminum plate. This allows two counter-rotating coils each almost two inches wide over the equatorial seal.

To avoid eddy currents, there was a slot cut in the aluminum hemispheres from near the polar pipes to the edge, which is then filled with epoxy. Also there was insulation in the baffles preventing current from completing a circular path around them. Later, when the magnet was abandoned, I took out the epoxy from the hemisphere slots and had them welded shut.

Access to the interior for probes, video, gas pumping and supply, and so forth is almost entirely limited to the polar pipes, which must be relatively small to ensure the proper shape to the magnetic field. In the prototype reactor I use aluminum 1 ¼ inch nominal schedule 40 pipe. The only other opening is in the thin gap between the hemispherical magnets that allows the coax cables in, which is only about 4 cm wide. It is also quite challenging to devise a flange that can be bolted and unbolted; one of the magnet hemispheres would be removed while the flange is fastened, then the magnet can be replaced. This is a rather major operation since all the fittings on the polar pipe must be removed. Also, the pipe must be completely smooth to allow the magnet to slide on and off, which complicates the engineering for the various fittings that must lead into the pipe under high vacuum. My initial attempts at this involved rubber sleeves that leaked rather badly and had to be abandoned.

The power supply is a capacitor bank supplying between 5 and 8 kV and about 11 kJ of energy with a time constant of a few milliseconds. The shape of the pulse current is critical for maximizing the heating and compression. The imploding plasmoid surface should have a velocity greater than the sound speed of the cold gas or cool plasma within, to form a shock wave; but the velocity must be less than the sound speed in the plasmoid itself. Thus the ramp-up time has to be adjusted to the proper implosion rate. (For hydrogen this would be shorter than 0.2 ms.) After reaching full strength, the current needs to decay slowly enough so that confinement mechanisms can be studied; also, should conditions become extreme enough, longer time constants result in detectable numbers of nuclear reactions. An actual thermonuclear device would almost certainly require superconducting magnets, which would be much smaller and cheaper than those required in standard magnetic confinement schemes.

This concludes the 2006 paper, reprinted with suitable edits.



Figure 3.14: Acrylic magnet spindles; never wound the wire on them

3.3 Construction starts, August 2006

3.3.1 The history of the research continues

My faculty advisor, Dr. David Aspnes, had some spare space in his lab in Research Building II in the Centennial Campus here at NCSU. In August 2006, I started construction. Two hemispheres arrived from Vancouver, and the physics instrument shop welded plate onto them and drilled holes for the antenna feedthroughs. Magnetrons, capacitors, and other gear came in largely from eBay, and the reactor took form—although a very early form, to be repeatedly torn apart and reconstructed over the next three years.

For the first several months of construction, I anticipated winding magnets and fitting them around the pressure chamber as in the original 2006 proposal (section 3.2). However it became obvious, after I had constructed trial spindles for the magnets, that this would be expensive, elaborate, and probably impossible for me to accomplish alone in the time required and with only meagre student loans for financing. After operating the reactor it became clear that my original proposal was entirely too tidy and optimistic, and that the idealistic simplifications would not apply in the real world. The reactor design and hardware

configurations continued to evolve dramatically all the way to the fall of 2009, when active experimentation halted.

3.3.2 Pressure Chamber, Early Version

The pressure chamber is an aluminum sphere. Spheres and hemispheres in the U.S. are available in stock sizes graduated in inches; custom sizes require substantial cost for tooling. The nearest size to the 21.5 inch spherical resonance node for 2.45 GHz is 22 inches, and so in the early days when I was considering resonance, this was a reasonable choice. It allows ample room for one-wavelength long antennas. For strength and to accommodate extra holes, fittings, and changes expected in a prototype, the first sphere has a wall thickness of 0.34 inches (3/8 nominal). The two hemispheres are side-by-side; each mount on strong steel shelving on casters. (A year or so later, I used two 8 foot long channel irons for the caster wheels, which was a great improvement. This guides the wheels in a set track.) The entire apparatus divides into two parts, allowing full access to the inside of the sphere. The hemispheres can be separated from each other and remain rigidly fixed to all attachments, such as pumps, power supplies, cables, grounds, etc. with minimal disruption to connections, and no lifting. Each half of the reactor measures 18" by 36" and is 64" tall, which fits through standard doors. At first, the hemispheres sealed with a neoprene skirt and hose clamps, but this was highly unsatisfactory and could only yield a pressure of about 3 Torr. Later I replaced this with bolted flanges and a 23 inch diameter O-ring.



Figure 3.15: Initial mounting of hemispheres on two shelves, August 2006

3.3.3 Magnetrons

There is a limited range of appropriate wavelengths for SMC in this configuration. Power transmission favors longer wavelengths, while reasonable reactor size and the extreme savings (a factor of up to a thousand) of using 2.45 GHz are major factors as well. With the upper frequency limit of about 5 or 6 GHz for the antennas and the power limits of semi-rigid coaxial cables, the practical frequency range in this type of reactor is from 2 to 5 GHz. The frequency must be high enough to influence only the electrons, and leave the ions untouched due to their higher mass.

The most economical microwave sources, by several orders of magnitude, are 2.45 GHz magnetrons, easily available in 1000 W rated power appropriate for the reactor. This is the only practical option for the test reactor. Dividing power from one magnetron to the 20 antennas is prohibitively expensive in this initial reactor, and results in relatively low power levels if using a household oven magnetron; 20 oven magnetrons of 1000 W rating are far cheaper. Future research, detailed below, will have a far more sophisticated and expensive microwave circuit to maximize the reactor's efficiency. (It is probable that this improvement is required to prove the concept.)

The most difficult aspect of the present reactor is the difficulty in even distribution of power to each antenna. It is not yet possible to test each individual circuit as I do not have a spectrum analyzer or signal generator, or tools to tune each coax cable to the proper impedance. Also, each magnetron requires a current source, and tends to take more current as it warms up. Once the plasma forms, it changes the load impedance seen by the magnetron. A magnetron that draws more current than the others will form more plasma, thus leading to even more current draw, heating, lower resistance, destabilizing the discharge. In this manner, the lack of a matching network severely limited the ability of the reactor to function as all too frequently one or a few antennas would take all the current. The 500 ohm current dividing resistors did not keep the power evenly divided, and on occasion blew up. For now,

coax adjustment to alter the impedance is ad hoc and approximate, and despite much trimming, ineffective.

While I was warned before construction by microwave engineers of dire consequences, in practice the opaque plasma provides ample separation between antennas, minimizing cross-talk and resulting arcs in the magnetrons. This is no longer true above about 200 Torr, far above the pressure range of interest for SMC, but well within range for ball lightning experiments. I also tested CW operation for a few seconds at low pressure with one antenna powered by the usual microwave oven power supply it is designed for, and damaged the test antenna and magnetron severely, as well as the connector just outside the sphere. Thus the present setup is clearly adapted for pulsed operation only, which typically lasts about 0.2 s.

The magnetron power supply is in two parts. The cathode filaments require a HV insulated floating 3 V at 10 A, which can be AC from the center feed of oven transformers. On top of this comes a -6kV pulsed bias from a capacitor bank that decays to -4kV, at which point the magnetrons stop functioning. The peak radiated power in this reactor is about 20 kW minus losses which are not yet measured; future reactors of this size will require much less microwave power.

The magnetrons are connected in groups of five, with one group above and another below each hemisphere. Each group shares air cooling by means of a 24 VDC squirrel cage fan. This is not really necessary since the pulsed operation is much too short for overheating the magnetrons; this cooling functions as insurance in case I forget to turn off the 60 W power to each filament, which is the main source of heat.

The magnetron power capacitor banks connect to the HV cable and magnetrons by means of a HV relay in the control panel, controlled by 110 AC. The current surge is well beyond the design limitations of the relays, which although capable of 12 kV, should not run over about a third of an ampere. As such, I put new contacts on the relays machined from a composite material made from copper, silver, and graphite specifically for electrodes like this. These worked well for the most part; however, EMF interference was always a problem,

even with shielding, from the rapid discharge of such a large capacitor bank and the inevitable sparks.



Figure 3.16: Group of five magnetrons, fan, HV relay



Figure 3.17: The Baffled Bill

3.3.4 *Baffles*

Cross-talk between antennas has a dire effect; microwaves from one antenna go into another, up the coax cable, into another magnetron, and causes an arc that can destroy the magnetron. Initially I tried isolating each antenna by means of thin sheet aluminum, bolted onto the walls via flanges using conductive silver epoxy. In practice, the baffles were not needed when plasma formed and thus shielded the antennas from each other. When the pressure was too high for plasma, cross-talk was severe even with baffles and the reactor could not operate without magnetron damage. Baffles also severely limited the camera's ability to observe inside the sphere, and sometimes suffered arc damage when using the sparker (discussed below).



Figure 3.18: Mounting baffles, and with early antennas

3.3.5 Coax Cable and Connecting Antennas to the Magnetrons

For economic reasons, and also since several fittings are custom and not commercially available, I have made coax connectors and adapters by hand for each of the 20 antennas and magnetrons. There are inevitable reflections and losses, not to mention leaks, in the circuit that would require several thousand dollars of equipment to avoid and correct. The reactor works reasonably well at the intended pulse duration, but it cannot be considered anywhere near to optimal in safety and efficiency, and cannot be run CW. Each magnetron produces 1000 W; this is within the power rating of the coax cable, but only standard connectors would be durable and reliable even with pulsed operation (at the usual 0.2 s).

The first connector required for the 20 magnetrons lead from the antenna stub usually used to feed microwaves into the oven waveguide, into the coax cable instead. This required an inner and an outer cone, proportioned for 75 Ohm impedance. The cable connected by sliding the inner connector into the inner cone and squeezing the outer shield onto the outer cone with a hose clamp and conical aluminum pieces. This technique worked very well and proved durable, with no evidence of leakage or damage over three years of operation.



Figure 3.19: Inner and outer cones connecting magnetrons to coax

I had significant problems with my connectors at the antenna feedthroughs charring and even sometimes igniting. Unless I coated the connectors with aluminum foil, significant RF noise interfered with the video camera. At first the empty space inside the feedthrough connectors were filled just with hot glue; after several surface breakdowns and a lot of soot, I coated the surface with a layer of porcelain (unfired) and BN ceramic paint. This helped a lot but was not a total cure. When the connectors had a reasonably divided power, they held up well; but when one magnetron sucked all or most of the current, failure was inevitable. The design challenge was that the antennas had to screw in from the inside of the sphere, but connect on the outside; most connectors require a 90 degree turn very close to the sphere to allow for the magnet spindle (such geometry is very handy even without the magnet as it allows a spherical shield). Even a commercial connector would suffer some reflections under these design constraints. My preferences would be to have a permanent feedthrough connector mounted on the sphere to which the antennas would connect on the inside, and the coax would connect on the outside, without ever disturbing the vacuum seal.



Figure 3.20: Feedthrough connector

As the intrinsic impedance of helical antennas in air, with a ground plane but otherwise unobstructed, is about 150 Ohms, I used 75 Ohm coax cable and appropriate dimensions in the feedthrough to lessen impedance mismatch. However, these antennas do not operate in open air; with the baffles, the impedance without plasma is probably close to 75 Ohms. Once plasma forms, I really don't know what impedance the antenna sees as load; it must change a great deal over short time scales. I do not have the required equipment to directly measure these things. The later antenna models, described below, dealt with these issues by trial and error, and eventually behaved as desired.

3.3.6 Video

The only diagnostic tool I had was a video camera. At first I used an elderly camcorder from the tape era, which worked well at first. I could arrange its settings and turn it on and off from the control panel by means of its power supply. However, due to a severe leak of the microwaves (whose source I discovered only after more than a year of operation), the power supply fried, and I had to rely on its own battery power. As such it would cut off on its own after five minutes, requiring much travel back and forth from my control seat. (I ran the reactor from several feet away as it was quite dangerous.) I shielded the camera in a Faraday cage made of perforated aluminum sheet metal, but this was never sufficient to prevent periodic outages and severe static on the recordings. Below I detail later cameras and improvements.

When first designed, with hemispherical magnets surrounding the pressure chamber, there was no access to the interior except through the polar pipes and the very thin gap between magnets (about 4 cm). The first design for video was by means of a fiberoptic borescope; I could get an affordable model designed for general use and with barely adequate resolution. Much more elaborate borescopes for use in medicine are far too expensive. Borescopes have excellent characteristics for this use; they have an internal light source, are (or can be) inert to microwaves, completely shield from x-rays, and the more sophisticated models can change their direction of view remotely.

My attempt to use the borescope ended badly since the vacuum pressure distorted the optical cable, leading to irreparable failure to focus. About that time I abandoned the magnets which allowed me to make a window on each hemisphere. The first windows were hand-made from $\frac{1}{4}$ inch acrylic with neoprene gaskets and four bolts epoxied into their holes. I used these until I moved the reactor to Duke in early 2009 and was able to find out what I had suspected, that they leaked.



Figure 3.21: First camera mount on monopod (minus Faraday cage) showing early plumbing

3.4 Early Plasmas (2007 through summer 2008)

3.4.1 Improvements to the Pressure Chamber

The early plumbing used hardware store gear with PVC fittings, hose clamps, stainless and brass ball valves, reinforced flexible vinyl tubing, and lots of plumber's sealant. Oddly enough, much of this proved to be secure from leaks within the detection ability of the leak chaser I used at Duke in 2009; parts of the system also held pressure to the limits of the roughing pump (20 mTorr) without indication of leaking. However there were deficiencies in the overall system, and I later replaced all of the plastic parts with KF-25 metal flanges and stainless flexible tubing. The plastic system was very handy when using the sparker as it allowed access through the polar pipe on the South hemisphere (the side opposite the pump). The main advantage of switching to all-metal plumbing was the ease of changing the setup without having to worry about leaks, and the ability to join to standard vacuum gear (such as the thermocouple gauge and turbo pump).

The early sphere relied on a neoprene sleeve and very long hose clamps to seal the equator. Clearly this was highly deficient; the original incentive for doing this instead of a flange with O-rings was that the connection needed to be secured underneath the magnets. However with the passing of the magnet concept, the virtues of this primitive system evaporated. In 2007 I dismounted the hemispheres and brought them over to the Instrument Shop in the basement of Cox Hall where much vital work has been done on this reactor. They added a flange on each hemisphere and a groove for a 23" diameter O-ring.

My initial feedthroughs for the antennas was simple rubber plugs inserted in the 3/8" thick aluminum wall through half-inch holes. While this was handy in some respects, allowing a certain flexibility with the antennas and preventing cracking of the ceramic during the inevitable bumps, it was hopeless to try and get pressures lower than 3 Torr. Finally in February 2008, I replaced the rubber stoppers with brass bushings and threaded the original holes from the inside with plumber's tapered thread. The 10 ga. copper wire at the base of the antenna fed through machinable ceramic epoxied into the bushing. This allowed a length of bare wire ½ inch long to protrude outside the reactor wall for connecting to the coax fitting.

Originally I used teflon-based plumber's sealant to improve the performance, after Teflon tape proved a failure; however I rapidly realized that it was imperative that the bushing have a good electrical connection to the chamber wall. Thus I converted to a copper-based conductive sealant with a silicone grease base that would never harden.

With these two simple changes, and the original helical antennas, I was able to reach pressures lower than at any other point in the experiment—all the way down to 16 mTorr, essentially the limit of the roughing pump. Evidently the homemade windows must have sealed well in the beginning, since they leaked badly by 2009; to be fair, I had to remove and remount them a couple of times, which couldn't have helped. Still, it is surprising that the initial reactor with just these simple improvements, while retaining some very approximate equipment, performed better than the much better reactor of later times. Much of this was due to the improved antennas, which could not be made free of outgassing given the budget restraints.

The baffles were quite difficult to build and obnoxious to use, as they obstructed the view. I was not convinced that they were required to protect the magnetrons. I especially tested this at higher pressures where the limits to the magnetrons lies, and found no difference with or without baffles as to the point where magnetrons could no longer function or would be damaged. I did notice at the relatively high pressures of the time (2 to 3 Torr, at the most prone to easy breakdown) that the plasma was less bright without the baffles. In fact under conditions where the video camera whited out with the baffles, it did not without them. Thus there might be some advantage to using them, but I did not have the capacity for plasma diagnosis that would clarify this point. Also I never had the chance to try the baffles at lower pressures. I was quite happy to discard them, and do not feel that they will play a part in any future designs.

An important addition starting in December 2007 was the grid; this merits its own section below.

The original shelves rested on hefty wood bases and four casters for each hemisphere, all of which freely swivel. My original thought was that this would allow easy adjustment in

position and rolling together and apart. This proved quite overly optimistic, since the minor motions required to line up the hemispheres had to contend with the swiveling of the casters. Finally I realized that putting the casters into two channel irons would simplify matters greatly. I got two eight-foot lengths of steel channel irons just big enough to fit the caster wheels. This was an enormous convenience and most certainly will be repeated in the event of future reactors.

3.4.2 *Sparker*

For initial plasma formation and introduction of experimental aerosols (vaporized organic powders), I used a miniature coaxial plasma jet at the end of $\frac{1}{4}$ inch outer diameter stainless tubing about 65 cm long. The inner electrode was a 5 inch long, $\frac{1}{16}$ inch diameter tungsten welding rod, with the cavity at the last half inch, the rest sealed with a low-temperature glass frit backed up with porcelain. The current pulse (negative from the capacitors) went along the central tungsten electrode, through the target material placed in the end (organic powder with carbon dust), and back through the stainless tube to ground outside the sphere. It ran in the south polar pipe and just past the inner baffles, carefully insulated from all metal contact, since any path to ground besides the intended one eroded a good deal of metal by intense sparking. The tube could be removed and reloaded with new powder between discharges with tolerable gas leakage (a few Torr starting from 3 Torr) by sliding it past a greased O-ring seal and then closing a ball valve. It had a capacitor bank pulsed power supply of 417 nF and no more than 2000 V. Higher voltages decreased the effectiveness of the sparker, require larger and inconvenient dimensions. For the initial tests, the sparker and magnetron capacitor banks fired simultaneously, but the sparker burst was over before the microwave power started any breakdowns. I first used an inductor made by connecting the HV secondaries of three oven transformers in parallel, then leading to a potentiometer for tuning the time constant. This gradually increased the power to the sparker relay until it triggers, allowing fair control of the delay between the magnetron and sparker capacitor bank discharges. I added a timer relay in 2008, and a pulsed timer relay in 2009.

However, it was never possible to coordinate the sparker with the magnetron pulse, as the magnetrons fired in a non-linear manner and so the timing was not predictable.

The tungsten electrode tends to warp after repeated use, and cannot be bent back to a central position without breaking. Later models used a 1/16 inch stainless rod that showed more erosion, but did not warp and could be bent to adjust its position.

After several months of experimentation, I found that a mixture of flour, charcoal dust, and agar powder packed into the sparker tip could give about a dozen bright discharges of impressive power without reloading. When tested in air outside the reactor, the sound was as loud as a rifle shot. Such tests were hazardous to the other equipment in the lab due to the EM pulse, so most of the shots were inside the sphere.

While there are aspects to the sparker design that are appealing, it does not suffice for a BL reactor in initiating a plasma. The explosion from the sparker flies out with considerable speed, supersonic for a few centimeters, and the residue continues on past the center. This does not result in a stable plasma after reacting with the microwaves due to the initial velocity and momentum.



Figure 3.22: Mounting for sparker, allowing entrance through South hemisphere polar pipe

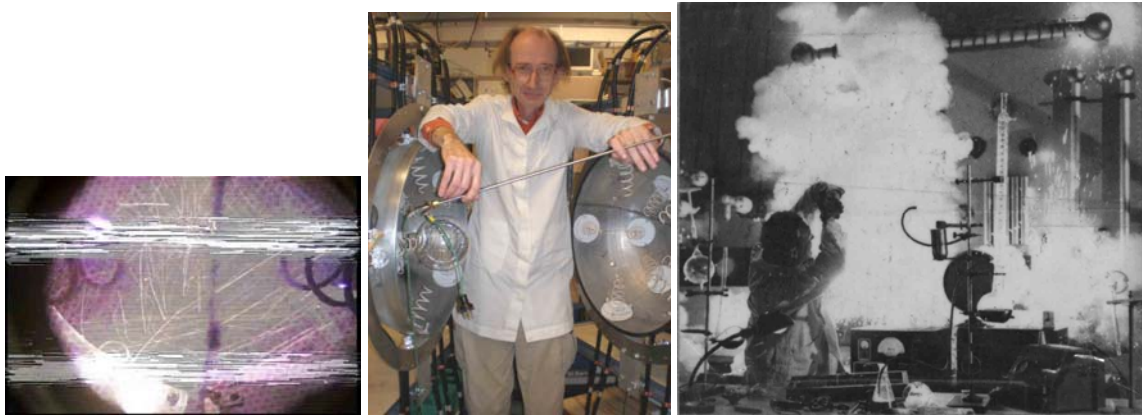


Figure 3.23: Sparker in action (October 2007), the sparker tube, and the biopic version

3.4.3 *Thoughts about BL Fuel*

My experiments included projecting a plasma formed from organic material shot from the sparker into various gases. This is because soot and aerosol are evident in many BL sightings, and from reports of acrid odor, typically of ozone or rotten eggs. The only available solids in air that would make soot are living things. Thus, I took the novel approach of using ground-up insects and other similar material in the miniature coaxial sparker mentioned above. This deposits glowing sparks explosively to form targets for the microwave pulse.

One disadvantage of the sparker is that the resulting blast has no coherence and consists of thousands of individual incandescent particles that fill a large proportion of the reactor volume. It may be that the desired plasmoid forms better with a more centralized single initial target. If this is the case then positioning such a target can be somewhat problematic. A sparker tube cannot be expected to penetrate close to the center as it is far too disruptive, and was limited to firing in from no more than halfway to the center. If the target must be vaporized to the point of being a seed plasma, then it could be suspended by wires thin enough to not interfere with the reaction but thick enough to not explode under the current pulse. This would be acceptable in a research reactor but is clearly not feasible for any power reactor, as shown in plans for fusion reactors. The pellet might be intrinsically

explosive and detonate either from the microwave pulse or an electrical trigger. For instance, a very fine wire coiled and coated with black powder or other thermally sensitive explosive could be at the center of a pellet; when the wire heats from the microwaves, the black powder would explode and could in turn detonate a coating of high explosive mixed with any test material. Alternatively a pellet could be shot into the center with a gas puff valve, timed to reach the center with the microwave pulse. This is something like the pellet technology of Inertial Confinement Fusion reactors. However this would be a strain for the current research program in terms of expense and complexity, and was far outside the limits of what I could build.

Another consideration in case a stable plasmoid develops is adding fuel while it is fully formed, instead of waiting for it to decay and forming another with fresh aerosol. This would be advantageous since the input power is entirely in formation of the plasmoid. The observed lifetime of natural BL is highly variable and probably has something to do with using up whatever fuel drives the reaction. Thus, to have a longer lifetime, more must be added, if possible. This fuel might be in the form of pellets to penetrate into the plasmoid, in the manner of feeding magnetically confined fusion plasmas with frozen hydrogen isotopes, or it might be better introduced as a spray of dust that is easier for the plasmoid to heat and incorporate into whatever process may be going on. Another possibility is an aerosol of particles fine enough to be easily suspended, such as thick smoke, that circulates through the reactor and is consumed by the plasmoid. Substantial mass is impractical to deliver in the form of smoke, vapor or gas, while powder on the order of a gram can fit in a sparker or a pellet. Liquid spray might also be possible and could deliver mass comparable with solids, but are limited in terms of possible operating pressures and temperatures external to the plasmoid.

The optimal gas pressure is entirely unknown. The most powerful, long-lived, and indisputably witnessed BL in history was the result of an undersea volcanic eruption in Japan. The huge plasmoid lasted over two hours, was many meters across, and terrorized an entire village. This implies that pressures in excess of atmospheric may be quite favorable for

power production and duration. Organic matter is unlikely in this case. The existing seals on the antenna through-hull fittings used in 2007 could not sustain positive pressures since they were simple rubber stoppers, and substantial positive pressure would also harm the windows as configured then. In early 2008 these stoppers were replaced by brass bushings.

3.4.4 Glass globe and carbon veil (December 2007)

The sparker technique did not form the kind of seed plasma that I had hoped for; even with very fine particles, the ejecta in partial vacuum was dominated by discreet sparks instead of the more generalized glow seen at atmospheric pressure. Since the material started off at supersonic velocities, and had less drag from gas than usual, the resulting ejecta transited the center very quickly, not giving the microwaves a chance to interact with it. In addition, it contaminated the chamber walls and antennas, although at this stage of very rough vacuum this was not a large concern. It did mean that the sparker experiments were incompatible with the other SMC runs requiring much higher vacuum.

My first attempt at containing the plasma was with a spherical 2 liter flask, seen in Figure 22. The intent was for the sparker to discharge into the flask, which would contain the ejecta long enough for the microwaves to interact with it. It was only possible to operate this at very modest pressures below atmospheric due to sealing difficulties. Also, I had to be very cautious about the power discharged by the sparker; a full blast at relatively high pressures (say, 200 Torr) would burst the flask. While the flask did solve the problem of contaminating the chamber with burnt ejecta, it does not appear to have functioned adequately in localizing a central seed plasma. The Pyrex was rather thin; to more fully investigate this method would require a hefty wall thickness capable of withstanding serious shocks. As the neutral gas accentuates the transmission of the impulse to the glass, full power operation requires relatively low pressures. I used 3 Torr as the minimum I could get at the time, but would prefer less.

I saw on several sites on the internet advice on various entertaining objects that formed dramatic plasmas when put into microwave ovens. The most recommended material

for the “ball lightning” experiments (far from natural BL but fun nonetheless) was carbon veil. This is a thin mat made of fine, randomly oriented carbon fibers, used in composite structures. By itself, it is very weak, and I needed some kind of framework to put it on. I ended up constructing a geodesic sphere of stainless wire, and wrapped the veil around it. To place it in the 2 liter flask, Dr. Aspnes sliced it in two with his diamond saw, and I epoxied PVC flanges to both hemispheres. This allowed placement of large objects like the wire/veil geodesic into the flask. The results were entertaining but not helpful. At the time I was having terrible problems with video interference, which worsened dramatically with increased pressure. Low pressures (the 3 Torr limit as used with the sparker) resulted in little glow with any material; higher pressures created brighter plasmas up to the limit tolerated by the magnetrons. While higher pressures showed copious plasma formation right on the test materials, there was no plasma whatsoever away from them. (For the record, fine steel wool was useless, and the carbon veil worked quite well producing a bright plasma on its surfaces.) Clearly the use of these solid substrates at pressures not much reduced from atmospheric did not lead in the direction of BL.

3.4.5 Grids and ceramic coatings

The basic justification for non-magnetic SMC was that the antennas would cause a non-neutral plasma, even if only on short time scales, in the center. This was rather hard to justify unless there was an electric field serving to help accelerate electrons preferentially towards the center. Also, with lower pressures came increasing difficulty producing opaque plasma quickly enough to ensure protection from magnetron damage; a ready supply of free electrons would hasten breakdown. To answer both these concerns, I added a grid at the base of the antennas, about 1” from the wall, charged at voltages up to -6kV. (This limit was handy since the magnetron capacitor bank already was at -6kV, insulation to that voltage is not difficult or excessively bulky, it is simple to use electrolytic capacitors in series to reach that voltage, and it was sufficient to produce copious plasmas at the pressures of interest reached by the reactor.) To ensure that the grid did not simply short out to the wall, I coated

the inside surface of the reactor with ceramic insulation. The only exposed grounded conductors were at the inner tips of the antennas, where the shields were free from the surrounding ceramic or epoxy (depending on the model). This provided a current of electrons moving inwards from the grid to the antenna tips. There was some video evidence that this current overshot the antenna tips and provided a space charge beyond the tips a few centimeters towards the center; this was rather faint and only visible after the bright glow from the magnetrons subsided, and if the pressure was at the lower end of the experimental range (below 50 mTorr).

As with most other features of this reactor, I did not simply build an optimal system all at once. Instead, there were several incarnations of both the ceramic and the grid. The first system was without a ceramic coating. I used teflon disks with thin stainless wire supported by nylon machine screws and nuts. There was a bright glow around the wire, but I felt that the small radius of curvature of the wire was making the field too strong at the grid. The Teflon disks did not stop strong plasma formation and charring at the wire entrance and between the disks and the wall.

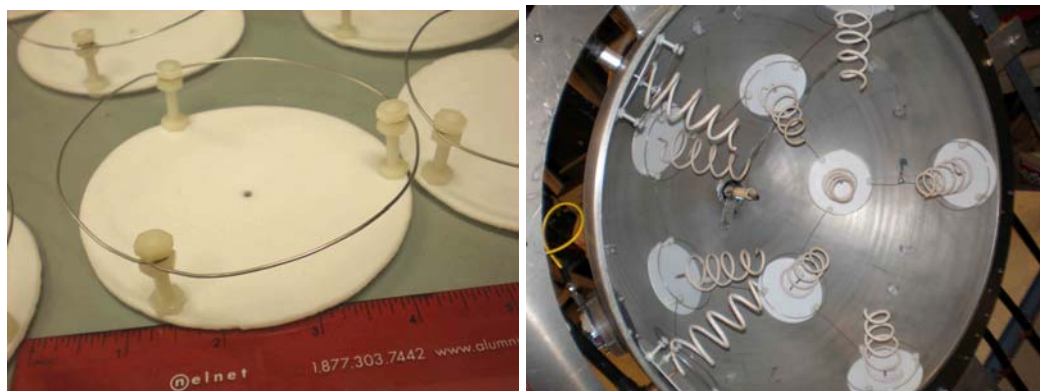


Figure 3.24: first thin wire grid and installed; showing sparker entering reactor at pole



Figure 3.25: thin wire in operation; replacement with sheet stainless circles

I replaced the thin wire grid with one made of 1/16" thick stainless sheet metal with rounded edges to make less localized breakdown; however this was clumsy and did not solve the problem of shorting to the reactor wall. Therefore the next step was to coat the reactor with an insulating layer. My first attempt at this was to use ceramic paint that required 90 degrees C for a few hours to cure. This turned into a nightmare as it refused to adhere sufficiently to the aluminum, and peeled off after heating. I ground off this paint (which adhered mightily on many places) and tried again with manifold paint bought at the local auto supply store. This also did not work. After grinding that off, I spray-painted the water-based ceramic that originally coated the antennas. While this looked promising at first, it turned out even worse. In use it released considerable dust, which then went into the mechanical vacuum pump and, over time, corrupted the oil, turning it into a thick goo well beyond my capacity to clean and repair. Thus, once again I had to grind off the ceramic. The final coating was with ZYP BN (boron nitride) hardcoat paint which worked very well. This paint is hard, shows no sign of outgassing, adheres strongly to the aluminum, releases no dust, provides adequate electrical insulation, and shows no damage from the plasma. It also did not require any heat curing. As the aluminum sphere stays at about the same temperature, there is no problem with cracking due to expansion. Any future reactor that gets hot will have to deal with this difficult design problem if insulation is required.

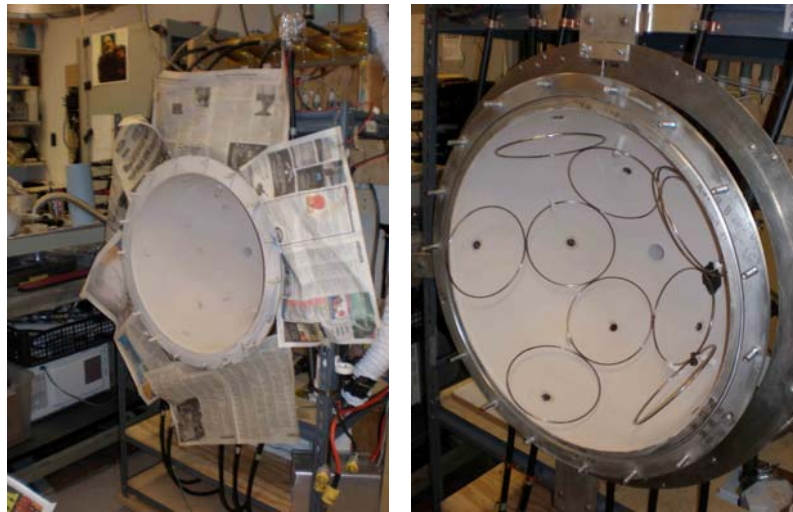


Figure 3.26: water-based ceramic spray job; final grid installed

After I had sprayed on the water-based ceramic and before the BN, I discarded the teflon disk idea, since such insulation did not work and would not be needed now. Instead of having the grid so close to the first turn of the helical antenna, I used circles of 10 ga. stainless wire spot-welded into arrays of ten, one for each hemisphere. These provided a potential equidistant from each antenna and as far away from each base as possible. The circles were mounted on machinable ceramic stand-offs so that the closest approach to the chamber wall was one inch. Later I reinforced the spot-welds on the five equatorial rings since their single attachment was tenuous. This grid works splendidly; the larger wire radius proves capable of a non-localized discharge until the pressure rises above 1 or 2 Torr, when the corona glow closes in around the wire. Ideally there should be no tight angles as there are where the circles meet, and my method for attaching the wire lead from the outside has some angular surfaces that should be smooth. It might be superior to have a more geodesic style of grid with straight sections welded together at the vertices. This would allow use of tungsten or other non-malleable refractory metals. For this experiment, stainless steel sufficed and showed no wear after heavy use. This final grid design is mentioned again in Section 4.2.2.2.

3.4.6 Solid Antennas; Mark I up to early Mark II

Initial tests were with a helical wire coil (the Mark I antenna) coated with a couple of millimeters of ceramic, designed similar to customary microwave antennas that give end-fire circularly polarized far-field radiation in atmospheric air. However these antennas ionize the low-pressure gas immediately and most intensely inside the coil; most of the radiated energy went to the plasma inside the antenna and at the base. This is highly undesirable. Also the gentle, radial taper of the first antennas is not suited to the near-field operation and electron acceleration. There were frequent scorch marks around the base of the antenna on the inner wall of the chamber.

I tried several approaches to keep plasma from forming prematurely at the base. The first was by fitting circular sheets of polycarbonate about three inches around the base of each antenna. (These can be seen in Fig. 24.) Shortly after fitting these on I mounted the first version of the grid on these circles, first with thin stainless wire and later with stainless sheet metal cut into circles. However the polycarbonate did not suffice and the wall still showed burn marks. Also, the volume inside the coils was where the brightest and longest-lived plasma formed, completely contrary to what the reactor needed.

During the summer of 2008, I used polyclay, a kind of moldable PVC putty that cures at about 140 F, to fill the insides of my Mark I antennas. It turned out that even though PVC is mostly, but not entirely, inert under microwaves, this PVC putty definitely absorbed the energy and burned, even after curing. All was not lost, however; I used the new solid antennas to test the general concept. I coated the outside of the plastic with high-temperature silicone, but this burned readily and was a poor substitute for ceramic. The microwave energy still came out at the base, even worse than before.

I then put several different patterns of aluminum foil and aluminum tape on the outside of the sold antennas, grounded at the base, with substantial aluminum around the initial antenna stub, to try and get the plasma to form all over the surface of the cone. After some trials I came up with the pattern that proved effective. Fig. 26 shows one experimental result, tested in air at 410 mTorr. The first picture shows antennas where the helicies are

filled with polyclay, then coated with high-temperature silicone caulk (which didn't work well!). The two antennas in the center were modified; the top has truncated triangular aluminum on the outside connected to ground, while the lower central antenna has similar shielding but with an outer layer of ceramic composite, primarily silica. While all the other antennas tended to produce plasma at the bases, the one with both shielding and ceramic overcoat produced plasma evenly distributed over the surface of the antenna. This was exactly what I was looking for, and so this was the basis for the design of the next antenna model.



Figure 3.27: Polyclay unshielded, shielded, and shielded coated with ceramic (lower center)

The Mark II antenna was the result. It solves all the problems of plasma formation and, in its latest form, survives service without damage. It functions well in the current reactor setup. The antennas are not ideal; the materials had to be compromised from what would be the first choice from cost and manufacture considerations.

The coil is conical, one wavelength long and 3 inches in diameter at the base. By casting the coil in solid epoxy, there is no chance of internal plasma formation. Over this plastic cone is an eighth-inch gap, initially filled with ceramic composite, followed by a copper sheet metal sheath made of eight triangles. This sheath protects against leakage of all the power at the base, and gradually tapers to fully open at the inner tip. By a long transition from coaxial geometry to bare wire (under dielectric), a full range of impedances occur along

the antenna length, matching whatever external conditions apply. The shield ceramic composite proved terrible for outgassing and had to be removed later.

At the tips of four of the shield triangles, brass electrodes protrude through the insulation. These form the grounded contact for the current from the grid. Brass is not the ideal metal, as it should be more refractory and less potentially chemically reactive with various gases, but it was much easier to fasten (by soldering) to the copper shield. Copper oxide formed after operation but not enough to hinder functionality. Future electrodes in this type of antenna would be something like tungsten spot-welded to low-expansion metal coated with ceramic and heat cured as a solid block.

The net result of this design, when tested as low as 20 mTorr, is a plasma that forms evenly over the surface of the antenna and extends out a few centimeters. The previous problems of plasma formation only at the base or inside the coil were solved immediately. There remained problems of feedthrough leakage, surface damage, and outgassing only effectively addressed in the spring and summer of 2009; these factors can only be fully cured by using much more expensive materials and with sophisticated fabrication beyond the scope of this research. The earlier record low pressures (15 mTorr) reached with just brass bushings and the simple helical antennas, with just the roughing pump, could never be matched with the Mark II antennas even with a turbo pump.

4 Chapter 4

4.1 *Later History of the Research (fall 2008 to Summer 2009)*

It became clear that there had to be a bifurcation between the BL trials, which were at a wide range of pressures and tended to be quite dirty, and the low-pressure SMC experiments. The two simply could not be alternated with any regularity, as the gear became quite different and incompatible. As I had no evidence of anomaly yet in the BL trials, I decided to convert to SMC only. This required finding and fixing leaks, which was an extended and difficult procedure over a year and a half. As I no longer was using magnets, it became attractive to see if Inertial Electrostatic Confinement could be enhanced and made to

operate without a grid by means of this reactor geometry. While at the end of this attempt the question remained open, I no longer believe this can be done. After August 2009 I converted the experiment back to BL.

4.2 Non-magnetic SMC as a kind of IEC

4.2.1 Confinement Mechanism

There follows a discussion of the theory as I understood it at the end of 2008, when I was proposing relocating the reactor to Duke to use the neutron-shielded target room at TUNL. Afterwards I explain the more current ideas of why radiation pressure and the ponderomotive force (without ECR) cannot enhance IEC to any worthwhile extent. However, the ponderomototive force and other effects with ECR, and hence the original magnets, is very promising, along with other effects that could make SMC work well. The magnets are incompatible with IEC.

4.2.1.1 Inertial Electrostatic Confinement

Here is a brief introduction to basic IEC ideas, especially those relevant to SMC. There is a large body of information now on the internet, especially due to amateur interest and experimentation, for those seeking more detail.

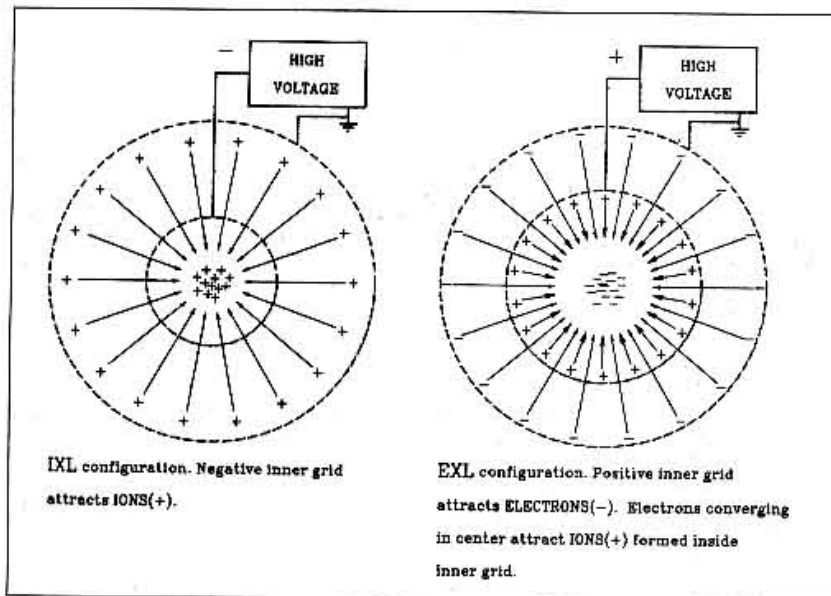


Figure 4.1.⁴³ The two basic spherical convergent focus fusion methods.

Plasma confinement, as defined by keeping the plasma physically separated from walls in a closed body, cannot be obtained by static electric fields alone. By use of a charged porous “wall” inside the plasma, an inner grid through which charged particles flow, a ballistic confinement can work. This is at the cost of losses to collisions on the grid and current losses from putting a potential across the conducting plasma. (This is still not true confinement since the plasma is not separated from the inner grid; I do not discuss here variants that try and protect the grid.)

As shown in Figure 1, there are two varieties of IEC. Ion accelerated (IXL) has the inner grid at negative voltage, causing a “virtual anode” at the center. Electron accelerated (EXL) has the inner grid at positive voltage and creates a virtual cathode at the center. This is a highly idealized view of a much more complex situation; angular momentum builds up inside the inner grid, especially among the electrons, leading to a double-well potential instead of a single focus.

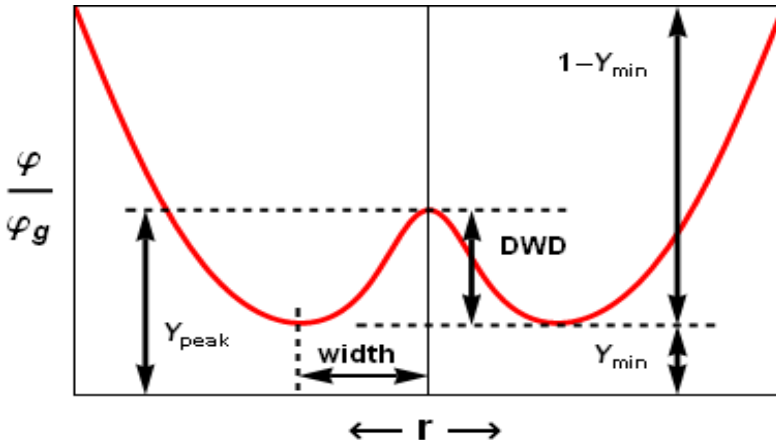


Figure 4.2:⁴⁴ Double well potential structure. The double well depth (DWD) is $Y_{peak} - Y_{min}$. Here, Y_{peak} coincides with Y_{core} . A double well is much more likely than a single well.

There are remarkable advantages of IEC over other fusion techniques. There are no magnets, which simplifies, shrinks, lightens, and cheapens the reactor by orders of magnitude, as well as avoiding synchrotron and magnet power losses. Very high temperatures are easy to obtain, and the geometry is simply-connected and convenient to build and maintain, unlike toroids.

However there are fatal disadvantages that are intrinsic to the design. The net reaction rate for any fuel in IEC is inversely proportional to both pressure and volume, which means that peak power is at densities far too low for power generation even if everything else worked perfectly. IEC reaction zones are typically about a cubic centimeter at the center, far too small for a reactor where plasmas are typically measured in cubic meters. (The upper limit for power in a thermal cycle is 100 W cm^{-3} .) The best power gain so far (Q) is about 10^5 . This can result in a good neutron source when using either D-D or D-T fuel (2×10^{10} at best so far) but this is about 10^7 too low for a power reactor.

Due to the way the potential is generated, the power scales as $1/a$ (with a = radius of plasma focus where most of the reactions take place) and also as $1/n$ (n = plasma density). Both of these factors are sufficient to rule out IEC for fusion power reactors.

The argument for scaling power as $1/a$ goes something like this. The applied potential on the center grid is balanced by the cloud of (roughly constant density) electrons that, being spherically symmetric, creates its potential at the surface of radius a , $\phi = Q/(4\pi\epsilon_0 a)$; and

$$Q = en(4/3)\pi a^3 \quad (4.1)$$

so $\phi \sim na^2$, in turn meaning that $n \sim \phi/a^2$. And since the power $P \sim n^2 a^3$, the result is that power goes as $1/a$. [The hope was thus to use SMC in some way to avoid these scaling factors, since the charge concentration is not obtained by the same mechanism. The eventual conclusion, stated in detail below, is that confinement is not possible using just electric fields even with microwaves and other variations, scaling factors or no.]

Collisions with grids are also prohibitive for power production; in terms of power loss, $P_{\text{gridloss}}/P_{\text{fusion}} > 3000$.⁴⁵ Ion upscatter and energetic tail loss time is about 1/1000 of the fusion rate; for both ions and electrons, the loss times are much less than the fusion time. There are substantial losses from ion-neutral charge-exchange collisions, where a hot ion takes an electron from a neutral atom and then, having no charge, is not confined. The plasma cannot ignite, in the sense of fusion products heating the fuel plasma, since the energy of the products is far greater than the potential well and they escape quickly with few collisions. The potential is created by a non-Maxwellian, non-equilibrium plasma; but this requires Coulomb collision losses far outstripping energy gained by fusion to sustain. Bremsstrahlung is the same or worse as in other reactors, which makes advanced non-neutronic fuels impractical, despite the attractiveness of the easily achieved extreme temperatures required (several hundred keV).

One interesting attempt to improve the situation is by means of the Periodically Oscillating Plasma Sphere (POPS), now being investigated at Los Alamos by R. A. Nebel and his team.⁴⁶ The ion cloud oscillates collectively due to the virtual cathode with this frequency;

$$\omega_{POPS} = \sqrt{\frac{2e\phi_o}{r_{VC}^2 m_i}} \quad (4.2)$$

Here, f_o = potential well depth, and r_{vc} = virtual cathode radius. POPS uses RF modulation of the grid voltage matching the ion oscillation frequency to preferentially heat the hottest ions, as well as greatly compress then expand the plasma, leading to adiabatic heating and fusion-relevant densities. Thus some ions are expelled, deepening and prolonging the potential well. Also, beneficially, POPS appears to aid in thermalization, thus minimizing Coulomb losses, while still allowing the small charge imbalance required for the virtual cathode or anode. (This space charge can limit the central density.) While the existing experiments show the concept is valid, the experimental RF voltage swing is on the order of hundreds of volts at pressures of $(0.1\text{-}10) \times 10^{-6}$ Torr, three orders of magnitude below practical fusion plasmas. The swing must be of kV in order to achieve volume compression ratios of about 50 for D-T, and 2000 for D-D fusion, for break-even in IEC reactors (other factors being optimized). It is highly unlikely that such RF voltages are possible, and certain that the power required would make a reactor far below break-even.

4.2.1.2 *Spherical Microwave Confinement*

A spherical chamber holds at least 20 inward-directed conical, helical antennas that radiate near-field 2 to 5 GHz microwaves into opaque plasma, much like magnetic SMC. Each antenna is designed to distribute energy evenly along its surface into the plasma by means of an inner coil surrounded by a metal shield gradually opening from base to tip. The variation in shielding provides impedance matching over a wide range of loads. All the metal is embedded in ceramic except for the inner tip of the shield. At the base of each antenna is a grid, a small distance from the insulated wall, charged to -6 kV or more. This external grid causes initial breakdown in the plasma and facilitates microwave-induced plasma formation up to opaque densities ($n > 7.45 \times 10^{16} \text{ m}^{-3}$ for 2.45 GHz microwaves). The opacity of the plasma lessens cross-talk between antennas and assists in protecting the microwave circuit from damage.

There is a current between the grid and small patches of exposed metal shield near the inner tips of the antennas. This electron flow is accelerated and forms waves of electrons flowing towards the center. Negative space charge just beyond the tips of the antennas prevents outward electrons from hitting the antennas, and the grid-to-antenna-tip potential confines the electrons all other places.

With electron confinement, ions rush in periodically to neutralize the plasma. However due to the rapidly changing environment, due either to phase and frequency differences between the microwave antennas, or RF frequency voltage modulation to the grids or to the microwave generator(s), the plasma never reaches neutrality. Ions, which are too massive to directly respond to the microwave fields, oscillate at MHz frequencies, and heat due to Landau damping.⁴⁷ The most energetic are expelled which leads to a net negative potential well. In case of fusion reactions, the well is insufficient to confine reaction product ions, leaving electrons behind to deepen the well and cause fresh fuel ions to rush in. SMC should have no problems refueling the reaction zone.

When using a single generator for the microwaves, it could be possible to detect the ion oscillation frequency, and by using amplifiers, use this signal to generate the RF modulation on the grid. This could create POPS in the SMC reactor without the limitations faced in IEC, and with higher ambient densities, could require much less compression for break-even.

Work done by Donald Ensley⁴⁸ in the early ‘70s showed that when a confinement mechanism depends on EM radiation, instability waves with wavelengths on the order of the driving radiation are damped. Thus by using RF frequencies for SMC that are roughly the size of the confined plasma, or at least on the order of the distance between antennas, instabilities should smooth out in a favorable manner.

IEC can also work in cylindrical geometries, with less efficiency. SMC might also extend to cylinders with hemispherical ends, although this would probably be in large chambers in applications where spheres are not possible. Spheres appear to be advantageous and so are the focus of initial research in SMC.

4.2.2 SMC Reactor Design

The goal of the test reactor at this time was to find out if SMC is a valid concept. The density must be low enough (about 1 to 10 mTorr) for a mean free path of one to ten cm, which I was not quite able to achieve, reaching only about 30 mTorr at best. The test reactor design described below was intended only to meet the first proof-of-concept goal. The critical test was with deuterium, measuring for resulting neutrons. No neutrons resulted with the current device; this does not disprove SMC, since the microwave circuit is very simple and largely hand-made, and may not be sufficient for fusion reactions. In addition, at the critical moment there was a general failure of the microwave circuit that could not be fixed, so the neutron tests could not represent a definitive outcome of the reactor concept. After trying SMC as an IEC device, however, my conclusion is that it is unlikely to be valid in that configuration and requires instead a magnetic field as originally proposed.

4.2.2.1 Pressure Chamber

I coated the aluminum inner surface with ceramic, to avoid conduction from the grid. As the ceramic cannot be baked, the options are quite limited. I tried several types, each time requiring a complete stripping and grinding of the inner surface of the hemispheres before the next trial. Finally, I found that BN ceramic paint adheres well to the aluminum, builds up a thick enough coating to insulate, does not outgas appreciably, and is mechanically durable.

Each of the 20 coax cables provide grounding points for the sphere through the coax sheaths and help short-circuit eddy currents. To function as a ground plane for the antennas, the pressure sphere needs many grounding points.

The equator of each hemisphere, arranged vertically, has a flange and O-ring seal with bolts. While this does not allow for bake-out, it is well suited to the frequent disassemblies required at this stage of development, and gives maximal access to the interior.

At each pole, a 1¼ inch nom. schedule 40 aluminum pipe welds onto the pressure chamber. This allows ample room for probes as well as openings for gas entrance and exit

ports. As a convenient result of earlier designs, which included two hemispherical magnet spindles that fit over the chamber (see photograph above), it is possible to encase the reactor with a blanket for absorbing neutrons that leaves open only the polar pipes and space around the equator for the coax cables. Such a blanket would be cumbersome and costly, and would be difficult to make effective enough to obviate the need for a neutron-shielded room for tests with deuterium, and still allow for neutron measurements.

4.2.2.2 Grid

The present grid, third to be built, is of 10 ga. solid stainless wire in 20 rings. 10 rings are spot-welded together in half-icosahedral symmetry to fit around each antenna in a hemisphere. Ceramic rods hold the ring assembly about an inch minimum distance from the chamber wall. To prevent conduction, there is a thin ceramic coating (hard BN paint) on the wall surface, which will be thickened with better material in the future. A feedthrough on each hemisphere connects the grid to its capacitor bank via a high-voltage relay. In the original setup, two water resistors helped split the current and slow the discharge with a time constant of about 3 seconds. This was necessary and worked well as long as the grid got its power from a capacitor bank and ran in a pulse. Later arrangements powering the grid from a transformer required another circuit, as the water resistors would overheat and boil.

Usually the grids handle -6 kV, and when fired at the same time as the magnetrons, there is about -5 kV charge on the grids when plasma peaks. I have a delay relay that can time the onset of grid charge to match the magnetron power, but for some reason the magnetrons fire with an unpredictable time lag between onset of its current supply and the peak plasma production. Usually the lag is a few tenths of a second. Future tests will have more advanced antennas (the Mark II design now under construction) and lower pressures, which may make results more repeatable.

Although the details remain difficult to decipher due to a paucity of meaningful measurements, the grid bias seems to be essential for proper functioning of the device. Whenever there is energy leaking from the microwave circuit, which typically occurs when

reflections dominate, the video camera will not operate properly. This tends to happen when the grid has no charge, while little or no such interference occurs with both magnetrons and grid in use. The most severe such indication comes when the pressure in the chamber is relatively high, above 200 mTorr, in which case the magnetrons can be damaged and grid charge is no help.

Higher voltages on the grid would require more insulation on the inner wall, more sophisticated feedthroughs, and a whole new circuit for the capacitor bank and relay. This may be required for fusion conditions, but it is a hope for SMC that not much more than the present voltage is required. With plasmas in the right density for fusion to be practical ($n \sim 10^{19} - 10^{20}$), resistance is so low that trying to maintain a grid voltage on the order of 50 to 100 kV would require severe power loads and destroy any hope of break-even. Such high conductivity and short Debye length (millimeters) eliminates most of the electric field from most of the reactor volume. This is one of the critical problems with conventional IEC. One of the main goals in this SMC configuration was to lower the potential required on the grid by means of the microwaves, thus allowing operation at higher densities. This goal was not reached by the time of the writing of this thesis.

4.2.2.3 Video

The video camera described above became progressively damaged and difficult to manage. I bought two security monitor cameras that worked very well for this purpose. I use 4 mm wide-angle lenses with fixed focal length, thus avoiding the focusing difficulties in more sophisticated cameras. (Most commercial camcorders have autofocus programs that are very difficult to override under remote operation, especially since most of the time the camera sees only darkness.) These relatively simple cameras go through 75 Ohm coax cable to a video acquisition card in the lab computer. The files then undergo editing with Adobe Premier software. Microwave power always mandated a metal mesh taken from the window of a microwave oven; when this was mounted inside the sphere, there were problems with grounding leading to sparks and unwanted discharges. Later I put the protective mesh outside

the window with the camera lens resting directly against it. Microwave plasmas usually required use of filters to avoid severe overexposure; in addition I used half-inch thick leaded glass to shield from x-rays after some unexpected camera failures. When operating with only grid power, filters were generally unnecessary, and I removed the metal mesh entirely.

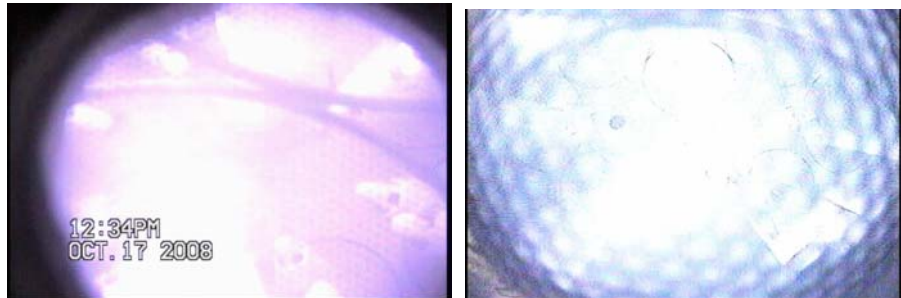


Figure 4.3: Tests from Oct. and Nov. '08 showing possible central glow

Some videos showed possible evidence for confinement, in the form of a central plasma when using both the grid and microwaves. Generally the brightest plasmas formed directly around the antennas; if there was a less luminous plasmoid in the center, as one would expect, it would generally be drowned out by the much brighter plasmas at the antennas. The main problem was, as always, uneven power delivered by the antennas. Only on those occasions when everything was reasonably balanced was there some indication that SMC without magnets might actually work. Only diagnostics beyond video cameras alone can determine this. It remains a disturbing possibility that what seemed like a central glow could in fact have been unbalanced high power from one antenna that happened to be directly across from the camera.

4.2.2.4 Other Details

I'm using surplus data acquisition equipment from undergraduate NCSU physics labs, which is relatively simple and quite adequate for the current use. When measurements become more sophisticated I will have to add more elaborate electronics.

Originally, there were two circular windows 2" in diameter, made of 1/4 inch polycarbonate. (These windows that I made myself I later replaced by one commercially available window and converted the other opening to a KF-50 port.) On the inner side is a metal grid taken from the window of a microwave oven to help block microwave radiation. In addition, I had two coatings of 20 dB plastic RF blocking film, which proved ineffective.

One window allowed in light from an LED lamp, over which was abundant aluminum foil to block x-rays. The other window was for the video camera, which was surrounded by an aluminum Faraday cage. This was to avoid static from stray leaking microwaves, which with some experience is now minimal. X-rays will not be able to leak through the camera and the cage, so this appears safe, but as noted above, after some difficulties with camera damage I added x-ray glass. The aluminum sphere will be transparent to x-rays above about 30 keV, but as the grid is never over -6 kV and the pressures are relatively high, any x-rays that would be a problem would be anomalous. All the EM radiation problems from the reactor were generated outside the sphere, to the best of my knowledge.

The magnetrons and grid are powered by two capacitor banks, made of series and parallel arrangements of 350 and 450 V, 5000 and 5100 microfarad electrolytic capacitors. Both banks are typically charged to -6kV, although the grid does have the option of alternate voltages from a -3kV DC power supply. The actual arrangements in the magnetron bank vary according to how many antennas are functioning; I am careful to have sufficient capacitance for roughly 0.2 s rise from -6kV to -4kV. There is sufficient capacitance in the grid bank, in series with two 15 kOhm water resistors to split the current between the two hemispheres, for the voltage to rise no higher than -4 kV by the time the plasma pulse has ended. Both cap banks dump charge through a 7 kOhm water resistor, one on each hemisphere.

I have made my own water resistors, as well as high-voltage cable and other circuit components. These water resistors functioned as designed, but proved problematic over time. They were made of vinyl tubing of 1" diameter and about three feet long. Each end was closed with brass fittings that in turn had terminals for wire connections. The only way to mount them on both the electronics rack, where I had three of them, and also on the reactor,

was vertically. This posed problems over long periods of time when the water level fell, causing a poor connection, overheating, boiling, and finally a complete lack of conductivity. Also, there were some problems with chemical reactions between the brass and the copper sulfate I used in the water to form the electrolyte. All these problems stemmed from using the resistors for years and under conditions of bursts of very high current. I later switched to large ceramic resistors, especially for dumping the charge on the capacitor banks.

Operation beyond -6kV on the grid would require substantial new construction and new connectors, no longer made by hand, and at considerable expense. Observations indicate that the present setup is sufficient for breakdown and microwave operation; indeed, without the grid there are difficulties getting the magnetrons to behave, as indicated by increased video interference. (It would be wonderful to be able to measure this process with some accuracy and detail but this requires equipment and resources not yet available.) IEC grids are typically at or above 50 kV when trying for D-D fusion; the hope was that SMC potential well depth would far outstrip the grid bias. This would be a great advantage in avoiding grid power losses and simplifying construction. Unfortunately I had no way of measuring this, and it was unlikely with the rudimentary microwave circuit I used. IEC experimenters have to go to extreme lengths to construct bulky HV feedthroughs and keep currents to a minimum in the sphere. Given the conductivity of the plasma, no reactor could possibly break even with grids running at 50 kV or more simply due to the lost power.

While I have an elderly Fluke 6 kV, 20 mA power supply set to negative bias, this is only to top off the capacitor banks to a well-defined voltage, when that is needed. A much more efficient, cheaper, and far faster charger is a microwave oven; I tap into the power supply via a diode and a resistor, which charges the capacitor banks to -6 kV from a cold start in just a few minutes. For most rapid operation, I leave the oven on and the capacitors recharge much quicker than I can recycle the test firings, due to data collection. Once the cycles have been going for a little while, recharging takes only about 30 seconds.

Air cooling for the magnetrons will suffice due to low duty cycles ($< 10^{-3}$). The magnetrons will be lined up in four groups of five, and each group has forced air cooling

from a squirrel cage fan; this is probably optional. There is little power loss in the antennas and they will not require cooling in the test reactor even though the ceramic coating and vacuum environment will make heat transfer difficult. Continuous wave operation is not possible in this first reactor but is a goal in future models. Power reactors will require active antenna cooling, probably with an appropriate oil.

The polar pipes allow for easy access to the interior and include mountings for probes measuring temperature, ionizing and microwave radiation; and plasma potential.

4.2.3 *What this reactor can and cannot do*

The SMC reactor has interesting capabilities, but also constraints due to the lack of funding, and the limits of one person's labor. This setup, with various modifications and improvements over time, could do the following:

- 1) try various gases; first was air, but next came hydrogen and deuterium. D-D fusion is the focus
- 2) with D-D, and perhaps in time D-T, measure neutron production, which would be proof of SMC and determine if it is viable for more development
- 3) test different ceramic coatings on the inner wall, with regard to thermal expansion, particle impact erosion, plasma contamination and other first-wall issues
- 4) test alternative antenna and grid designs
- 5) measure x-ray production under various conditions; any x-rays hotter than the grid potential indicates exothermic reactions
- 6) measure the potential through the radius to the center
- 7) use a spectrometer to measure density and temperature, assuming a nearly-Maxwellian plasma
- 8) apply RF modulation to the grid voltage to test POPS

The limitations are due to financial and engineering limitations that cannot be avoided. High vacuum systems are intrinsically expensive, and while this project has benefited greatly by borrowing equipment from past lab experiments in the current lab space, there are critical features that limit the lower pressures the chamber can achieve. The most important limitation was in plasma diagnosis

Until the end of 2008, the antennas mounted inside the hemispheres by screwing into pipe thread cut into the 3/8" aluminum wall. The connection must conduct, and pipe thread depends on sealant, which is usually an insulator. I used copper-based conductive pipe dope, as well as vacuum sealant varnish on the outside. While many of these feedthroughs were without detectable leaks, they were not always tight, and could not be relied on after dismounting and remounting antennas. I changed the seal to an O-ring flange on the inside that was tightened by screwing in the previous way with the pipe threads, without sealant this time.

The connection to the external coax is hand-made. It would be much preferable for these 20 fittings to be more vacuum-tight and to have standard coax connectors, but this application has custom requirements and will take some serious engineering and machining to improve for higher vacuum and better microwave performance. The current equipment cannot operate with CW power.

The microwave circuit is simple and sometimes worked as intended, although distribution of power evenly to all antennas was hit-and-miss at best, and a flaming failure at worst. The reactor needs a proper matching network for a comprehensive research program. Much more equipment, such as a spectrum analyzer and signal generator, would be required to improve and tune the circuit, change to a single generator, reduce power, protect against reflections, maximize the energy delivered to the plasma, and test CW operation. The existing system can only operate at 2.45 GHz, 1000 W pulsed power at each antenna, although I do have the option of running 10 antennas instead of 20 with half the capacitor bank. Successful neutron production with SMC might be dependent on an improved microwave circuit, so there is the unfortunate possibility of a false negative with the current reactor.

The O-ring between the hemispheres as well as the windows and antenna feedthroughs make bake-out impossible, limiting the low pressure range. An SMC reactor requires the ability to reach well below 1 mTorr, and thus back-fill to 10 mTorr for D-D tests. Since peak IEC neutron production is far below this density, it would be prudent to be able to test down to 10^{-6} Torr to compare the two systems.

4.3 Trials at Duke (TUNL), first half of 2009

In February 2009 I moved the reactor from NCSU to the Triangle Universities Nuclear Laboratory (TUNL). The main reason was that I was close to filling with deuterium and wanted to measure neutrons. I had no access to facilities here at NCSU for either neutron measurement with any precision, or to a shielded room to put the reactor. TUNL has a 10 MV accelerator and very large rooms designed to be shielded from high levels of radioactivity. They also are fully equipped for all eventualities, including neutron measurement with a multichannel analyzer, and could offer occasional help from a technician.



Figure 4.4: South Hemisphere, assembled reactor, and target room location at TUNL

Neutron shielding requires a thick wall with any pipes having curves to avoid allowing them to stream through. I had space in an adjoining room, just behind the wall shown in the third frame of the figure above, where I had the control panel in its rack along with power supplies, capacitor banks, and computers. All the many wires leading to the reactor passed through conduits under the base of the wall. I had two video cameras, one looking into the reactor and the other mounted on a tripod allowing me to see the reactor in operation. Although I had two computers and three monitors, there were problems getting all the video cameras to work all at once. Also, the coax video cables had to share the conduit with HV power cables delivering a considerable dose of power to the reactor. The usual shielding simply was not sufficient much of the time. However for the most part, after some weeks I was able to get the reactor back into its configuration as it was at NCSU.

My first challenge was actually getting into the target room. My health has always been a limiting factor during this research, as I have arthritis and suffer from severe fatigue. The half-hour drive each way wore me out and I found it impossible to go to the lab every day as was my custom; three days a week was more the norm. On top of that was the schedule of accelerator operation. When the accelerator was on, the target room that I used was frequently radioactive and off-limits, sometimes for a week or two at a time. This slowed progress terribly at first.

By March I had pumped the reactor down and put it through test firings, but the pressure problem was severe. At this time the Mark II antennas were in an early form that included porous ceramics, and were outgassing severely. The BN paint was peeling after firings, and even after pumping out for a couple of days, the pressure could not drop below 90 mTorr. Although I had set up a turbo pump (and all its complications with power supply and water cooling), I could not hope to use it until the pressure came down considerably. Thus I had no choice but to pull the antennas out, take them back to NCSU, and modify them to not outgas so badly.



Figure 4.5: Stripping off ceramic; casting in solid epoxy; finished before BN paint
(note the O-ring flanges covered by masking tape)

Stripping the ceramic, casting the antennas in epoxy, and painting with BN took one month. Returning to TUNL in April, I moved the reactor to a small adjoining room that would be accessible almost all the time regardless of the accelerator operation. There, John Dunham, a technician working at TUNL, helped me use a helium leak detector. At first, even with the new antennas, there was little to no improvement on the ultimate pressure; clearly there were external leaks as well as outgassing. (I didn't expect the new cast antennas to not outgas at all, but they certainly would do so much less, and at these modest pressures it shouldn't be a problem as long as the surface had some protection from plasma flashes.) We did find problems with several feedthroughs and the window ports. I replaced the homemade windows, and filled some voids in the O-ring space on the antennas with Apiezon Q putty. While not ideal, it did help, and after another three months of work, I got all detectable leaks resolved. Still, it was not possible to get the pressure low enough for the turbo to operate, and I had to settle for roughly 30 mTorr as a best result. When operating in something other than air, the situation was pretty bad since I had to backfill up from this pressure, resulting in running the tests at 80 or 90 mTorr. My goal was to operate from 1 to 10 mTorr in deuterium.

I ran the very real risk of a false negative due to running at pressures far too high, and with contamination from air and volatiles from the antennas.

As a further headache, I was using two different thermocouple gauges, which proved to be a real problem. They did not agree; the TUNL gauge read at about 70% of the one I brought with me from NCSU. In addition, thermocouple gauges are sensitive to the kind of gas used, and these were calibrated for nitrogen; and in any event, they can be off by a factor of 2. So, it was quite tricky to get a feel for what actual pressures were in the reactor. Should I get funding and thus have some choices, I would certainly use a pair of capacitance manometers, one high and one low range, that are indifferent to the gas type and quite accurate.

In mid-June, I took one antenna that had the worst problem with peeling BN paint, stripped it down to the epoxy, and applied several coats of silicone-ceramic engine paint. While this ideally needs heat treatment to fully cure, I decided to see if it would work on the antennas. By the end of my stay at TUNL, it showed no damage at all and no peeling, while several of the other antennas had significant problems with the BN paint adhesion.

To switch the -6 kV capacitor banks, both for the grid and the magnetron, I used two HV relays designed for up to 12 kV, but not this many amps in a short pulse. I replaced the contacts with a special amalgam of carbon, silver, and copper, which worked well and eliminated the melting at the contact points that happened with the original silver-plated copper. However with repeated use at excessive amperage, the capacitor bank relay (whose current was much greater than for the grid and over a shorter time) suffered damage and started shorting out and burning some of its insulation. I had a spare and replaced it; but this was just the start of mysterious problems.

In late June I could get the pressure down to a minimum of about 45 mTorr and started tests again, at first in air. The first two runs, at 95 mTorr, were with the grid only and went normally. However when I included the magnetrons, the discharge was very short, only lasting one frame of the video (recording at 30 frames per second), even though the capacitor bank discharged normally over about 0.2 seconds. The discharge was so bright that it caused

a white-out of the image, so further diagnosis was impossible. I added Polaroid filters but the problem persisted. Next I pumped down and filled with hydrogen repeatedly with similar results. When I used 4 filters, it showed that only one antenna was firing, but as it was near the window, and my field of view could not include looking sideways, I could not see details. It did not help that I was not in the same room as the reactor and could not see what was happening.

To add to the frustration, something was causing a pulse that was knocking out my data acquisition. I used a voltage divider to turn the -6 kV of both capacitor banks to -6 V, since the DAQ hardware can handle -10 V. As a result this important diagnostic tool became useless. By observing the reactions of the radiation detectors with sensors in the target room, it became clear that something was setting them off—even when no gammas, neutrons, or x-rays could be coming from the sphere. There must have been some sort of EM pulse as a result of a malfunction that I simply could not locate. Oddly enough, I tested each magnetron individually and found all of them in working order.

Regardless of this obnoxious and potentially dangerous undiagnosed defect, I decided to go ahead and try a measurement of neutrons while it was possible. TUNL was kind enough to give me a lecture bottle with 50 psi of deuterium which was more than enough for my experiments. Dr. Robert Golub, on the NCSU faculty and working at TUNL, had a small scintillator detector that I connected to a video camera. Dr. Chris Gould, also from NCSU and with an office at TUNL, assisted in calibration and moral encouragement. I used a brick of paraffin to moderate the neutrons that was about 2 inches thick. There was no sign of any activity during the trials.



Figure 4.6: Scintillator detector with camera, and mounted on reactor with paraffin

As a result of the malfunction and null neutron count, as well as the difficulty of working with a commute, I decided to move back to my old lab space at NCSU at the end of July 2009.

5 Chapter 5

5.1 *Recent History of the Research (from Fall 2009)*

5.1.1 *Return to NCSU*

Even with the dramatic and unrepairable magnetron failure at Duke, there was no reason to believe that the reactor actually confined any plasma in the center, or functioned as an IEC configuration even in a glow discharge mode. One frame from one test with grid power only did show some glowing past the tips of the antennas that was very intriguing and may indicate the existence of the desired space charge that could protect the antennas, but this was only visible because the magnetrons were not on and so plasma of small luminescence could be detected.

Once back in Research Building II at Centennial Campus, NCSU, I found a few problems as a result of taking the reactor apart and reassembly due to the move. However

these did not fix the near-complete inability for the magnetrons to fire. At Duke, I had been separated from the reactor by a radiation-proof barrier; now I was in the same room with the reactor, several feet away, as were my computers. Power was reaching the magnetrons from the capacitor bank, and all the circuits tested fine; but still something bad was happening. Worst of all, the EM pulses from firing off the capacitor banks, for either the grid or the magnetrons, was damaging my computers, forcing them to reboot and making me worry that serious permanent damage was entirely possible. Shielding with metal panels and foil did not work. Eventually I had to conclude that the problem was not fixable in a reasonable time with the equipment available. As it was already August 2009, it was nearing time for me to start writing this thesis in order to graduate in May 2010. As a result I reoriented the final few weeks of lab work from SMC to BL.

5.1.1.1 Theoretical Aside: Why RF can't enhance gridded IEC

There was no sign of confinement without an inner grid, while there clearly is a bright plasma inside the inner grid of a conventional IEC reactor running at the pressures reached in the SMC experiments (~40 mTorr minimum). Would there be a way of using microwaves to compress, heat, and help confine the core plasma in an IEC reactor?

The answer appears to be no, at least not enough to make it worth the bother in equipment and power. For radiation pressure to apply to the plasma, it must exceed the critical plasma density (n_c) at which point transmission into the plasma stops. This happens when the plasma frequency ω_p equals the microwave frequency ω :

$$\omega_p = (n_c e^2 / \epsilon_0 m_e)^{1/2} \quad 18 \pi n_c^{1/2} = \omega \quad (4.3)$$

as shown in the magnetic SMC discussion in Chapter 3. At glow discharge densities as done in my experiments, with pressure no lower than about 50 mTorr, the gas is so easily broken down by strong microwaves that plasma forms around the antennas and the microwaves are strongly attenuated after that. IEC is marginal at these densities anyway due to excessive collisions with neutrals. Therefore, to apply microwaves effectively to the central plasma, the fill pressure must be low enough to prevent immediate breakdown next to the antennas. This

also allows IEC to work far better as the mean free path must exceed the dimensions of the chamber to have ballistic confinement.

The typical plasma density for a 100 kV IEC reactor is about $2 \times 10^{14} \text{ m}^{-3}$ in the core region. This means that the maximum frequency that would find this plasma opaque is 130 MHz, with a wavelength of $\sim 2.4 \text{ m}$. Supposing a cylindrical vessel of this diameter and height contained numerous small IEC units, each consisting of outer and inner spherical grids. The gaps in the grids would have to be small enough for symmetry, but with gaps smaller than 0.05 times the wavelength, they form effective barriers to RF transmission. Also, due to the grounding of each outer grid, they all act as antennas to absorb the RF energy, leading to extreme losses.

Even if this trial reactor design could find a way around these problems, the pressure density is equal to the energy density of the RF field;

$$\frac{\epsilon_0}{2} E_{\max}^2 = \frac{(0.9) Q \text{ Power}}{\omega \text{ Volume}} \quad (4.4)$$

with (0.9) being an estimate of the antenna efficiency. With a Q of 2 (very optimistic), power of 20 kW, frequency of 127 MHz, and volume of 10.3 cubic meters, the pressure is a staggering $4.4 \times 10^{-6} \text{ Pa}$. This is actually comparable to the IEC effective pressure, at least within an order of magnitude, but not any more than that; and the centers of the inner grids will be where the RF is at its very weakest.

The only way I see of making radiation pressure significant is to do something like the original magnetic SMC proposal, with magnets, a closed surface at ECR, circularly polarized microwaves in short intense pulses, and a lot of money. Then things are very different. The ponderomotive force becomes quite large and the microwave coupling to the plasma is very efficient.

5.2 Reorientation to BL

5.2.1 Why a gridless IEC device can never be a fusion power reactor

As a result of more careful thought, review of the literature, and looking at the results of my experiments, and reading proposals for gridless IEC reactors, I came to the general conclusion that the long-standing conclusion that there is no way to confine a plasma with electric fields alone is quite correct. (IEC with grids does *not* confine plasmas; it puts the first wall inside the plasma in the form of the inner grid.) The failure to confine is most easily seen in the context of the extreme conditions required for fusion reactors, but the general conclusion is unavoidable for several simple reasons relating to conductivity, charge mobility, and Newtonian mechanics.

For any non-explosive fusion reactor, to meet the Lawson criterion and produce a useful amount of power per volume of reacting plasma, the plasma density must be on the order of 10^{-20} m^{-3} , which corresponds to a fill pressure of from 1 to 10 mTorr. Below this density results in reactors that cannot break even, and above this density plasma cannot be confined at the temperatures required. Thermal cycle reactors are limited to power densities of 100 W/cm^3 and those using direct conversion (impractical for spherical IEC) will not be able to exceed this limit by very much. Thus the Debye length ($[\epsilon_0 kT / n e^2]^{1/2}$) will be on the order of 10^{-5} m , the plasma frequency ($[n e^2 / \epsilon_0 m]^{1/2}$) will be $\sim 10^{11} \text{ Hz}$, and the reacting plasma volume must be at least many liters, if not cubic meters, in any practical power reactor.

This series of requirements poses impossible demands on any IEC system. No substantial electric field can be sustained beyond a few millimeters; non-neutrality can only persist for nanoseconds; and the small size of the central focus, always less than a cubic centimeter, can never be scaled up to fusion reactor sizes. As mentioned above, gridded IEC power scales as $1/a$ and $1/n$, both of which mean IEC power will always be minute.

The hope of a gridless IEC reactor is to establish and maintain virtual anodes, cathodes, or both, in spherical symmetry around the center, which would allow ballistic confinement of ions to circulate the thousands of times required before fusion. (Such a large

number of turnarounds is required since the collision cross-section is at least 10^4 , and usually much more, times larger than the fusion cross-section.)

The Debye length dictates the limit in physical dimensions of non-neutrality beyond durations longer than the plasma frequency; as such, sustained separation of charges for virtual anodes or cathodes would require some mechanism that appears to be missing. Free electrons would neutralize any virtual anode in nanoseconds. There would have to be some way of introducing hot ions into the center, or possibly heating them when there. To turn around the ions heading out of the center, an excess of electrons must provide a potential commensurate with the ion temperature. For D-T fusion, the coldest possible, this would be - 10 kV just to turn around roughly half of the ions. To turn around all but one part in 10^4 , the required potential would be prodigious, and would be a function of the energy distribution of the plasma, which is not quite Maxwellian. About 10 times more potential would be required for D-D fusion and about 50 times more for p-¹¹B. Space-charge repulsion alone would guarantee that this electron excess would disappear in nanoseconds.

Ballistic confinement only makes sense when the mean free path is on the order of the size of the reactor. Otherwise the particle path becomes randomized before the particle can complete an orbit and return to the center. Any fusion reactor cannot possibly operate at pressures this low and produce useful energy, as mentioned above.

Another problem with having sufficient non-neutrality in the core to turn around the fuel ions; fundamental Newtonian mechanics requires that the plasma pressure must transmit a force to the reactor in order to be confined. In magnetic confinement the magnet coils feel the plasma pressure due to distortion of magnetic fields. In gridded IEC, the inner coil feels an outward pressure due to interaction with the charged particles it turns around in the space between the inner and outer grids. This pressure is constrained by tension in the grid. With no grid, the force of reaction would be felt by the excess inner electrons mentioned above required to make the enormous negative inner potential, which would make these electrons fly outwards as there is no way to sustain tension in a gas or plasma. These forces are very considerable in a fusion power reactor. With D-T reactors, the plasma pressure is of the order

of an atmosphere, and for a p-B reactor, at least 15 times that or more. Since the reactor pressure (magnetic or electrostatic) must exceed the plasma pressure to avoid instabilities, the resulting pressure to be constrained by a p-B reactor would be on the order of 30 atmospheres. With no inner grid, all of this pressure goes entirely to dispersing the electron excess in the center.

Such Newtonian considerations also rules out the methods I originally proposed for magnetic SMC for plugging the cusps with local magnetic fields in the skin of the plasmoid. There is no way to transmit the plasma pressure to the reactor, and no way to sustain tension. The cusps can be plugged to a certain extent by means not very far removed from the original idea, as has been done in ECR ion sources. Magnetic SMC remains of interest as detailed below in Section 6.3.

5.2.2 *Changing the reactor to BL for one last shot*

I saw that with the arrival of fall 2009, it was time to wrap up the active phase of the experiment and start to write this thesis. There appeared to be no way to diagnose the problem plaguing the microwave system with the equipment and time available, and considerable danger in trying to keep operating it. Also, using a capacitor bank to power the grid was continuing to cause interference problems of significant size. I decided to eliminate the microwave circuit, magnetrons and all, leaving only the coax connections and cables to the antennas. In its place I installed 20 electrolytic capacitors, rated to 450 V and 2400 microfarads where the magnetrons had once been. On top of each I placed two Schottky diodes to rectify any incoming RF, and connected the capacitors in parallel to a voltmeter and my DAQ sensor. Each diode array connected to the old coax cable leading to an antenna in the sphere. Thus I could detect by the capacitor bank voltage the existence of EM radiation in the sphere of any frequency up to tens of GHz.



Figure 5.1: O-ring seal with Q putty; painting the antennas; mounted on South Hemisphere

The grey BN coating on the antennas was clearly deficient, and I removed the antennas, sanded off the paint, and recoated with five layers of black silicone-ceramic engine paint. This paint had worked well on the test antenna at Duke. All problems with surface damage ended for the rest of the experiment, although the antennas were no longer having to deal with microwave plasmas. If there was any outgassing problems with this paint, it was less than the background.

For the grid, I removed the capacitor bank formerly housed in the lower part of the Southern Hemisphere (the designations are arbitrary; the stationary North holds the vacuum pumps, vacuum gauge, various plumbing, and the wire connections to the control panel, while the more mobile South has gas entrance and camera window). First I experimented with powering the grid straight from the microwave oven, but this was not successful. Instead, I wired up a combination of one of my oven transformers (of which I have 20), a diode rated to 3000 V, and a 100 Ohm HV ceramic resistor. This is controlled by a relay triggered from the control panel which in turn has two delay relays. As a result I can deliver timed pulses ranging from 0.2 sec apart to arbitrarily gaps, and of any duration. The voltage is half-rectified 60 Hz peaking at 3000 V.



Figure 5.2: Diodes on capacitor; top of SH; bottom of NH

The result was very well-controlled, predictable discharges at any pressure up to several tens of Torr, in both air and hydrogen. There were no more interference problems or any appreciable dangers in operating this final system. While this was certainly a relief, there also was no anomaly detected; no particular reason in this configuration to suspect confinement in the central region. The collected voltage in the capacitor bank was extremely small (a fraction of a volt) and was due to the grid current and AC cycles, not any BL microwaves.

6 Chapter 6: Results and Conclusions

6.1 Summary

The reactor is a practical design that held a vacuum, generated plasmas, and could be scaled up and modified for further experiments. It includes HV power supplies, capacitor banks, control circuitry, video gear, vacuum systems, magnetrons and microwave cables, and custom antennas.

IEC is ruled out (without inner grids). BL experiments did not work yet; SMC could be valid with magnets for either low-pressure plasma confinement or instigating BL, but not for fusion.

To understand BL I propose an extension of physical theory that still lies within the constraints of experiment, but that allows extrapolation at a later date for more general uses not now associated with science.

This kind of research is important if we want to continue a technologically advanced civilization for the indefinite future; a concentrated, practical, endless energy source is mandatory. Without it, we will return to subsistence agriculture and hunter-gatherer societies in just a few hundred years at most, and possibly much sooner.

6.2 What was accomplished

While this research did not succeed in reaching either of the twin goals of unambiguous evidence of confinement or generating some reasonable analog of ball lightning, it did form the basis for further work in these directions. There were *ambiguous* signs of possible confinement, but detailed diagnosis was not possible.

There is no substitute for actual construction of a prototype for finding out what works and what doesn't, and much of that occurred during these years. The basic reactor geometry solved some fundamental problems with any device of this type. Spheres are clumsy constructions in some ways, when compared to the ubiquitous cylinders. This reactor design allowed full access to the entire interior by means of opening into two hemispheres. By having the equatorial seal vertical, no lifting was required. Since both hemispheres were solidly mounted in their own frameworks, all fittings and connections were geometrically stable, and only the flange and a series of electrical connections required disconnection to open the reactor. With both frameworks on wheels set in rails, alignment was guaranteed and separation was quite easy. This basic concept can be scaled up to quite large sizes, although once a sphere is big enough to enter via a hatch, it really doesn't need to come apart into hemispheres, and so it shouldn't.

The main computational work in SMC was in the original magnetic SMC proposal. Much is badly dated, such as the now-abandoned ideas for plugging cusps via a strong localized magnetic field in the skin of the plasmoid. However, the magnet design is quite valid and would be the basis for the design of hemispherical magnets for a future reactor. Such magnets would work well with the current basic design for the reactor on two frames with polar pipes for access. The magnet spindles that I built, mostly of acrylic, would not be sufficiently strong for the purpose, but served as reasonable mock-ups and proved their practicality.

Antenna design was a major area of development. They started as conventional far-field truncated conical helicies, following designs used in the atmosphere and very high vacuum. They ended up, after three years, as entirely custom shielded solid conical helicies well suited to high power and near-field applications in pressures of 50 to 500 mTorr. Feedthroughs and mountings posed very difficult design and fabrication problems which could only be partially solved with the resources and time available. My final solution allowed the antennas to be screwed in from the inside and fairly well sealed, such that the remaining vacuum problems were dominated by outgassing instead of external leaks. However the entire system could not be baked out, and especially not these feedthrough seals. Below I will detail how the next reactor can improve on this design.

Unique to this reactor, antennas using near-field radiation created opaque plasma surrounding each antenna quickly enough to shield each from the microwaves coming from the other antennas. Thus, for a range of pressures (< 10 mTorr to 100 Torr), the plasma itself protected each of the 20 magnetron from reflected power which otherwise would cause internal arcing and severe damage. In future systems, a single microwave generator would be protected by the matching network.

The grid also went through considerable evolution before its final stable, reasonably efficient form. Experience shows that the microwave discharge with the inadequate circuit required the grid to enhance quick plasma formation. There was little advantage gained from grid voltages over a few thousand volts; while the maximum attempted was -6 kV, there was

no particular advantage in going higher, and considerable disadvantage in wasted power, dangers in operation, difficulties in making and switching HV capacitor banks, and the considerable insulation as used in IEC systems. The system as constructed was dangerous enough.

While I did not construct a matching network for the magnetrons, and simply had one magnetron per antenna with an attempt at even current supply, I did show what would be required for a more advanced system, which I detail below. It was possible to operate the existing system much of the time, but this was hit and miss, with considerable risk of equipment damage. When the reactor chose to cooperate, the discharge was extremely bright, possibly with the desired plasma in the central region, and lasted 0.2 sec, long enough for useful observations with simple equipment. In its appropriate pressure range, the magnetrons escaped damage; this happened only when the pressure was too high (>100 Torr), and would have happened if the pressure could been too low (>1 Torr). This in itself was a bit of an achievement, and not exactly expected; the power was so high that the plasma became opaque quickly and isolated each antenna.

The reactor required custom control circuitry that evolved over the years, including various relays ranging from 12 V systems to HV relays running on 110 AC and switching the 6 kV, 5 A cap banks. There was data acquisition hardware and software coordinated with multiple video cameras, providing the results of each test. The control panel handled power supplies to cap banks, magnetron filaments, lights, fans, and pumps. The pumps could be timed to turn on and off at any given hour, and the grids were timed to pulse in any regular simple pattern desired.

The vacuum system was limited by financial constraints, but ended up limited more by the materials in the antennas than by the reactor integrity itself. The ultimate pressures reached (30 mTorr) were not low enough to test the full possibilities of this reactor, and must be considerably exceeded in the next. I was able to explore a full range of pressures above this in air and hydrogen.

6.3 What is left to be done; Magnetic SMC

6.3.1 Generalities

(From here, I will call magnetic SMC simply SMC as this is the direction for future development.)

SMC is not a candidate for a fusion reactor in the conventional sense. The magnetic field cannot be strong enough to use for confinement of fusion plasmas, nor can the cusps be plugged sufficiently for hot ions to use for a power reactor. The two reasons for the reactor, then, are as a pulsed hot ion source, and in hopes of instigating BL.

The previous work indicated the need for the magnetic field. Without the field there is no good way to get the plasma formation away from the antennas and to a defined volume in the center of the reactor. The prospects for a gridless IEC system are very poor and should be abandoned. ECR and similar situations at somewhat higher pressures and field strength allow strong coupling between the plasma and the microwaves at locations of our choosing.

To explore this kind of reactor, considerably more funding is required than what I did in this research. There will have to be a settled location with adequate facilities. A team of at least several people will have to include people with training in microwave engineering and plasma diagnosis. The vacuum system will have to be of high quality for much lower pressures and greater gas purity. And critically, the antennas will have to be made of advanced materials, especially if they must be solid cones.

6.3.2 Technical details

The closest existing art to SMC is for ECR ion sources (ECRIS). The definitive text on the subject is by R. Geller (1996)⁴⁹.

6.3.2.1 Magnets and Microwaves

ECRIS use either a simple magnetic mirror or a cusp field similar to SMC, where an oblate spheroid surface is at ECR. (The cusp field is superior as all the curvature is good, that is, negative.) On application of a circularly polarized microwave field from one end, a

plasma forms on and around the oblate spheroid ECR surface. The results depend on the fill pressure; when using very low pressures and high-Z ions, quite high ionization levels can result. Usually ECRIS operates at low enough pressures to form collisionless plasmas, and generate hot electrons and relatively cold ions. (In this discussion, “low pressure” is defined as below 5×10^{-4} Torr, while “high pressure” is above 10^{-4} Torr.) The hope is that the SMC geometry can scale up the yield and increase efficiency for ion generation, and form the basis for BL research as well. This is due to a more even application of circularly polarized microwaves instead of from only one antenna, using a spherical chamber instead of the more typical cylinder, and possibly the addition of grids.

SMC magnets are designed for pulsed operation. The ECR surface, then, would start in spherical shape near the reactor walls, and move inwards as the field increases. The ECR is self-maintained in a growing **B** field and yields high-energy electrons since

$$\omega_{RF} = \frac{eB_c}{m_e} = \text{constant} . \text{ The rate of increase } dB/dt \text{ should not exceed } 2\pi k_F E/c.$$

While SMC or ECRIS devices are not suited to fusion as the open magnetic fields are too prone to losses, these can be minimized enough to contain quite hot plasmas and ions with multiple ionization. SMC already has grids that can serve to produce a blocking voltage at both the polar and rim cusps. (This requires more research, as electric fields disrupt the constant magnetic moment required for mirror confinement.) More effective is the acceleration of electrons in the direction perpendicular to **B**, which increases the angle in velocity space. Typically, ECR accelerates electrons *only* in this perpendicular direction, which has the effect of changing the “loss cone” to a “loss hyperboloid”. While high-energy electrons can still escape, below a certain energy virtually all electrons are confined, except those lost via 90° Spitzer collisions. Experiments indicate that this idea is valid.

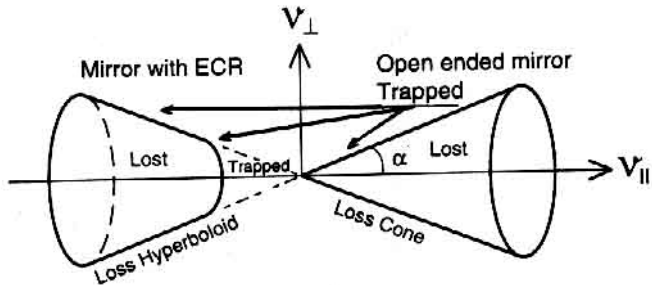


Figure 6.1: Loss cone in velocity space (Geller 1996)

The SMC reactor is much larger than the wavelength, which means that the cavity is multi-mode (TE_{xyz} and TM_{xyz} with $x, y, z \gg 1$). As a result, E is not calculable, the fields are generalized, and Q is quite low. Chambers such as these are rarely treated in the literature, due to few uses and the intractability of the math. (Spherical chambers are especially ignored and are generally useless as they cannot be adjusted in size.) In order to have radiation of circular polarization in the desired orientation interacting with the plasma in various locations, it is desirable to have as little reverberation as possible, and maximized near-field radiation directly from the antenna closest to the plasmoid. Thus it would be ideal to have an anechoic chamber. Much of the radiation will be absorbed by the plasmoid surface anyway, so the relative coherence of the near-field radiation on first pass should assure the desired result. The only practical manner of investigating how well this works would be to construct the reactor and carefully measure the results. If grids are not useful, and thus insulation is not required, the walls could be coated with carbon as an effective RF absorber and refractory, low-Z first wall. Multiple passes of RF lead to stochastic heating which is very undesirable; we want heating to be concentrated at or near the ECR surface to ensure definition to the plasmoid. Stochastic heating will contribute to RF diffusion. This being said, it remains true that ECR heating results from an unknown mechanism about which there is much debate.

The question of grids and coatings for the reactor wall is significant for another reason as well. Breakdown relies on secondary electron emission since the cascade time is longer than the average electron lifetime. Such electrons could come from the corona

discharge around the grid, or from the walls. If there are no grids, the first surface on the wall can be doped so that the work function is low and copious electrons result.

The great advantage of low-Q chambers is that the impedance matching between the radiation and the plasma adjusts itself to tend to keep the coupling high; modes that are mismatched tend to disappear in favor of better-matched ones. Another advantage is that the shape of the chamber is arbitrary as long as its characteristic dimension is much greater than the wavelength. The SMC spherical chamber is handy for reasons other than for any preferred spherical resonance. It is reassuring that the many variations from spherical, due primarily to the many antennas but also for any other reason, do not matter to the functioning of the RF field. In a typical high-Q microwave chamber, tiny deviations from the ideal dimensions have dramatic effects, and the frequency must be tuned and stabilized to considerable precision. Thus, the norm is to allow for well-measured calibration of at least one dimension of a chamber. While cylinders and rectangular prisms allow for this, spheres do not.

6.3.2.2 *Power levels*

The microwave power input for maximum temperature plasma is a complex and incalculable function of reactor geometry, gas composition, fill pressure, and magnetic field strength. The proposed reactor will run at a wide variety of all these parameters, and so the microwave power will likewise vary experimentally to find the optimum power for maximum plasma conditions of density and temperature. If the power is too high, ECRIS experience shows that opaque plasma forms outside the ECR region and disrupts the process. Excess **B** can combine with excess microwave power to continue to make hot plasma, but this is outside the most efficient regime and is a marginal effect. Extrapolating from existing ECRIS designs would indicate that for a one-meter diameter sphere, the maximum microwave power required under any anticipated conditions would be about 4 kW; this is the power level point design for the magnetic SMC proposal covered in section 3.2. In actual operation the power would be considerably less than this, probably 1 to 2 kW.

There is one way to increase the maximal RF power level. By increasing the magnetic field above B_c it is possible to have a similar surface at extra power at higher pressures than the usual operating range, even as high as 0.1 Torr (roughly the range of the present experiment). The general effect of this would be to have the plasmoid larger in size than at lower power and lower density, and with cooler temperatures, but significantly higher plasma density.⁵⁰ This could be useful for exploring BL. Whenever the RF power goes above 1 W cm⁻³, the interactions are nonlinear and unpredictable. This could be easily reached in very short pulses, as from radar equipment, superimposed over a lower power longer pulse. The power levels in the present experiment are hard to estimate, but since the microwaves were absorbed very quickly in plasma close to the antennas, the volume where most of the microwaves existed was much smaller than the whole 90 liter sphere. Thus the power levels in the plasma itself probably well exceeded the nonlinear threshold.

One significant problem with the existing SMC reactor was the unwanted breakdown and plasma formation inside the initial open helix antennas, and also plasma formation at the base where the wire entered the chamber. At typical ECRIS pressures, and at lower power, such breakdown would not occur, and open helix antennas could once again be used. These antennas are far easier to make, lighter, and far cheaper than the solid cones required in the present reactor. The Paschen minimum for breakdown is about 3 Torr for most gases. At ECR, the electric field required for breakdown remains about the same as at this minimum as pressure goes down to quite low levels. This means that at low pressure operation, even with open helix antennas, the breakdown will occur at the ECR surface and not elsewhere unless the radiation becomes excessive. The antennas would still require ceramic coatings and thus would be of expensive low-expansion metals, but even so would be simple to construct and cheap enough to allow for multiple experimental models.

The magnet is intended for pulsed operation, as the reactor is large and fields, currents, and heating are considerable. Prolonged fields would probably require superconducting magnets and a huge budget. Breakdown in the ECR surface will typically take on the order of 1 msec from initiation to high density plasma; thus the pulse must last in

conjunction with RF for at least that long, and preferably appreciably longer. That said, there is much room for shaping the current pulse in the magnet and also the strength of the RF field.

ECRIS devices generate electron energies up to several MeV, resulting in considerable x-ray generation and hazard. Any SMC reactor would have to have significant shielding in addition to the reactor walls, even if they are of steel, and even the magnet windings. ECRIS devices typically use thick lead plate for this purpose.

6.3.3 Next generation details

Antenna mounting is quite intricate for the proposed reactor. Experience with the present reactor shows that it is mandatory for the antennas to be mounted, and removable, from the inside. The wall mount and feedthrough should be permanent and leakproof, allowing the microwaves to pass without reflection through the wall, with a standard coax connector on the outside. One alternative to this is to have each of the antennas permanently mounted onto a plate that has a Conflat seal big enough for the hole to allow the antenna to pass through from the outside. This is expensive and poses some geometrical difficulties with a hemispherical seal. With this option, it is likely that the sphere would be welded into one piece and access to the inside would be through the antenna holes.

Instead of the present 20 antennas, better spherical coverage occurs with 32 antennas in soccerball (or buckyball) symmetry. This also makes division of power somewhat easier in the microwave circuit using a single power source, avoiding division by 5.

The antennas will be monolithic like the Mark II antennas of the present experiment. However they will be constructed of much more advanced materials; the metals will be low-expansion, typically Invar, and instead of epoxy the bulk will be of monolithic ceramic. This should avoid the outgassing problems and can withstand plasma flashes. If there are exposed electrodes at the inner tips as in the present antennas, these should be of more refractory metal like tungsten instead of brass.

Should the new reactor use a grid at the antenna bases like the current reactor, this grid should be welded of at least stainless steel, and possibly of more refractory metal, in a polygonal shape instead of the rings used now. (Stainless worked without any degradation in the current grid.) This avoids the sharp angles and resulting high electric fields. The mounting of about 3 cm. from the wall works well. The wall would then have to be insulated; BN hardcoat paint is inappropriate for a reactor that can change appreciably in temperature, so probably some kind of ceramic tile will be required.

The vacuum system will be capable of 10^{-5} Torr and the whole vacuum part of the reactor will be baked out.

With this system comes significant x-ray generation, so the reactor will have adequate shielding. The magnet will help in this regard.

Plasma diagnosis will be sophisticated and a major change from the present relatively crude system. Video will be challenging since access to the sphere is limited mostly to the polar pipes, where space is shared with all the other probes and wires. Fiber optics that can hold the vacuum pressure without breaking like the one I used would be a good option.

6.4 Reactor design should BL reaction occur

6.4.1 Design for BL

There are some missing ingredients with regard to triggering BL in an SMC-type reactor, and no clear way at present to discover them. It seems reasonable to suppose, though, that someone will eventually construct a reactor which will initiate, contain, and get energy from BL, since after all it does exist in nature. And the general geometry of such a reactor could very likely be quite similar to the SMC concept.

If this is the case, some general ideas are apparent. The most desirable aspects of BL are its potential for high energy density ($\sim 10^9 \text{ J m}^{-3}$), benign environmental aspects, common fuel (whatever it is!), and power output via microwaves. The last characteristic is a defining one for reactor design and is a strong suit of SMC. The microwave circuit can supply a short intense burst of microwave power to the antennas to trigger the plasma formation. Should BL

generate microwaves, they can be picked up by the same antennas; isolators can shunt the power to Schottky diode-based rectifier circuits and then to a combination of capacitors, voltage controllers and batteries. This array can convert the RF from BL to useful electrical power with no moving parts, very high efficiency, minimal heat loss and no thermal cycle. As a result the reactor can have relatively high power output for its weight and size, and can be used in situations where disposing of waste heat is difficult, such as space.

Without knowing BL physics, we have a difficult time anticipating the optimal fuel. Presumably we can start with what is available in nature, but this can hardly be assumed to be the best for BL. There is a large range of possible gas mixtures, and also quite a few possibilities for sources of aerosol. Nature provides only biological sources of airborne solids of any consequence; birds, bats, and bugs. It might make sense to start with these. Gas density is another unknown, especially since most plasma phenomena work better in lab conditions at considerably below atmospheric pressure. With BL reacting rather weakly in response to its environment, it is not clear how to keep the plasmoid centered in the chamber. Nor is it clear when the anticipated microwaves are generated. If they come during the lifetime of the plasmoid, for which there is some evidence by means of radio interference, then it would be advantageous to go for long BL lifetimes. If on the other hand most of the power comes out at the end, then a succession of bursts is preferable, with the downside of more power going to BL formation and complications in RF rectification and energy storage. And finally, it is not clear what is the best scale for reactors. The general pattern one would expect is that bigger is better in terms of economy of scale, up to at least 100 MW, and that the advantages of a large volume to surface area ratio would work in favor of large reactors. Still, one expects that reactors small enough to put into airplanes, for example, would be practical given the size range of natural BL and the upper limits of known energy density.

6.5 The need for Transcendental Physics

6.5.1 Historical overview

This chapter could be book-length, but I will limit the discussion to the context required for BL research. That said, the context is quite large, and a full exposition even of this limited aim is beyond the scope of this thesis. A complete treatment would include relevant aspects of the history of the scientific method and physical theory, as well as religions and mythologies.

From the earliest efforts at cosmology, the understanding of our place in the universe included existence beyond the physical spacetime continuum. The Indian Vedas and the Buddhist cosmologies refer to other “*lokas*”, cognate to our “location”, to describe this. The Neoplatonists had a relatively advanced understanding that heavily influenced European thought for two thousand years. Proclus Diadochus⁵¹, a late Neoplatonist, was the first to use the term “*platos*”, which has since been Anglicized to “*planes*”. These planes are seen as interpenetrating and co-existing with the physical plane, and forming a series of which the physical plane is the most dense. Later Europeans used this general idea with the Great Chain of Being, which was included in scientific thought up to the nineteenth century. Vitalism was a kind of transcendental physics, but suffered from poor theory, lack of reproducible experiments, occasional fraud, and no mathematical framework. It fell to the triumph of materialism only about one hundred years ago.

The details of the old cosmologies, especially when applied to what we can observe, are at wide variance both to physical reality and to each other; different cultures result in different mythologies. The methods for investigation at these times were predominantly introspection, personal experience, and reasoning. The power of observations using the new tools of the Renaissance and the utility of calculus and other mathematical innovations drove the idea of transcendental planes from science. Thus by the early 20th century, Einstein could assert that all existence was limited to events in spacetime, strictly limited to our four spatial dimensions and time. (There was much speculation at this time about the meaning of higher spatial dimensions and possible relationship to higher planes, but just adding a physical

dimension does not suffice to produce a transcendental plane. Also, curvature through a higher dimension is equivalent to a change in the metric with no extra dimension, so measuring a curvature of space does not directly imply displacement through another spatial dimension.)

However if we collect the commonality of the global traditional understanding of other planes and their relationship to the physical plane, we see some factors that can be quite useful. As a result I will use what terminology remains relevant. The basic idea is that there is a spectrum that includes a variety of planes, although the critical variables separating and defining planes are not at all clear.

6.5.2 *Characteristics of a general theory*

Historically, the sweep of traditional cosmologies was as large as possible, trying to include everything that was thought to exist, from God to rock. This application stresses the physical plane and what lies closest to it in a general spectrum, and which therefore would be easiest to measure with physical instruments. If this near field can be established with some clarity on the basis of repeatable experiments, then those parts of the larger spectrum can be eventually addressed in a systematic fashion. At the same time, any proposed theoretical framework must be capable of expansion.

Any general theory must be well-formed and unique; there is a presumption in science that Nature exists only one way. This has made perfect sense so far, as it would be quite absurd for an electron to be fully described in two incompatible ways. (Our puzzlement over waves and particles is *our* problem, not that of the electron; QED is one theory, not two.) If there are two different theories of the same thing, applying at the same scale and accuracy, then either they have to be equivalent, or one or both are invalid to some degree sufficient to account for the difference. The observations at hand for transcendental physics are almost all subjective, and as such highly dependent on the belief system of the observer. But if we look closely, this is nothing new, and applies in some degree to all of physics, and all of science. It simply assumes central significance in this field and cannot be ignored as it

can be in, say, classical mechanics. Thus we have the critical importance for simple instrumentation with physical measuring tools and repeatable experiments that systematically include as data the mental state of all involved.

Just as with all other physical theories, the physical plane as currently described by quantum mechanics, general relativity, QED, and other very strong theories must be retained as a limiting case. At the same time, QM and GR have mysteries and incompatibilities of their own that might be profitably approached with the advantage of transcendental physics. The present efforts of string theorists to address some of these problems are certainly sophisticated, but do not qualify as transcendental; the extra dimensional states are curled and result in a purely physical plane. These string theories are neither well-formed, unique, nor answerable to experiment. It is quite possible that there can be an eventual application of something like strings or membranes, especially as membrane theory can be the basis of very interesting cyclical cosmologies such as that of Steinhardt^{52,53} and Turok, but currently the field is incomprehensible even to the experts and useless. It may be, for instance, that BL could be the result of one extra dimension uncurling to the size of the plasmoid.

It is very likely that planes result from a tendency for matter (however that ends up being defined!) to exist in certain well-defined places in the spectrum. Whatever is in-between planes could be energetically disadvantaged and would tend to migrate to a more stable place. This could be analogous to quantum bound states, although analogies are dangerous things. There is an intriguing coincidence in that the most common number for major planes (excluding the hyperfine splitting frequently mentioned) is a total of seven, sometimes eight. Most string theories have three spatial dimensions that are uncurled, and a total of 10 or 11 dimensions (including time). If one spatial dimension were uncurled at a time, this would result in seven or eight planes.

The initial assumption can be that the physical plane is characterized by a high degree of polarization (in terms of the strength of charges, small particle sizes, very dense nuclear matter, the effects of physical constants and so forth). We should expect variability in the direction of less extreme conditions elsewhere on the spectrum. Also, other planes are

universally reported to be more responsive to the thoughts and desires of the observer; this reaches some rather extreme levels in the higher planes where the identity of the observer typically becomes unrecognizable from our usual context and can even be temporarily obliterated. Stray desires and resistance to dissolution of the boundaries that define our “self” are the main barriers to experiencing these states in person. (Unfortunately, the practice of science in the usual way tends to increase these barriers.) The physical plane is also responsive to thoughts and desires, but in a very clumsy and usually very slow, manner; unless one looks for it, such can be easily overlooked, even when our entire environment is artificial. We can expect little progress when looking for near-physical phenomena if this interplay between consciousness and physics is overlooked or denigrated.

We suffer from a disadvantage in measurement as it is probable that observing a more-dense, or “lower”, plane is much easier than observing one that is less dense, or “higher”. If this is true then it would serve notice that our physical plane is the lowest.

Time is another factor with interesting characteristics. Our usual causality is a product of being limited to spacetime. However, if it is possible to transfer from one plane to another, or even to observe (gather information) between planes, then such limitations no longer apply. Subjective experience frequently mentions a very different meaning for time in relation to other planes, and we should expect such effects. We may gain some traction on this issue by means of quantum mechanics; for instance, there are problems with regard to transitions between states that require instant change over a finite volume of space, which is not possible.

Eventually a general theory will address issues currently left to fields other than physics, so that a more cross-disciplinary approach will be required. These will have to include our own awareness, the nature of consciousness, and other matters now the subject of psychologists and religions. It is a good measure of the primitive state of our understanding that we find such a range of philosophies, mostly incompatible, to describe the same universe.

At the same time, little is gained by attempts to force-fit unquantifiable subjects to literal measurement. There is a tendency in the physics of today to regard anything not reducible to a variation in voltage as an illusion. For certain contexts this is an understandable habit that doesn't matter much, but in this context it is fatal. We can profitably consider the natural laws that stand behind the full spectrum of planes without requiring a clockwork universe; in short, we need a higher understanding of mechanics. Then we can more gracefully study and develop what used to have the much preferable name of Natural Philosophy.

6.5.3 Physical applications and experiments

While my focus is on BL, there are many reasons to believe that transcendental physics will greatly enhance the conventional physics of the physical plane. There are many puzzles that have eluded resolution that could be addressed to a useful degree with a multiplane approach. This does not imply that mysteries will ever be eradicated, especially since the scope and recalcitrance of mysteries tends to expand the harder we look at the universe. It does appear, though, that using only physical tools and physical senses has given us a very partial picture of reality, and any partial picture is an illusion—especially when we don't know what's missing.

There is a range of research paths from the purely organic and parapsychological, to the more conventional physics routine. While there is much to be gained from investigating near-death experiences (some of the best accounts of other planes come from these), placebo effects, twin connections, and similar, my focus is on the physics experiment side. Rupert Sheldrake⁵⁴ has very interesting ideas and suggestions for research, but his expertise is in cell biology and so has that bias. (Some of his conclusions, such as suspecting a sizable variability in the speed of light in vacuum as measured over the last century, could use some more background in physics. This would result in refraction of starlight as it passed through regions of variable speed that would be very easy to detect.)

One interesting possible application is in the search for dark matter and dark energy. The characteristics of the gravitational anomaly that we can image around galaxies might result from interactions from other planes. If so, then the search for physical particles will come up either empty or misleading; we could misinterpret a positive experiment that actually registered a transcendental interaction for a detection of weakly interacting physical particles. Our conceptual framework could determine not only the experiments but the results, so we can only hope that we are not misled. We could expect cosmological consequences for any reasonable transcendental theory, and with such a large proportion of the universe unspoken for, this is a major inducement for research.

There are many quantum puzzles related to the nature of the observer, what it means to collapse the wave function and when that actually occurs, and so forth. These many questions have been in play for the entire history of QM, and there is no consensus on solutions. Indeed, there are many philosophical interpretations of QM that are compatible with the mathematics. Many existing experiments take advantage of quantum weirdness to explore the relationship of consciousness and physical reality.

The Princeton Engineering Anomalies Research group was a notable organization that did this, and related experiments, for 28 years until 1997. “The enormous databases produced by PEAR provide clear evidence that human thought and emotion can produce measurable influences on physical reality.”⁵⁵ (Their work is now transferred to the International Consciousness Research Laboratories.⁵⁶) This kind of work by many researchers, with a full range of credibility from excellent to execrable, has been going on for the entire history of science; a full account of the field is beyond the scope of this paper.

6.5.4 Why BL needs Transcendental Physics

BL does not have any excuse to exist under the known laws of physics, as detailed above in section 2.3.2. We have no choice but to expand the physics to include observations. Without laboratory BL, though, we have little chance to get enough data; and our mode of

thinking must be flexible enough to allow us to accept a valid result. The proposed theories constrained to the present understanding of physics are all woefully inadequate.

BL does not interact with its environment in a way shared by any other physical object. Despite its luminosity strongly implying temperatures well above ambient, BL has felt cool to the touch to many observers who have had contact with it. (A minority of these report warmth and a few have been burned; as some BL has a smooth surface and others have flames, indistinct boundaries, and even smoke, there may be hot regions in some BL that is peripheral to the inner core and interacts differently.) BL has neutral buoyancy and frequently moves without regard to wind direction; thus it does not fall under the usual constraints of fluid dynamics. It does not interact with the atmosphere by thermal conductance or physical pressure. If air passes freely through it, this air has no cooling effect. If air does not pass through it, that is even stranger since the air is not displaced by what should be a less dense object, given its high temperature.

From this argument, it is probable that BL is a superposition of two states. The underlying physical environment stays as it was before, and BL also exists *in the same volume of space*. This would help to explain the lack of interaction with barriers, limited thermal energy loss by conduction or convection, the indifference to wind direction, and no upward buoyancy. After all, the main idea of transcendental physics is that the full spectrum of states are superimposed over each other and interpenetrate; we can see the BL because it is only slightly and temporarily displaced.

It is not clear whether BL responds to gravitational forces or not; it does tend to fall out of clouds but usually keeps some distance off the ground, frequently hovering or moving laterally. Any motion of a plasmoid in the atmosphere would be influenced far more by fluid dynamics and electrical and magnetic fields than by gravity, so this question cannot be resolved out of the laboratory. However difficult, a gravitational test is important since the “force” is really fictitious and comes from the acceleration of inertial frames by mass. If BL exists in a way that refers to a different kind of inertial frame, then it might easily have a much different gravitational interaction with the local field.

BL sometimes bounces off of physical objects, but frequently passes through them. Most of the time this results in no change to either the object or the BL. Sometimes there is damage to the object, such as shattered windshields on cars and holes burned in glass windows. There are no macroscopic physical objects that have any such characteristics for unhindered passage through solid barriers. Investigators have carefully measured objects that have recently interacted with BL for residual radioactivity and have found none. Thus there seems to be no interaction even on the nuclear level, which strongly constrains subatomic particle passage. (The only particles that could penetrate walls and still be part of a low-velocity object that lasts long enough would be neutrons, which clearly are not the main constituents of BL, or a microscopic black hole, which cannot form and disappear in the manner required.) All the physical forces that we know of that could serve to confine BL rely on electrical charges, on ions or electrons, which are precisely what would cause very high collision cross-sections and immediate interaction with any solid object. Reports of underwater BL are maximally anomalous for these reasons, and are strong indicators of a superposition of states.

The extreme energy density of high-energy BL is another key example of the inadequacy of physical theory. The total energy of such a volume of gas at roughly 5000 K is quite small given the low specific heat of air and its low density, and is incapable of doing the damage reported. Much of the hard evidence left behind shows signs of exposure to high levels of microwave radiation, for which there is no physical mechanism known, either to supply the energy or generate the RF. As BL can form without linear lightning, as has been witnessed repeatedly, there is no correlation between energy needed for formation and that released during its existence or at its dissolution. Thus all of our tools for using conservation of energy do not seem to apply. We should expect conservation laws to be in effect, but if there is an apparent violation, then we are failing to see everything that is going on.

BL observations are consistent with the following idea. Suppose the physical plane is a stable state at or near one end of a continuum which has a series of other stable states along its range. Outside these states is not favored, probably for some kind of energy minimization

analogous to our customary physics. For some unknown reason, a volume of physical space becomes dislocated slightly, becomes a dual superimposed physical-near physical state, and interacts with its surroundings primarily by means of EM radiation. We could figure out some characteristics of the continuum by considering the behaviour of BL during the time of this dislocation. Some BL appears to be a mixed state with outer coatings that are purely physical and that interact as expected, trailing smoke and sparks in some cases. At the moment that the volume of space returns to a purely physical plane, the BL acts just as it should by our understanding of physics and immediately decays. Intermittent BL, which has been seen to flash into and out of existence, could be explained by its variable distances from the physical plane; when too far away, the radiation interaction fails. Energy could be conserved as excess energy would simply be transferring from other planes; another possibility would be exotic reactions not possible under purely physical conditions.

Not just anything is possible, of course, and some more detailed understanding of the proposed continuum is required before any progress can be anticipated. This is a rough conjecture pointing in a direction that could be developed when the time is right. There must be an explanation of why a given volume of space would exist in a different way than the usual, how it becomes defined and why it ends.

6.5.5 *Problems in Transcendental Physics*

The whole of the scientific method—at least in its idealized form—relies on a separation of observer and observed, as well as on reproducibility of measurements. While purely observational sciences like astrophysics get a pass on the strict sense of reproduction, such is not the case for a near-field subject like BL, or transcendental physics in general. As put by Tetens (1995)⁵⁷;

“While the requirement of reproducibility is largely uncontroversial in physics, chemistry, and biology, the possibility of reproducible experiments in behavioral science, psychology, and cultural science is questionable. The reason is that in experiments about the behavior and action of human beings the test persons *know* that an experiment is

repeated. This reflexive knowledge changes the initial and boundary conditions of the original experiment in a way which is essential for its outcome. As a consequence, the original experiment cannot be repeated under the same initial and boundary conditions.”

Any system showing a direct relationship between mental and material states produce problems currently intractable without modification of standard scientific procedure.⁵⁸ The case of a skeptic who insists on being shown the results of an experiment that shows sensitivity to the mental states of participants is analogous to a person who denies that film is sensitive to light, and that photographic negatives can be developed in a darkroom. To prove his point he insists on bringing in a flashlight to make sure things are done without fraud.

The advantage of BL is that it could be a phenomenon only slightly displaced from a physical state, and thus one would expect much more indifferent to the thoughts of observers than for something far removed from physical. Thus the plans for further experiments do not specifically focus on mental states, nor would this be diplomatic or advantageous to stress in grant proposals (here I indulge in understatement). Still it would be a very good idea to keep records of the general thought patterns of participants and treat them as an experimental variable just as a matter of course, since generically this would be important in any transcendental physics experiment. With practice from a nearby case like BL, such a research protocol could be extended and refined for investigating further away from the physical plane.

There is a great deal of information to be gained from seeing what kind of information cannot be demonstrated. Personally, I have no problem accepting the existence of higher planes, as I have experienced them hundreds of times, as well as occurrences that would be impossible with only physical existence. This is true of millions of people over the whole course of human history. But we find it impossible to actually demonstrate the existence of anything but physical reality. This is true even though the very existence of self-awareness is clearly transcendental, so that every thought and experience is fundamentally beyond just the physical plane.

This planet is safe for scientific materialists. Any hard-core skeptic who insists on unequivocal, undeniable demonstration that the physical plane is not all there is, will be satisfied. James Randi will not have to pay his prize money to anyone. Why is this? The shadow left by this peculiar condition is itself a kind of evidence, even though the existence of the shadow is not possible to demonstrate to a skeptic. I term the phenomenon “blockage”. It’s a necessary mechanism for the moment, but times change. Blockage is the impediment for any incontrovertible, undeniable, verifiable and repeatable evidence for the existence of anything beyond the physical plane that can be shown to others, especially skeptics. The evidence for blockage is itself blocked, since it could only exist if the physical plane was not unique. Blockage does not necessarily apply to individual experience, as the idea is that the general culture is shielded from evidence. However, almost all individuals do experience it internally as well, such as the general rule that people forget past lives.

This would at first blush appear to be off-topic for this thesis, but my understanding is that it is central to the mystery of BL, and why we have no theory for it nor laboratory recreations. My proposal for the fundamental nature of BL cannot be acceptable or be the basis for technology, such as a reactor, until there is no longer blockage of transcendental physics in the consensus reality.

Once this blockage lifts—as I believe it will in time—we can start to extend science to the greater reality. Fundamental to this is instrumentation; we need simple measuring tools before there is any hope for transcendental physics. Very interesting experiments have shown activity with nuclear decay⁵⁹, but while it poses interesting quantum mechanics philosophical quandaries, it does not yet rise to the status of a voltmeter. Living organisms are already examples of physical objects that interact strongly with other planes, but we have to translate this interaction into something measurable. I have tended to favor such experiments with very simple organisms such as plants or micro-organisms.

6.5.6 *The Oracle experiment and ITC*

Another approach, one tried by a long series of inventors and scientists including Thomas Edison, is to build a device that can pick up transmissions sent from other planes. This could be thought of as a SETI program for astral physics instead of astrophysics. As one might imagine, this also is blocked; it is quite interesting to see the blockage in action once one looks for it. Experimenters have found over the years that quite simple devices can be effective, but to avoid blockage, the mental and spiritual orientation of all the people in the group involved must be correct; and whatever tangible evidence that results must always be consistent with something that could have been faked, even if such fraud is far-fetched and everyone connected to the experiment knows that it is genuine.

Mark Macy⁶⁰ has been active in instrumental transcommunication (ITC), which is a term coined in Europe some years ago to describe this field. Many of the groups making good progress in the ‘80s and ‘90s have dissolved and the times are frustrating for all involved.

I was active in ITC from 1979 to 1990, working full-time during the last half of the ‘80s. I called my device the Oracle, and have a paper on the project listed on my website. The details are beyond the scope of this thesis as ITC is not directly involved in BL, although it would be a critical tool for understanding the physics. Unfortunately the Oracle did not work, as it was premature and, as you might imagine, blocked. My emphasis was on the device and only secondarily to the personal and group dynamics that are the only way ITC can work at the moment.



Figure 6.2: Oracle experiment. Control room with optical resonator, April 1990

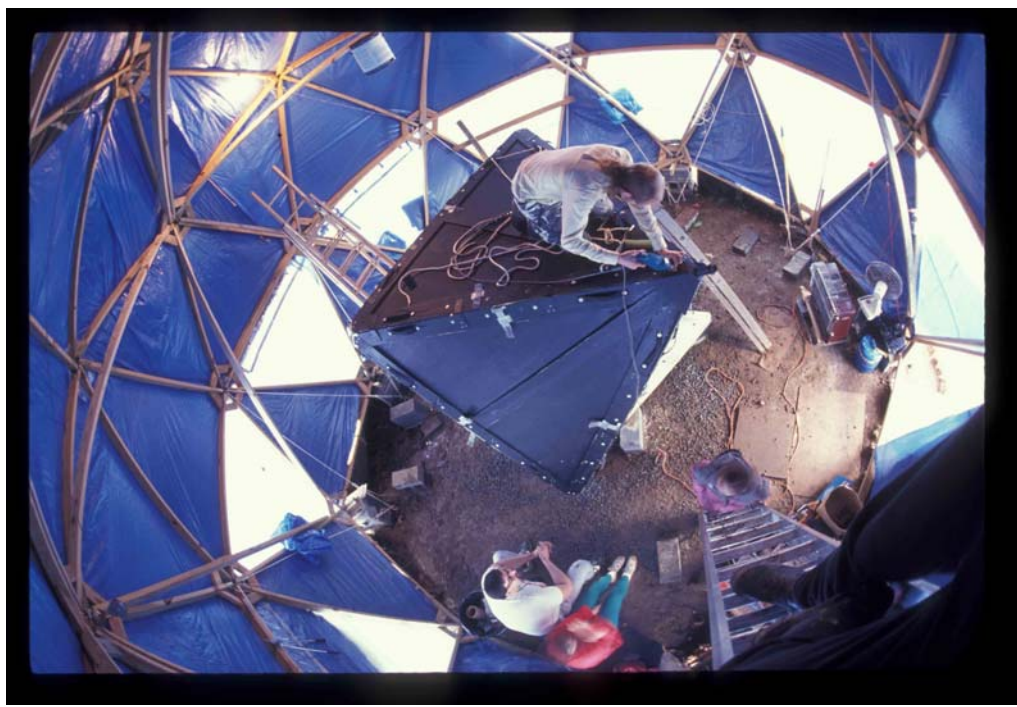


Figure 6.3: assembling the antenna in its dome

REFERENCES

¹ Reuters Friday Jan. 30, 2009

<http://www.reuters.com/article/newsOne/idUST8310320090130?rpc=64>

² John B. Calhoun, MD, Proc. Royal Soc. Med. **66** (January 1973).

³ Seth Putterman, Scientific American, February (1995).

⁴ M. Brenner, S. Hilgenfeldt, and D. Lohse, Reviews of Modern Physics **74**, 425 (2002).

⁵ S. J. Putterman and K. R. Weninger, Annual Review of Fluid Mechanics **32**, 445-446 (2000).

⁶ D. Shapira and M. J. Saltmarsh, Phys. Rev. Lett. **89**, ISSN 1079-7114 (19 August 2002).

⁷ Steven Krivit is a excellent journalist on CF, see his <http://newenergytimes.com>; also work by George Miley, Edmund Storms

⁸ Edmund Storms, Infinite Energy **4**, #21 (1998).

⁹ E. Yamaguchi and T. Nishioka, Jap. J. Appl. Phys. **29**, No. 4, L 666-L 669 (April 1990).

¹⁰ Y. Iwamura, T. Itoh, and I. Toyoda, Fusion Technol. **26**, #4T p. 160 (1994).

¹¹ A. G. Lipson et al., The Sixth International Conference on Cold Fusion, Hokkaido, Japan, Vol.2, 433, (1996), edited by M. Okamoto

¹² http://www.absoluteastronomy.com/topics/Ball_lightning

¹³ Ball lightning Page, <http://www.amasci.com/tesla/ballgtn.html> (a major source of current information and archived eyewitness accounts)

¹⁴ Ball lightning photographs,

http://www.ernmphotography.com/Pages/Ball_Lightning/Ball_Lightning_ErnM.html

-
- ¹⁵ Vladimir Dikhtyar and Eli Jerby, Phys. Rev. Lett. **96**, 045002 (3 Feb. 2006).
- ¹⁶ M. D. Altshuler, L. L. House, and E. Hildner, *Is Ball lightning a Nuclear Phenomenon?* Nature **228**, 545-546 (1970).
- ¹⁷ Warner Cowgill, US Consulate, letter to Scientific American **55**, 389 (1886).
- ¹⁸ Eugene Garfield, *Essays of an Information Scientist*, (1974-76), Vol. **2**, p.479-490.
- ¹⁹ John Abrahamson and James Dinniss, Nature **403**, 519-521 (3 February 2000).
- ²⁰ S. L. Friedlander, H. D. Jang, and K. H. Ryu, Appl. Phys. Lett. **72**, 173-175 (1998).
- ²¹ B. M. Smirnov, Phys. Rep. **152**, 177-226 (1987).
- ²² J. D. Barry, *Ball Lightning and Bead Lightning* (Plenum, New York, 1980)
- ²³ D. J. Turner, Phil. Trans. R. Soc. Lond. A **347**, 83-111 (1994).
- ²⁴ G. S. Paiva et. al., Phys. Rev. Lett. **98**, 48501 (2007).
- ²⁵ Artificial Ball Lightning produced in the laboratory, Martijn Goossens, Pascal de Graaf, and Ronald Dekker <http://www.dos4ever.com/bolbliksem/bolbliksem.html>
- ²⁶ Susan Fontaine, private correspondence
- ²⁷ 2002 Melbourne BL photo and testimony,
http://www.ernmphotography.com/Pages/Ball_Lightning/Ball_Lightning_ErnM.html
- ²⁸ M. Hirsh and H. Oskam, *Gaseous Electronics* (Academic Press, 1978)
- ²⁹ Dan Green, James Leggett, and Richard Bowtell, Magnetic Resonance in Medicine **54**, 656-668 (2005).
- ³⁰ F. Chen, *Introduction to Plasma Physics and Controlled Fusion* (Plenum Press, 1984), Vol. **1**
- ³¹ J.D. Barter, J.C. Sprott, and K.L. Wong, Phys. Fluids **17**, 810 (1974).

-
- ³² J.D. Barter, J.C. Sprott, and K.L. Wong, Phys. Fluids **17**, 810 (1974).
- ³³ P. Baille and Jen-Shih Chang, J. Phys. B: At. Mol. Phys. **14**, 1485-1495 (1981).
- ³⁴ J. D. Huba, *NRL Plasma Formulary* (Naval Research Laboratory, Washington, DC, 2000)
- ³⁵ Xue-Heng Zheng, Phys. Lett. A **148**, 463 (1990).
- ³⁶ N. J. Fisch, J. M. Rax, and I. Y. Dodin, Phys. Rev. Lett. **91**, Number 20 (14 Nov. 2003).
- ³⁷ Donald L. Ensley, Shape stability for a plasma contained within a standing electromagnetic field, Phys. Fluids **22(12)**, 2359 (1979).
- ³⁸ F. Chen, *Introduction to Plasma Physics and Controlled Fusion*, (1984), p.308.
- ³⁹ Erich Weibel, in *The Plasma in a Magnetic Field*, edited by Rolf Landshoff (Stanford University Press, Stanford, CA, 1958)
- ⁴⁰ A. Komori, Y. Takada, A. Yonesu, and Y. Kawai, J. Appl. Phys. **69**, 1974-1980 (1991).
- ⁴¹ D.T. Emerson, The Gain of the Axial-Mode Helix Antenna
<http://www.tuc.nrao.edu/~demerson/helixgain/helix.htm>
- ⁴² ITC ceramic information: <http://www.bigceramicstore.com/Supplies/ITC.htm>
- ⁴³ Tom Ligon, Infinite Energy, issue **30** (2000).
- ⁴⁴ Ryan Meyer, *IEC thesis, U. of Missouri-Columbia*, 2007
- ⁴⁵ Todd Rider, A general critique of inertial-electrostatic confinement fusion systems, Phys. Plasmas 2 Vol. **6**, (1995).
- ⁴⁶ J. Park, R. A. Nebel, and S. Stange, Physics of Plasmas **12**, 056315 (2005).
- ⁴⁷ F. Chen, *Introduction to Plasma Physics and Controlled Fusion* (Plenum Press, 1984), Vol. **1**
- ⁴⁸ Donald L. Ensley, Shape stability for a plasma contained within a standing electromagnetic field, Phys. Fluids **22(12)**, 2359 (1979).

⁴⁹ R. Geller, *Electron Cyclotron Resonance Ion Sources and ECR Plasmas* (IOP Publishing Ltd., London, 1996)

⁵⁰ Y. Rao, Jiannan Wu, Yuhong Yan, Yong Zhang, and Lei Qi, Rev. Sci. Instrum. **65** (4), 1127 (April 1994).

⁵¹ Proclus Diadochus, in *The Elements of Theology*, 2nd ed.th edition, edited by E. R. Dodds (Clarendon, Oxford, 1963)

⁵² Paul Steinhardt's web page, <http://wwwphy.princeton.edu/~steinh/>

⁵³ Bill Robinson, Cyclocosmos (a research paper in antiquarian verse concerning the Cyclic Universe cosmology of Steinhardt and Turok)

<http://www.billrobinsonmusic.com/Documents/CyclocosmosPDF.pdf>

⁵⁴ Rupert Sheldrake, *Seven experiments that could change the world : a do-it-yourself guide to revolutionary science* (Fourth Estate, London, 1994)

⁵⁵ PEAR, <http://www.princeton.edu/~pear/publications.html>

⁵⁶ ICRL

http://www.icrl.org/home/index.php?option=com_content&view=frontpage&Itemid=1

⁵⁷ H. Tetens, Reproducibility, in *Enzyklopädie Philosophie und Wissenschaftstheorie Band 3*, edited by J. Mittelstrasse et al. (Metzler, Stuttgart, 1995)

⁵⁸ Harald Atmanspacher and Robert Jahn, J. Scientific Exploration **17**, No. 2, 243-270 (2003).

⁵⁹ Henry P. Stapp, *Theoretical model of a purported empirical violation of the predictions of quantum theory*, Phys. Rev. A **50** No. 1, (July 1994).

⁶⁰ ITC homepage, <http://www.worlditc.org/>

⁶¹ Cold fusion website <http://www.mit.edu/people/rei/CFdir>

⁶² E-Quest information from the Sono Fusion Sonoluminescence Home Page, <http://www.hooked.net/~rgeorge/sonof.html> and links

⁶³ Los Alamos National Laboratory Report on Production of Tritium in Glow Discharge Cold Fusion, <http://wwwnde.esa.lanl.gov/cf/tritweb.htm>

⁶⁴ H. R. Taplin, Infinite Energy **18**.

⁶⁵ Sonofusion history, <http://home.fuse.net/clymer/sn/>

⁶⁶ R. Lofstedt, B. Barber, and S. Puterman, Phys. Fluids A **5**, No. 11, 2911 (1993).

⁶⁷ Margulis M. A., (1995) *Sonochemistry and Cavitation* (Gordon and Breach)

⁶⁸ Gaydon A. G., Hurle I. R. (1963), *The Shock Tube in High-Temperature Chemical Physics* (Reinhold Publishing Co.)

⁶⁹ Thompson P. A. (1972), *Compressible-Fluid Dynamics* (McGraw-Hill)

⁷⁰ Andresen A. F., Maeland A. J. eds. (1978) *Hydrides for Energy Storage* (Pergamon Press)

⁷¹ H. R. Taplin, Infinite Energy **18**.

⁷² Reader G. T., Hooper C. (1983), *Engines* (E. & F. N. Spon)

⁷³ Rosa, R. J. (1987) *Magnetohydrodynamic Energy Conversion* (Hemisphere Publ. Corp.)

⁷⁴ Sutton G. W., Sherman A. (1965), *Engineering Magnetohydrodynamics* (McGraw-Hill)

⁷⁵ Messerle H. K. (1996), *Magnetohydrodynamic Electrical Power Generation* (Wiley & Sons)

⁷⁶ G. Kistiakowsky and P. Kydd, J. Chem. Phys. **25**, No. 5, 824 (1956).

⁷⁷ Gaydon A. G., Hurle I. R. (1963), *The Shock Tube in High-Temperature Chemical Physics* (Reinhold Publishing Co.)

⁷⁸ R. H. Wiswall and J. J. Reilly, Inorg. Chem. **11**, No. 7: 1691 (1972).

⁷⁹ Dushman, S., Lafferty, J. (1962) *Scientific Foundations of Vacuum Technique* (John Wiley & Sons)

⁸⁰ Stone, Richard (1993), *Introduction to Internal Combustion Engines*, 2nd Edition (Society of Automotive Engineers, Inc.)

⁸¹ Maly R.R., (1984) “Spark ignition: its physics and effect on the internal combustion engine”, in J.C. Hillard and C.S. Springer (eds.), *Fuel Economy of Road Vehicles Powered by Spark Ignition Engines* (Plenum, NY)

⁸² Kistiakowsky, G., Kydd, P. (1956) “Gaseous Detonations. IX” *J. Chem. Phys.* 25, No. 5, 824

⁸³ Thompson P. A. (1972), *Compressible-Fluid Dynamics* (McGraw-Hill)

⁸⁴ Vargaftik, N. B. *Tables on the Thermophysical Properties of Liquids and Gases*, 2nd ed. (Wiley & Sons)

⁸⁵ Cohen H., Rogers G.F.C., Saravanamuttoo H.I.H. (1987) *Gas Turbine Theory* (John Wiley & Sons)

⁸⁶ *Infinite Energy*, journal and website <http://www.infinite-energy.com>

⁸⁷ US Patent 5522905 - Diesel fuel containing an additive which improves the combustion of soot

⁸⁸ Dan Green, James Leggett, and Richard Bowtell, *Magnetic Resonance in Medicine* **54**, 656-668 (2005).

APPENDICES

7 Appendix A: Warm Fusion I (1998)

Note [2009]: Both parts of this warm fusion paper were from early stages of my research in alternative energy schemes, before my beginning studies at NCSU in 2001. Shortly after writing this it became obvious that for the idea to be valid, the hydrides involved would have to behave as high explosives—which they clearly do not. As a result, the idea is quite imaginary and cannot be the immediate basis of further research. This paper does provide the approximate requirements for reactions in hydrides which would make detonation shocks possible. I include the two parts of this paper as an appendix to the main thesis for purposes of context. As there are anomalies reported, I do still think that some kinds of LENR are probably happening, but they will take some time to discover, reproduce at will, study, and utilize. Many of the references are to sources that have since proven pathological, but the complete sorting out of which are valid and which not is an unfinished process.

7.1 Warm Fusion I: TiD₂ and D₂ Gas

Abstract.

Given an aerosol at moderate temperature of D₂ with a fume of extremely fine particles of TiD₂, a Chapman-Jouguet detonation shock wave could provide a suitable environment for a self-sustained reaction. This reaction (or reactions) would be of the type already demonstrated in bulk hydrided titanium when stimulated by microscopic shock waves in heavy water, and termed “cold fusion”; the detonation “warm fusion” process increases the severity of the heat and temperature, increases the surface area of the catalyst powder maximally, and scales up the process to macroscopic size. The resulting high power density is comparable to conventional combustion, with the result that the hot gas finds utility in similar fashion to combustion gases. No radioactivity is anticipated as none has been observed in previous cold fusion experiments. This paper concentrates on the mechanics of the shock, and includes a brief overview of applications in piston fusion engines and fusion turbines.

7.2 Cold Fusion

7.2.1 Show me

No cold fusion experiment yet is able to generate useful work, despite several demonstrations in different labs of excess heat beyond chemical capacity to produce, and isotopic and elemental transmutation.^{61 62 63} Something is certainly happening--there are philosophical and political reasons to denigrate what appears to be solid evidence of anomaly, as the degree of anomaly is great and some of the CF science has been shoddy--but any disinterested observer must conclude by now that something indeed is observable, beyond conventional theory. Few observers, sadly, are disinterested. Nuclear transmutations such as have been claimed would be expected to produce well-defined radiation which is not observed--and there is no understanding why not. This and other fundamental oddities make acceptance of CF absolutely dependent on a viable and unambiguous application for acceptance into the general culture.

7.2.2 Work to date

While techniques vary, they usually have in common:

- presence of deuterium and/or hydrogen either in gas or water, in proportions from 99%+ D to H (heavy water or D gas), to one atom of D to 4000 or 5000 of H as with light water.
- presence of a catalyst, usually palladium (Pd), nickel (Ni), or titanium (Ti); these three have worked the best in most experiments. In some experiments the metal transmutes, and thus is part of the fuel, such as $\text{Li}^7 + \text{H} \rightarrow 2 \text{He}$.
- application of electrical current; generally this is in an electrolyte with voltage at modest levels applied to electrodes, one of which is the catalyst. This is missing when either other methods insert H or D into the metal catalyst, or when the reaction doesn't involve H or D in a solid lattice, as with the Li-H reaction noted above⁶⁴.
- radiation output (of the sort expected from the transmutations if done with conventional thermonuclear methods) that if present at all, is entirely insufficient to account for the excess energy. This is one aspect of the complete ignorance of the actual reactions.

Some experiments try to amplify the reactions by methods like ultrasonic stimulation and cavitation⁶⁵, or modifying the surface of the electrodes, or trying new catalysts like high-temperature ceramic superconductors. The highest temperature shown yet in any macroscopic scale with pure CF is that of boiling electrolyte at 1 atm. pressure, and only in very small cells. These techniques reach neither useful heat-engine temperatures, nor high pressures, nor significant volumes for the zone of reaction, nor even robust repeatability, all of which--in addition to a high yield/energy input ratio--are required to apply whatever's going on to any useful purpose. And without an unequivocal application that cannot possibly be faked, cold fusion will continue to have the reputation of pathological science.

7.2.3 *Why they wimp out*

Conditions in existing electrolytic CF experiments are relatively moderate for two basic reasons; the limitation on the applied electrical power, and the low catalyst surface area. As the electrolyte is a good conductor, no appreciable electric field can occur across electrodes, and application of voltages much above about 2 V leads to dissociation of the water. To make more extreme conditions would require passing a spark through pure water, but with solid electrodes as catalysts this is ineffectual. Sparks underwater are very difficult to produce and control due to the high dielectric constant which reduces any electric field by 80 times, and by the high current and voltage required to achieve breakdown.

The second problem is the catalyst geometry. Thin films, wires, plates and foil don't work well. Some show signs of microexplosions, others of various effects of small-scale events within the lattice and at the surface. Sometimes there is plain evidence of transmutation of the metal, some of which would absorb energy, some release it. Whatever is going on is locally highly energetic and not generally spread out as a low-density reaction over either the surface or the volume of presently-used electrodes. Were any such electrode to produce useful power levels it would disintegrate; as a macroscopic solid it's unlikely to be able to produce such power anyway, not to mention conducting it to a heat engine or other application. Interaction with H or D, and giving up heat to a working fluid, is a function of

surface area--which in proportion to volume is evidently insufficient with macroscopic solids to provide sufficient mass flow or heat transfer for practical power production.

There is an additional problem with current cold fusion development. Should the most practical reactors only boil water, especially if the reactors are complex and bulky, most power production would remain in electrical power plants, ships, or facilities using large amounts of hot water or steam. Fuel synthesis could substitute for fossil fuel in transportation as hydrocarbon supplies diminish, but all the liabilities of carrying a flammable and finite fuel supply would continue. This would make unavailable the benefits of having a fusion reactor on hand--no fuel to buy, range limited only by maintenance, and nothing to burn in an accident. Also, the existing prime mover infrastructure, based mostly on internal combustion (i.c.) engines and worth untold hundreds of billions of dollars, would be unconvertible to fusion, and dependent on inevitably costly synthetic fuels once the petroleum runs low. More ominously, oil and other carbon-based fuels would continue to have a prominent role in the energy economy as long as the cost of production beats that of synthetics--which would be for a long time yet even with cold fusion in operation as currently envisaged.

7.3 *History of this Research*

7.3.1 *Beginnings*

The first 14 months of my research in fusion, starting in early 1995, was in the context of deuterium bubbles in water (or heavy water).⁶⁶ This was intended to use conventional hot fusion reactions with inertial confinement. At first these bubbles were from ultrasound, modeled after the many recent experiments with sonoluminescence. Later as I got into the details, I tried forming bubbles with sound and then hitting them with other energy sources for inertial confinement fusion. None of these methods stood up under even rudimentary study, and I turned to other interests.

In the spring of 1997 I saw on the Internet that cold fusion research was in much better shape than I had thought, so I started converting my old ideas to cold fusion methods. After some time I found that none of the well-known methods of generating ultrasound work

well under conditions of both high pressure and high temperature, nor are they economical when near pressure and temperature limits either in money to build or energy to run. This is especially true since sound intensity must be more and more severe to cause cavitation as ambient pressure rises, and the volumes affected are minute.

The next step was finding a schematic for a simple device for forming tiny sparks underwater in a Russian text on sonoluminescence and related chemistry⁶⁷. It works like a doorbell, with a probe closing the circuit when in contact with its target, and that circuit including a coil around a magnetic core connected to the probe. This pulls the probe away from the target, causing a spark gap until the distance is too great and the circuit opens. In the original, gravity pulls the probe and magnetic core down again to the target, completing the circuit again and starting the cycle. Margulis found that the sparker caused sparks starting in the range of 20 to 60 V, with typical sizes of fractions of a millimeter.

There are great advantages to making cavitation bubbles with sparks instead of sound or dynamic methods. The spark causes vapor bubbles in degassed water with high temperatures and pressures, with an outwards shock wave. When the spark stops the cavitation implosion also causes high temps and pressures. This ability to create bubbles continues even under high ambient pressures, although with a sacrifice of bubble volume.

7.3.2 *Turning point*

However, making such bubbles was not in itself sufficient. I then came to understand that addition of fine metal powder to the water in high density would solve many problems, as the current, heat, and pressure would include the catalyst metal and dissociated hydrogen. Also the surface area of the powder maximizes the catalysis. The limitation that the water be non-conductive for spark formation is not a problem, as the colloid is no more conductive than the original pure water. The effective gap is reduced by the volumetric proportion of metal, which is a minor factor. As sparks will form hydrogen peroxide and nitrogen compounds if there is air in solution, the water should be nearly gas-free.

After some consideration I understood the probable limitations of this method, especially the problem of powder condensation from plasma with interaction with oxygen

from the water, and also the need to hydride the powder--not possible in water by this method.

7.3.3 *D₂ and Aerosol Catalyst; Warm Fusion*

On abandoning water as the medium of choice, this left deuterium gas with aerosol metal powder as the catalyst.

There are major advantages to gas. With water, if D₂O were required, any reactor would use so much as to be extremely expensive. The mass of D₂ gas would be far less and much cheaper as a result to fuel a reactor, even if at considerable pressure (which is unlikely). D₂ is a very good working fluid for heat engines as it has a high heat capacity and low viscosity. Hydrogen embrittlement requires the use of non-corrosive materials like ceramics, high alloy steels, and non-ferrous metals. D₂ is a prime candidate for *shock tubes*, and shock formation in general.⁶⁸ This is an efficient and practical method for attaining in bulk the same extreme conditions at the microscopic center of cavitating bubbles. Most importantly, the metal powder should recondense from plasma onto cool aerosol powder without oxidation or other water-related problems.

Currently I focus on starting and propagating the reaction by means of a Chapman-Jouguet shock wave.⁶⁹ This may not be sufficient, in which case ignition may require a high-power laser. This would make any reactor large and costly, and hard to achieve break-even. Since first experiments will be exclusively with shocks, I mention the laser alternative only in passing--and will deal with it in detail if shocks do not work.

I now call the reaction *warm fusion* (WF), thus emphasizing the higher temperatures and pressures than previous cold fusion experiments.

After close study of various stable binary metal hydrides, the best candidate for straight D-D reactions--on which this paper focuses--is titanium deuteride (TiD₂) for the aerosol powder.⁷⁰

Currently I am investigating another kind of reaction with a similar method, Li⁷ + H → Be⁸ → 2 He, as well as Li⁶ + D → ⁷Be + n. Crystal Energy Inc. proposes the first reaction as the explanation for anomalous energy release from lithium additions to fossil fuel in

external and internal combustion applications⁷¹. As they detect soft gamma rays, x rays, and alpha particles of appropriate energies, there is some compelling evidence; note however that this is not conventional thermonuclear fusion since the radiation is in no way enough to account for the excess energy. They have not been able to get the reaction to work without fossil fuel; therefore the possible use of Li⁷H particles in H₂ gas or Li⁶ in D₂ in the same reaction chambers as used for warm fusion holds great promise. This will be the subject of the second paper in this series.

7.3.4 Reactor types

Two applications come directly from developed heat engines. One is the *fusion engine*, which uses the explosive nature of reactions just like internal combustion engines. This could be an easily designed and constructed reactor, especially as the i.c. engine technology is so well developed. However there are serious problems with seals, rings, and lubrication that may result in WF engines resembling Sterling engines in materials and machining tolerances. This would make them at least 1.5 times more expensive than conventional i.c. engines even in mass production.⁷²

The other application is the *fusion turbine*, an adaptation of gas turbines in closed cycle. This requires reaction chambers providing a steady flow of gas within the temperature limits of the turbine inlet. There are any number of ways to do this, with one method mentioned in this paper. Otherwise the function and design would be little changed from current turbines, assuming materials do not suffer from deuterium corrosion; powder will be so fine as to not cause abrasion. As anticipated compression ratios are modest, small fusion turbines could be quite practical, although facing the same difficulties in application to cars and trucks found with gas turbines with regard to small speed range and high rpm. The most immediate and appropriate uses would be anywhere now using gas turbines, such as in aircraft.

The most efficient, simple, lightest, and cheapest way to get electrical energy from a high-velocity hot gas in large plants is by *magnetohydrodynamic (MHD) generators*.^{73 74 75} Overall efficiencies of up to 55% or more are theoretically possible in very large hybrid

reactors using combustion gases. Thus there is great interest in whether MHD is useful with warm fusion, especially in hybrid reactors bottomed out by a Rankine cycle.

The major difficulty at this point is anticipating the temperature of the gas after reaction; insufficient heat leads to low conductivity and thus little interaction with the magnetic field. Current estimates place equilibrium temperatures after reaction well below levels associated with MHD. Reactions will probably have to occur in the MHD ducts to take advantage of the relaxation time for recombination of electrons and ions. There are other complications such as the unknown degree of inhomogeneity of the gas, problems associated with gas density (reactors will operate well above atmospheric ambient pressure) and metal ion cross-section inhibiting electron mobility, and several other factors. These combine with the impracticality of small MHD reactors to make any WF application a step to take well after the initial phase of research, and after design and testing of turbines and engines. As a result MHD will be the subject of future papers and will not be developed here.

One interesting small-scale method which shares the advantage of simplicity and direct energy conversion with MHD is to use *plasma diodes*. These can operate at high temperatures with high efficiency.

For some uses, heating water or other working fluid is enough, and a wide variety of shock tubes or reaction chambers would be suited to this less demanding service. As such designs are of great variety and are relatively self-evident once warm fusion is understood, and as the engineering for such is highly developed, they are not covered in this paper beyond this mention.

7.4 Overview of the Warm Fusion Reaction

7.4.1 Terminology

There's a presumption that this reaction occurs in the context of a Chapman-Jouguet detonation, denoted by **C-J**. Subscripts are as follows:

- 0 the initial filling pressure and temperature

m manifold conditions--the sealed circuit will heat with use and thus have higher ambient pressure than when filled, but the same density

H₂ values for H₂ in similar conditions

H values for dissociated H in similar conditions

REACTION ZONES:

1 ambient conditions before the C-J shock; this will be different from **m** when using engines or turbines requiring compression

s the von Neumann peak before reactions occur

d the equilibrium after reactions just behind the shock; this lasts a short time before the rarefaction wave gradually decreases the pressure, temperature and density

2 the equilibrium after the shock and rarefaction wave dissipate and the entire cavity is in one condition

I use some terms in a somewhat unconventional way, since C-J detonations generally are chemically caused and not by tiny nuclear reactions. Details are in the text below.

C_p heat capacity at constant pressure

C_v heat capacity at constant volume

D speed of shock, m/s

P pressure, in MPa except for P₀ which is in atm

T temperature, always in Kelvin

T_c critical temperature for decomposition of hydride powder, a function of pressure

ρ density, in kg m⁻³

γ ratio of specific heats

γ_{1d} average ratio of specific heats between γ₁ and γ_d

γ₁₂ average ratio of specific heats between γ₁ and γ₂

σ ratio of densities compared to ρ₁, such as σ_d = ρ_d / ρ₁

π	ratio of pressures compared to P_1 , such as $\pi_d = P_d / P_1$
$M\#$	Mach number, with regard to sound speed in ambient gas (zone 1)
M_x	molecular weight of gas at zone x ; only includes metal when in vapor form
M_{H2}	molecular weight of hydrogen gas at a given pressure and temperature
N_x	number of moles in gas phase at zone x ; includes metal vapor
n_{Ti}	molar fraction of TiD_2 powder in initial conditions
R_x	gas constant zone x
R_0	universal gas constant
rc	compression ratio
Δhd	energy evolved by the reactions influencing pressure and temperature in zones s and d , averaged over the whole mass of gas and powder, in MJ/kg
Δhp	Δhd treated as if only the powder were reacting, thus showing the energy levels in the powder after reactions and before distribution to the gas, in MJ/kg
J/cc	energy yield density per shock over entire uncompressed volume
PW	power estimate of engine per swept cylinder volume, based on 55% mechanical efficiency, Otto cycle, 3000 rpm, 4-cycle, in kW/l (or J/cc)

7.4.2 Chapman-Jouguet Detonation Shocks

The great majority of shocks through explosively reacting gas follow C-J dynamics due to this being the process with least entropy. Since warm fusion consists of chemically-induced nuclear reactions, the same requirement for a finite time for reaction initiation applies as for chemical reactions. This finite time, which will be of the order of tenths of a microsecond, causes the front of the shock to be a spike of pressure and temperature, known as the von Neumann spike after the author of the definitive paper published in 1942.⁷⁶ Von Neumann used hydrodynamic theory to describe C-J detonations in formulas used below to investigate its properties. The spike represents a maximum of pressure during which, in a normal chemical detonation, the gas receives the energy required to initiate the reactions. The time required, and thus the duration and thickness of the spike, lessens with increased

ambient pressure, and the contrast between the spike and ambient conditions lessens with increased ambient temperatures. This is the spike denoted by subscript s .

Next, after the reactions have occurred and the resultant energy has spread around the local gas, is an equilibrium lasting on the order of hundreds of microseconds where temperature is at its maximum, considerably greater than in the spike, and pressure somewhat less than in the spike. This is denoted by subscript d . Following this stable region is the rarefaction wave, which in a shock tube results in a linear decline of pressure and temperature back to the beginning of the shock (assuming the shock starts at the end of the tube). Once the shocks and waves are mostly settled down and the energy is in equilibrium, in a constant volume chamber the pressure and temperature are both greater than the original conditions; in a constant pressure reaction chamber, such as used in a turbine, the temperature is greater but less so than in the constant volume chamber. This final equilibrium state is denoted by subscript 2 .

7.4.3 *Conditions required*

There must be D_2 gas, solid and stable metal hydride powder finely divided, a chamber of a shape suitable to contain and direct shock waves, and an initial plasma sufficient to start a shock wave and consequent reaction.

The gas has to be high enough in pressure (P_1) so that the peak temperature reached before reaction in the shock wave (T_s) is not too high to decompose the hydride before reaction. The temperature of decomposition (T_c) is a function of powder type and pressure. (There is only the supposition of the requirement for solid hydride to give an *a priori* estimate as to reaction conditions, but much can follow from that one idea.) Dehydriding is endothermic, so not only does it interfere directly with the reaction by separating the catalyst metal from the D, it also takes heat away from the front of the shock wave. This provides a limit to shock strength and reaction yield, which makes calculation of reaction characteristics possible. Since there is a relaxation time involved in the dehydriding, T_s will be able to be a bit above T_c , although this excess is well beyond my ability to predict. In practice, the von

Neumann relations give a slightly higher value to all the parameters than seen in practice due to the idealization of the gas and neglect of loss factors; any excess of T_S over T_C would act against this tendency.

Note that in chemical detonations in gas, in general the speed and temperature of the detonation wave is independent of P_1 .⁷⁷ The condition of $T_S \approx T_C$ (or just a bit greater) makes WF different in this respect, since T_C is a function of pressure and temperature..

The ambient temperature T_1 must be low enough to allow sufficient reaction energy yield to sustain the shock without T_S excessively exceeding T_C . The **Table of Shock Characteristics** shows how profoundly the effects of varying T_1 have, most particularly when elevated due to compression as required in engines and turbines.

Contamination with H_2 can be harmful out of proportion to its fraction of the gas due to the possibility of preferential absorption into rehydrating powder, so the gas should be of high purity. (Actually, while most hydrides are more accepting of H than D, whether this is the case with Ti is not clear from existing research.)⁷⁸ Buildup of He dilutes the D in the hydride and reduces the energy required to cause a given T_S and P_S , which is the main limiting factor. This will shorten operation time between gas replacement in a small reactor; on larger units it will require continuous He removal.

The reaction depends on the shock wave for propagation, and so the reaction chamber must be shaped so as to keep the shock from excessive dissipation or disruption to the shock front. Also the wall surfaces must not preheat the cool gas before reactions or cool the hot gas after reactions too much, nor react at high temperatures with D_2 . This places a lower limit on chamber dimensions for a given pressure and powder density, and constrains the wall material choice.

7.4.4 WF Shock from Ambient to Final Equilibrium

In any practical reactor, the initial level of P_1 will be well above atmospheric, to increase power density. Generally T_1 will be above external ambient levels for two reasons;

first, due to the incomplete equilibrium with coolant in heat exchangers, and secondly because of pre-reaction compression in reactors such as engines and turbines.

Minute particles of TiD_2 float as a fume in this D_2 gas. As long as the fume is in solid or liquid phases, it doesn't affect the colligative properties of the gas, but does add to the overall density and lowers γ slightly. Thus the sound speed and the strength of the shock decrease as powder density increases and the aerosol behaves less like an ideal gas. (Observe the details in the equations below.)

The leading edge of the shock progressing through the aerosol is the von Neumann spike. This spike is of very brief duration, defined by a few hundred collisions in time and a corresponding number of free paths in width. This is approximately the required number of collisions to transfer energy to the D_2 gas, dissociate it, and have it act on the powder. The spike becomes extremely quick and thin at elevated P_1 , being of the order of tenths of a microsecond in duration. Gas atoms bombarding the surface of the fume particles produce conditions in the hydride similar to that in the most extreme locations found in E-Quest's bubble cavitation CF experiments. As a result, whatever the currently mysterious process of chemical induction of nuclear fusion is should happen here as well--only on a much larger scale, involving the large majority, or possibly almost all, of the particles.

There are lower limits which must be exceeded in order for the shock to propagate. One is, that the large majority of particles must react, and they must be both fine enough and densely packed enough to provide sufficient homogeneity to the shock. In this paper I assume that the reaction is general enough for the average value of heat produced per unit mass of hydride to be a meaningful term and a useful approximation. Also I assume that the distance between particles is such that the aerosol achieves the post-spike C-J equilibrium close enough to the norm in chemical gas detonations for there to be a negligible difference between the two types of detonation.

The heat evolved in each particle--which in current CF experiments is the only form of energy released--first must dehydride the TiD_2 , which absorbs 125 kJ/gmol(D_2), or 2.67 MJ/kg(TiD_2). Next the heat goes into the heats of transition for Ti, first melting then

vaporizing, which totals 8.83 MJ/kg(Ti). The heat must exceed the sum of these (11.69 MJ/kg(Ti) or 12.52 MJ/kg(TiD₂)) in order to result in hot Ti vapor and D, which in turn heats the surrounding gas.

Here lies the reason behind a rather exotic manner of keeping track of the energy. In chemical reactions, there is a known value for the heat of formation of the product of the reaction. Each reaction in the detonation can be summed and the expected enthalpy change then provides a good basis for predicting shock characteristics. This isn't the case here, since the "enthalpy" base line for fusion must include the mass equivalent of energy lost in transmutation. That method of bookkeeping is essentially meaningless for this context since only on the order of one in ten million D atoms react in a given shock. Instead, I use two more useful terms; $-\Delta h_p$, which is the above-described energy while concentrated in the original hydride (the "p" is for "peak"), and $-\Delta h_d$, the energy averaged over the entire aerosol. (The minus sign keeps the numbers positive and complies with the usual thermodynamic sign convention for exothermic reactions.) It is important to note that only the energy that exceeds the dehydrating and transition requirements and actually is available to heat the gas between zones **s** and **d** count towards either term. This is an important detail in terms of quantitative analysis and determines the form of the equations below, where these terms are defined in more detail.

The next zone after the spike is the C-J equilibrium. Here, the heat has spread throughout the spaces between exploded powder particles and made a generally stable condition. The temperature T_d is significantly higher than T_s and T_c . The Ti is in supersaturated vapor form as there are insufficient nuclei and not enough time for condensation during the roughly 100 μ sec of the C-J equilibrium; as a result it figures into the molecular weight and γ of the gas and the colligative gas properties. Since the Ti doesn't condense it does not contribute any heat of transition during zone **d**. P_d is the highest pressure at any point in the process. ρ_d is lower than its maximum value of ρ_s , but higher than ρ_1 , which equals ρ_2 .

After the C-J equilibrium the rarefaction waves create a gradual and roughly linear decrease of temperature and pressure going back to the beginning of the shock. Eventually the waves die down and leave a final equilibrium (zone **2**). I'm assuming that re-hydriding takes place well after zone **2**, so this doesn't factor into the energy balance and influence the temperature and pressure; however, the D atoms liberated by dehydriding in zones **s** and **d** should have a chance to reassociate to form D_2 , so the heat of formation does increase T_2 and P_2 .

For the purposes of this paper, there are two fundamental types of reaction chamber; constant volume (CV) and constant pressure (CP), each of which have somewhat different final post-shock states. CV chambers have a fixed volume which is entirely swept by the shock; shock tubes with closed ends are in this group, as are the compressed phase of engine cylinders. (Of course the piston doesn't really stop for any appreciable time at top dead center, but I take the volume as fixed as a close approximation due to the speed of the shock.) $P_2 > P_1$ for closed chambers. The strength of the chamber determines the upper limit of P_2 , which in turn limits the power density more stringently than any other factor.

CP chambers have $P_1 = P_2$, as with turbine combustors in conventional gas turbines. This type is useful in fusion turbines between the compressor and the turbine; also it can find use in a Rankine cycle where the pressure gradient through the circuit is very small and only used to promote circulation. Typically this would be in a boiling water or other heat-oriented application.

Such chambers are not limited by having to withstand high P_2 levels, requiring such strength only for P_d (higher but transient) and T_2 . As a result there can be a considerable power/weight ratio advantage for CP chambers despite lower thermodynamic efficiency from lower CVT_2 values.

7.4.5 Reaction products

CF experiments have been especially perplexing in the area of reaction products, leading to the most serious reasons for skepticism on the part of the mainstream scientific

community. It does make intuitive and qualitative sense that low-temperature induction of nuclear reactions should have a different family of reaction products than those caused by extreme collision velocities. The various theories put forward so far to explain anomalous experiments are all insufficient and unconvincing, especially when they try and use conventional quantum mechanics and nuclear physics to cover what is plainly forbidden by what is currently accepted theory. The course of research proposed here is quite devoid of details as to the nature of the reactions, concentrating only on a very rational method of causing and sustaining whatever is going on. A profound physical explanation must wait until after more experiments with robust reactors with high energy density levels, which would follow in the tradition of the founding of thermodynamics and engineering *after* the start of the Industrial Revolution and the advent of the practical steam engine.

The major problem with CF experiments to date has been low energy density levels. The yield per atom is so large that accumulation of appreciable reaction products requires large energy production in reasonable times and volumes. WF, if it works as hoped, would certainly provide sufficient energy density for unambiguous investigation at long last.

Should WF follow the trends in CF experiments, the bulk of products should be ${}^4\text{He}$, with a much smaller amount of ${}^3\text{He}$. Tritium is anomalously low in CF, with some experiments showing none and others very little. Otherwise the only anticipated product is heat, with no neutrons or gamma rays. However there should be UV radiation from powder explosions, which are masked in the electrolyte of CF experiments--and should be observable with WF. (Preheating of the cool powder ahead of the shock could be a real problem, which I have not yet addressed. This would be because of the high peak temperatures of the powder not found in chemical detonations, which can be several tens of thousands of degrees Kelvin, and also because TiD_2 can absorb UV radiation which passes easily through the gas.)

7.5 Metal Hydride Powder

7.5.1 Powder type

Most CF experiments to date have concentrated on Pd, Ni, and Ti as electrodes. The requirements for electrical D absorption are significantly different from WF conditions, since there is no externally applied electrical potential to the powder particles. (They will carry a small negative charge from friction effects but not enough to make an appreciable difference.) Instead WF depends on hydride formation from a combination of pressure and temperature after the metal condenses from vapor in the cooling gas after reactions. In addition, the requirement for withstanding the spike temperatures in the C-J detonation shock wave necessitates as great a stability as possible.

One more requirement is the right kind of bonding between the metal and D. Ionic or saline bonds as found with Li, Cs, Mg, Ca, Sr, Ba, Eu and Yb are not used in CF experiments as catalysts. (LiH, LiH & TiH₂ and LiH & Ni are subjects of the second paper of this series.) Covalent hydrides are weakly bound between molecules and are liquid or gaseous at room temperature, clearly ruling them out. Compounds between metals used in CF for catalysis and non-metals, when they form hydrides, are not stable enough to withstand conditions in zone s, and pose problems in the condensation phase of the cycle.

This leaves metallic hydrides. Alloys are not practical as pure catalysts in this context. Not only would condensation in proper proportions be hard to maintain, but also all intermetallic hydrides are much more unstable than binary hydrides. This makes them suited to hydrogen storage but not to withstanding high temperatures. This leaves binary metallic hydrides as suitable candidates.

Hydrides in general follow a linear relation between the temperature at which the compound dehydrides (T_C), and the log of the pressure. When solved for the temperature, which is the most useful version in this application, it is as follows;

$$T_C = -A / (B - \ln P_S) \quad (8.1)$$

The physical meaning of the constants is as follows: $A = 2 \Delta H_f (s R_0)^{-1}$, and $B = -2 \Delta S (s R_0)^{-1}$ where ΔH_f = heat of formation, s = stoichiometric number for D, R_0 = universal gas constant, and ΔS = entropy of formation. Putting the numbers in for the remaining elements to consider leaves Ti, Zr, and U as the best candidates.

U, the third most stable of the three, is not a good candidate. U and UD₃ powder ignite in air at 25° C, leading to risks of severely toxic pollution and fire. Zr may be possible, but its stability is not as great as that of Ti (the constants for Zr are A = -28,000, B = 27).

Ti has the highest stability (A = -14,900, B = 15.1) under the spike of any metallic hydride. Also it is stable in air or water, so that TiD₂ in powder form can be added to an empty reactor that is then evacuated and filled with D₂. TiD₂ has the highest D density of any form of D at atmospheric pressure, liquid or solid or any other hydride, at 9.2 D atoms / 10⁻²² cc . It absorbs more D or H for its weight than any other element, and is second only to Pd in volumetric ratio of gas absorbtion. Ti has shown activity in CF experiments, including the E-Quest devices that come closest to WF in peak pressures and temperatures. Therefore Ti is the metal of choice for promotion of pure D-D reactions.

Should Ti work, Nature will have been kind--it is quite abundant and, in the modest quantities required, relatively cheap and easily available. Ti powder is carcinogenic, so there are precautions required.

Ti used in WF must have low levels of impurity to absorb D to its maximum capacity; Al contamination in particular must be avoided, making aerospace scrap unusable without further refining.

In bulk metal, TiD_x (as is generally true with metal hydrides) does not have integral stoichiometry; "x" reaches the highest values at low temperatures, only starting a noticeable decline at around 600 K.⁷⁹ Uptake of D or H is faster at higher temperatures but the solubility is lower. This leads to the idea of holding tanks before and after the heat exchanger in any reactor cycle, one for the initial hydriding and the second to finish the job. This application differs from most in the minute size of the particles. Since the range of T_m in practical

reactors is well within the high-solubility limit for TiD_x , this paper assumes that the hydride goes to $x = 2$.

7.5.2 *Powder size*

TiD_2 prepared outside the reactor will crumble with minor effort to about micron size. Grinding it smaller is a real challenge--and probably not worth the bother. Commercial powdered Ti of 20 μm radius is easily available; this powder, once hydrided, should be suitable to addition to an empty reactor. Then the reactor is sealed, evacuated, and filled with D_2 . There should be a compressor or fan of some sort to provide forced circulation through the reactor before startup.

Stoke's Law for spherical particles gives the terminal velocity. Putting in values for the density of TiD_2 and the viscosity of D_2 gas at probable T_m levels, with viscosity in poise, density in g/cc, gravitational acceleration in cm/sec^2 , terminal velocity V in cm/sec , and radius of particles r in μm , $V = .0973 r^2$.

The settling velocity for 20 μm powder in D_2 is 40 cm/s, so powder should be no bigger than this to start with, even if the inhomogeneity problem noted above is inconsequential. After going through WF reactions, the Ti ranges from plasma at peak temperatures to supersaturated vapor at T_d to fume again at T_2 . As a result, a very few cycles should reduce the average particle size to the order of tens or hundreds of nanometers.

One potential problem is the powder sticking to cool wall surfaces, especially when not in operation. This also is hard to anticipate. It may be that a slow circulation must continue even when the reactor is cold. The particles will be a fume and easy to suspend, as their terminal settling velocity is very low. The problem is most acute in heat exchangers.

7.5.3 *Powder density*

There is a balance between excessive and insufficient TiD_2 molar fraction (n_{Ti}) that is quite elegant. Higher n_{Ti} means, for a given energy limit posed by $T_s \approx T_c$, lower powder peak temperature from $-\Delta h_p$ distributed over more mass. When the peak temperature is

below a certain value, there will be too much of the powder remaining unvaporized due to the anticipated distribution of particle conditions; this in turn will hinder the formation of the C-J equilibrium and the shock will fail. Only experiment will tell what that value would be, and it will vary according to the geometry of the reaction chamber and the ambient gas conditions. I'd be surprised if the peak could go below 5,000 K in a reliably repeatable shock, and it may be that 8000 or even 10,000 K is more realistic. The effects of the peak being too low would likely be similar to running an internal combustion engine too lean, leading to sporadic and unpredictable performance in borderline conditions. Note that many factors determine what the lean limit is in i.c. engines; such may be the case in determining a minimum T_C for a given reactor.

At the same time, high nTi allows $-\Delta h_p$ to be smaller before reaching shock energy limits. This means that the effectiveness of the shock induction of WF reactions need not be so high as with low nTi and high $-\Delta h_p$ values. Since there is no way to anticipate what the upper limits are to $-\Delta h_p$ before experiment, it is wise to find a full range of possible values and design towards the lesser levels. As there are many factors that can degrade the ultimate possible $-\Delta h_p$ value found in extremely pure substances in optimal reactor conditions, the greater the difference between the permissible $-\Delta h_p$ and the ultimate $-\Delta h_p$ the better--and we can only alter the former.

Another effect of low nTi is the increased distance between particles and resulting gas inhomogeneity. Given particle sizes at fume levels, well below micron diameters, it's likely that this will be a secondary limit. However, new unreacted powder as placed in reactors will have to be small enough to not inhibit initial shock waves. In the lower limits of density this could pose problems with inhomogeneity, since TiD₂ powder smaller than a few microns is hard to produce and handle, as well as being a carcinogen. Once the reactor has gone through a few cycles the powder will reduce to fume sizes and the problem will likely vanish.

A third effect of high nTi values is the strengthening of the shock and related increases of T_d , P_d and P_2 , M#, and the energy produced by any of the several measures. All these effects show up in the **Table of Shock Characteristics**, especially when compared to

those parameters that can be estimated as they would be in the absence of any powder at all ($n_{Ti} = 0$). This table samples the probable range of n_{Ti} from .01 to .02. The actual practical higher and lower limits depend on specific reactor configuration and will be a prime area of experimentation.

7.6 Spark Plasma WF Initiation

7.6.1 Basic spark physics

The following excellent summation of how sparks function in i.c. engines is, except for minor changes, from Richard Stone;⁸⁰

1. *Pre-breakdown.* Before the discharge occurs, the material between the electrodes or conducting materials is a perfect insulator. As the spark pulse occurs, the potential difference across the gap increases rapidly (typically 10-100 kV/ms). this causes electrons in the gap to accelerate towards the anode. With a sufficiently high electric field, the accelerated electrons may ionize the molecules they collide with. This leads to the second phase--avalanche breakdown.
2. *Breakdown.* Once enough electrons are produced by the pre-breakdown phase, an overexponential increase in the discharge current occurs. This can produce currents of the order of 100 A within a few nanoseconds. This is concurrent with a rapid decrease in the potential difference and electric field across the gap (typically to 100 V and 1 kV/cm respectively). Maly⁸¹ suggests that the minimum energy required to initiate breakdown at ambient conditions is about 0.3 mJ. The breakdown causes a very rapid temperature and pressure increase. Temperatures of 60,000 K give rise to pressures of several hundred bars. These high pressures cause an intense shock wave as the spark channel expands at supersonic speed. Expansion of the spark channel allows the conversion of potential energy to thermal energy, and facilitates cooling of the plasma. Prolonged high currents lead to thermionic emission from hot spots on the electrodes and the breakdown phase ends as the arc phase begins.

3. Arc Discharge. The characteristics of the arc discharge phase are controlled by the external impedances of the ignition circuit. Typically, the burning voltage is about 100 V and the current is greater than 100 mA, and is dependent on external impedances. The arc discharge is sustained by electrons emitted from the cathode hot spots. This process causes erosion of the electrodes, with the erosion rate increasing with the plug gap. Depending on the conditions, the efficiency of the energy-transfer process from the arc discharge to the thermal energy of the mixture is typically between 10 and 50 per cent.

With currents of less than 100 mA, this phase becomes a glow discharge, which is distinguished from an arc discharge by the cold cathode. Electrons are liberated by ion impact, a less efficient process than thermionic emission. Even though arc discharges are inherently more efficient, glow discharges are more common in practice, because of the high electrode erosion rates associated with arc discharges.

7.6.2 Desired traits

The extreme conditions of breakdown are very attractive to get WF reactions started, which will in turn add heat to a growing plasma. Also this first phase is the most efficient in transferring spark energy to the aerosol. However it lasts but 10 or 20 nanoseconds, and occupies a very tiny volume before amplification by reactions. Thus for practical reasons of expanding the duration and volume of plasma and consequent reaction energy released, there must follow the arc phase. In plasma jets (described below), the arc phase is far shorter than with simple spark gaps, as the plasma must complete heating before ejection.

Reactions occur within the metal hydride powder particles, turning those that do react into plasma and generating high-temperature electrons. Thermionic emission of electrons from the metal plasma will supply copious electrons in the reaction zone. Electron density will remain high for some time after the shock passes due to the finite relaxation time for electrons to recombine with ions; however, how this translates into conductivity is a complex and as-yet unsettled question due to variability in gas and metal ion densities. Glow discharge will have little role to play in promoting WF as the reaction proceeds just behind

the expanding shock wave. Therefore electrical energy delivered to the plasma after the detonation commences is wasted, leading to a shorter period of power supply than used in i.c. engines. This favors capacitative ignition systems over coils for spark gaps.

7.6.3 Spark gaps

A simple point of ignition suffices to initiate a detonation in chemical explosions of flammable gases; but looking at the very beginning of the process indicates that simply putting a spark in D₂-hydride aerosol will not work. WF behaves in the manner of high explosives, although probably with C-J and not strong shocks, and as such must start either with a shock already formed or with comparable compression and heating. Spark gaps do form shock waves, but as the spark is small compared to the chamber, the initial shock is spherical, weakening it quickly, and much faster than the plasma expansion. As a result, in conventional spark ignition in flammable gas, the shock separates from the slower plasma and flame front, which never catches up. When the reaction zone finally establishes at the shock front this usually is from spontaneous ignition, and in a non-coherent turbulent manner. Spontaneous ignition and subsonic flame fronts are not traits of WF, so a simple spark gap is not a good candidate for starting reactions.

These faults can be improved by placing the gap at the apex of a steep cone, so that the initial shock is somewhat confined and directed. Such a solution or something like it would be required if electrode erosion makes plasma jets impractical.

7.6.4 Plasma jet

[See Fig. 7.1] The plasma jet is essentially a way of fitting a small initial chamber around the spark so that the resulting shock is coherent, well-directed, and intense. From there the larger reaction chamber geometry can aid in shaping the resulting WF shock wave. In the context of shock tubes, this is straightforward--as long as the granularity of WF is not too great and the diameter of the tube is sufficient (at least 1 inch) there's every reason to expect clean shocks, although convex in the direction of the cool gas as is usual. However, for conditions as in fusion engine cylinders, the cool gas is highly turbulent, the shape is

generally far from ideal, and turbulent detonation is probably unavoidable. It won't make a great deal of difference as long as the whole chamber reacts; whether this is the case requires much experimentation.

Engineers working with i.c. engines have long sought methods to ignite lean mixtures for better mileage and pollution control. One showing promise has been plasma jet plugs to replace spark plugs. For automotive engines these consist of a coaxial design and power supply as shown in the drawing. This also is appropriate for WF. Typical dimensions have an inner chamber length of 7 mm-1 cm, and a radius of .75-1 mm. These deliver plasma of about 1 eV and a velocity of $\sim 5 \times 10^3$ m/s.

This velocity can vary by a factor of 2 depending on the size of the exit hole, which can vary from the full diameter of the cavity to half that size. The smaller diameter has the highest speed, but also suffers more from electrode erosion, the chief problem for plasma jet plugs.

The above figures are for a variety of gases at roughly NTP in non-WF conditions. Electrical energy from the circuit for the sample plug is about 1 J per shock, which converts to plasma energy at from 7 to 10%. As the thermal energy released by a typical automotive i.c. engine is about 100-200 J per ignition per cylinder, the plug power is not excessive--but is near the upper practical limit before becoming a major design problem.

One major benefit is that plasma jet plugs work best in hydrogen atmospheres, to such an extent that automotive test applications have included a small inlet tube keeping the plug filled with H₂.

Currently plasma jet plugs are not used in i.c. engines because electrode erosion limits them to about 10^5 shocks before requiring replacement. This is a major problem facing WF reactor design. However there is real hope of long-lasting plugs, since WF in the plug itself contributes to conductivity by partially ionized powder. This means that thermionic emission from the cathode to support the arc phase may not be required or caused by hot spots. Hence there is the possibility of little or no melting and ablation. (Interestingly, plasma jet performance suffers most from erosion from the exit electrode, since the size and shape of

the exit hole is important for shock speed, and the core electrode's length is not so critical. However the polarity of electrodes has no effect on erosion rates, so making the exit electrode anodic doesn't help.) The current for the arc phase can be smaller and shorter than customary since after breakdown the bulk of the heating is from WF, avoiding erosion.

The current choice for electrode material is thick 316 stainless steel, as tungsten would likely react with the D, and is harder to incorporate into the body of the plug, resists machining, etc.

7.6.5 Wire explosion

One other spark producer, impractical for power generation but of interest for experimentation nonetheless, is filament ignition. A thin wire, ideally of the same metal as the powder, runs through the aerosol. On application of a high current the wire vaporizes, causing a plasma channel in its place. This would then proceed to expand into the gas in the same manner as other spark plasmas, and causes reactions in the normal manner. Although a lot of energy is required to blow up the wire, this would be an excellent way to maximize a single blast. The problems of wire replacement, and the great lengths required for repeated operation, make this a special application only for single explosions.

7.7 C-J Shock Analysis

7.7.1 Equations

To prepare the circuit or reaction chamber for operation, first D₂ gas fills the previously evacuated volume which contains TiD₂ powder. The initial filling pressure and temperature are P₀ (in atm) and T₀. For evaluating various conditions with a standard base of common features, I take T₀ = 293. P₀ varies and is generally higher than 1 atm in order to have reasonable power densities. Any actual reactor will have the initial temperature before compression (if any) higher than the coolant temperature; for this paper's estimates I take this manifold temperature T_m = 350. This would be realistic for air-cooled engines or turbines.

The manifold pressure P_m will increase proportional to the temperature increase over P_0 , in this case by $350/293 = 1.194$.

The initial density ρ_0 follows easily from the filling pressure P_0 and n_{Ti} by the following equation, which is conceptually

$$\rho_0 = P_0 \text{ (moles m}^{-3} \text{ of ideal gas at 1 atm at } T_0) \text{ (kg mol}^{-1} \text{ of D}_2 + \text{kg mol}^{-1} \text{ of TiD}_2)$$

Numerically this is

$$\rho_0 = 41.57 P_0 (.00403 [1 - n_{Ti}] + .0519 n_{Ti}) \quad (8.2)$$

When there is compression, it is by the ratio rc , so that $\rho_1 = rc \rho_0$.

Shock tubes will not have initial compression as do engines and turbine reaction chambers, and so $P_m = P_1$ for them. With compression there is adiabatic heating and pressure increase. Therefore the expressions for P_1 and T_1 for compression are;

$$P_1 = P_m rc^{\gamma_1} \quad (8.3) \quad T_1 = T_m rc^{\gamma_1-1} \quad (8.4)$$

In the early 1940's, John von Neumann, along with Zeldowitch and Doering, predicted and described the reaction zones described above.⁸² The equations derived from hydrodynamic properties of ideal gases allow quantitative estimates of all the principle variables in each zone--successively the spike, the C-J equilibrium, and the final equilibrium.

For the spike:

$$\pi_s = \frac{P_s}{P_1} = \frac{2 D^2}{R_l T_1 (\gamma_{1d} - 1)} - \frac{\gamma_{1d} - 1}{\gamma_{1d} + 1} \quad (8.5)$$

$$\sigma_s = \frac{\rho_s}{\rho_1} = \frac{\pi_s (\gamma_{1d} + 1) + (\gamma_{1d} - 1)}{\pi_s (\gamma_{1d} - 1) + (\gamma_{1d} + 1)} \quad (8.6)$$

$$T_s = T_1 \pi_s \sigma_s^{-1} \quad (8.7)$$

For the C-J equilibrium:

$$\sigma_d = \frac{\rho_d}{\rho_1} = \frac{\gamma_d + 1}{2\gamma_d} + \sqrt{\left(\frac{\gamma_d + 1}{2\gamma_d}\right)^2 - \frac{M_d T_1}{\gamma_d M_1 T_d}} \approx \frac{\gamma_d + 1}{\gamma_d} \quad (8.8)$$

$$\pi_d = \frac{P_d}{P_1} = \frac{M_1 T_d \rho_d}{M_d T_1 \rho_1} = \frac{M_1 T_d \sigma_d}{M_d T_1} \quad (8.9)$$

$$D = \sigma_d \sqrt{T_d \gamma_d R_d} = \sigma_d \sqrt{\frac{T_d \gamma_d R_0}{M_d}} \quad (8.10)$$

M_1 is the molecular weight of the D_2 gas alone, as the TiD_2 is in solid form. (I approximate the degree of dissociation of D_2 as being the same as for H_2 in the same conditions, as molecular weight tables are not available for D_2 as for H_2 .) As the temperature is moderate and the pressure adequate to negate dissociation, M_1 will always equal 4.028.

For M_d , the TiD_2 has dehydrated completely, and the D from the hydride I treat as not having time to reassociate as D_2 . For the surrounding D_2 , usually the M_{H_2} value (mol. weight of hydrogen at the same conditions) at the C-J equilibrium is not much below its maximum undissociated value of 2.016, except in the case of shock tubes operating with gas not subject to compression and heating before shocks. The molecular weight of the Ti must be included in the gas because it is in the form of supersaturated vapor. The molar proportion nTi applies to the hydride powder in zone 1; after dehydrating and with atomic D, the proportions will change as follows:

molar proportion of Ti at d = $n_{Ti} / [(1 - n_{Ti}) + n_{Ti} + 2n_{Ti}] = n_{Ti} / (1 + 2n_{Ti})$

where the denominator is the sum of the proportions of D₂, Ti, and D. Likewise,

molar proportion of D = $2 n_{Ti} / (1 + 2n_{Ti})$

molar proportion of D₂ = $(1 - n_{Ti}) / (1 + 2n_{Ti})$

The equation for M_d is

$$M_d = \{2 (\text{mol. wt. H}_2 \text{ at } d \text{ conditions}) (\text{proportion of D}_2) + (\text{mol. wt. of Ti}) (\text{prop. of Ti}) \\ + 2 (\text{mol. wt. D}) (\text{prop. of D})\} / (\text{sum of proportions})$$

$$M_d = (2 M_{H_2} (1 - n_{Ti}) + 47.9 n_{Ti} + 4n_{Ti}) / (1 + 2n_{Ti}) \quad (8.11)$$

To have any validity for any of these equations, as close an approximation as possible of γ in all zones is a strong requirement. This is very difficult unless n_{Ti} is small, in which case the γ for H₂ is available in tables and close to valid in the shock. In fume form, the powder will be small enough to heat and cool with negligible lag behind the gas, and so must be a factor in γ . As with M and R and other thermodynamic variables, I assume that values from tables for H₂ are close enough to D₂ (with corrections for molecular weight) to be useful.

There are two causes of error that I cannot yet correct beyond a reasonable approximation. One is that I do not yet have access to thermodynamic tables for TiD₂, and so must treat the compound as if its heat capacity is about that of Ti--something that is surely not the case. This influences γ_1 only.

The second cause of error is an uncertainty of the influence of the fume on the overall heat capacity of the aerosol when the fume is in solid or liquid form, and when there is a significant divergence of $C_{p,Ti}$ and $C_{v,Ti}$ --that is, when $\gamma > 1$. For γ_1 the temperature is moderate enough so that $C_p \approx C_v$, so the equation for determining γ_1 should be reasonably good once I have valid figures for the heat capacity of TiD_2 or TiH_2 . For γ_d the Ti is in supersaturated vapor and the equation below should work. However, for γ_2 the Ti is solid and hot enough so that C_p diverges from C_v , which approaches the Dulong and Petit value of nearly 6 cal/mol deg. I include both C_p and C_v in the equation for γ_2 , but the flaw is that the solid particles do not act as a gas. I have not yet been able to find out what their influence would be on the overall γ in such conditions. The effect of this inaccuracy is moderated by the fact that the only way γ_2 is used is as an average value with γ_1 . For the formulation of the **Table of Shock Characteristics**, I have approximated this average in all cases as being 1.38, and left more detailed and accurate estimates for later. This standard value is probably too large in the cases showing high energy density, but it would be fairly close in the more moderate examples. In any case the use of one value does help comparisons between cases even if the actual values are not quite accurate. (The tendency of the whole process will be overestimation of real values since losses are not included.)

The formulas for γ_x depend on the stage of the shock. For zones 1 and 2,

$$\gamma_x = [C_{p,H_2} (1 - n_{Ti}) + C_{p,Ti} n_{Ti}] / [C_{v,H} (1 - n_{Ti}) + C_{v,Ti} n_{Ti}] \quad (8.12)$$

This formula distributes the effect of the heat capacity of the TiD_2 according to its molar fraction; note that I assume that the heat capacities for Ti and TiD_2 are close enough to treat as equal. When I can get figures for thermodynamic values for TiD_2 this will be a big improvement, as noted above. When solid and at T_1 , $C_{p,Ti} = C_{v,Ti}$. Ti exists in two different solid forms with slightly different heat capacities. The α form predominates up to $T = 1155$, and the β from there to melting at $T = 1940$. (These numbers are for atmospheric pressure and would be higher at operating conditions.) T_1 will always be < 1155 , so γ_1 will reflect the

α heat capacity--although the difference is, for the moment, well below the other errors in these calculations. In the equations below, $\gamma_{H_2} = \gamma$ for H_2 in each of the respective zones.

For zone **1**, with solid fully hydrided TiD_2 and $T < 1155$, using the polynomial approximation for Cp_{H_2} and using cal / gmol throughout:

$$\gamma_1 = \frac{\frac{(1-nTi)(6.62+0.00081T_1)+nTi(5.25+0.0025T_1)}{(1-nTi)(6.62+0.00081T_1)} + nTi(5.25+0.0025T_1)}{\gamma_{H_2}} \quad (8.13)$$

Condition 2 has Ti in solid (β) and dehydrided form, with $1155 < T < 1940$, although T may be a bit below the lower limit in CP reaction chambers and the weakest shocks. Cv for Ti is very nearly the Dulong and Petit value since the Debye temperature for $Ti = 290$ and this range is several multiples of that. So, $Cv_{Ti} = 6$ cal/mol deg. The difference between the equation above and the one below in practice is very minor since nTi is so small.

$$\gamma_2 = \frac{\frac{(6.62+0.00081T_1)+7.5nTi}{(6.62+0.00081T_1)} + 6nTi}{\gamma_{H_2}} \quad (8.14)$$

For zone **d**, a more accurate equation is not as difficult. The TiD_2 is dehydrided and the Ti is in supersaturated vapor as described above for finding M_d . As such Ti is primarily a monatomic gas with $\gamma = 1.63$, and $Cp_{Ti} \approx 5$ cal / mol. For D, $\gamma = 5/3$. The proportions of D_2 , D, and Ti are as for M_d , and as the proportions are in ratio form the denominator cancels. Cp_H , the heat capacity of atomic hydrogen, varies so greatly that values must be interpolated from tables. As a result:

$$\gamma_d = \frac{(1-nTi)Cp_{H_2} \cdot Cp_{Ti}(nTi) + Cp_H(2nTi)}{(1-nTi)Cp_{H_2} + 0.61Cp_{Ti} + 0.6Cp_H(2nTi)} \quad (8.15)$$

Numerically this is:

$$\gamma_d = \frac{(1-nTi)(6.62 + 0.00081T_1) + 5nTi + Cp_H(2nTi)}{(1-nTi)(6.62 + 0.00081T_1) + 3.07nTi + 0.6Cp_H(2nTi)} \quad (8.16)$$

For a perfect gas, the Mach number (M#) for the detonation wave comes from;

$$M\#^2 \rho_1 P_1 \gamma_1 = \rho_d P_d \gamma_d \quad (8.17)$$

Because the C-J equilibrium is connected to the spike and the ambient gas, continuum arguments yield the following expression for the heat energy transmitted to the gas as a whole during zones **s** and **d**,⁸³

$$-\Delta hd = .5 (P_d - P_1) (\rho_d^{-1} + \rho_1^{-1}) \quad (8.18)$$

This is the heat energy per unit mass of the entire aerosol, and as explained above is not the same as the enthalpy change in chemical detonations. From $-\Delta hd$ comes the same energy when concentrated in the powder alone; Δhp is Δhd divided by the mass fraction of TiD_2 , which has molecular weight of 51.93.

$$\Delta hp = \Delta hd [4.03 (1 - nTi) + 51.93 nTi] / (51.93 nTi) \quad (8.19)$$

To find J/cc , which is the power density over the whole uncompressed volume of the reaction chamber, conceptually the equation is

$$J/cc = [-\Delta hd + (J/cal) (gmol/g) (g/kg) (mole fraction / molecular weight) X (J/kg)] \quad (8.20)$$

$$\{(heat of transition for condensation of metal) + (heat of formation for D_2)\] \rho_0 (10^{-6}) (cal/mol) (cal/mol) (kg/m^3) (m^3/cc)$$

Numerically this is

$$J/cc = (-\Delta hd + 4184 nTi [106,000/47.9 + 104,200/4.03]) \rho_0 (10^{-6}) \quad (8.21)$$

which simplifies to

$$J/cc = (-\Delta hd + 117.4 \times 10^6 nTi) \rho_0 (10^{-6}) \quad (8.22)$$

This equation takes into account that the Ti goes from vapor to solid, and the D from TiD_2 has a chance to reassociate to D_2 .

J/cc , with the compression ratio, can give an estimate of power per unit of swept volume to compare with typical i.c. engine values. Conceptually the equation is;

$$PW \text{ (in W/cc or kW/liter)} = (J/cc)(total volume/swept volume)(indicated } \eta/\eta_{0otto})(\eta_{0otto})(rpm)(min/sec)X (power strokes/stroke) \quad (8.23)$$

The ratio of entire volume/swept volume is $rc / (rc - 1)$. A good sample value for indicated efficiency over Otto cycle theoretical efficiency is .55. The efficiency for the Otto cycle (η_{0otto}) is $(1 - rc^{1-\gamma})$. The sample values I use in the table for the engine parameters are 3000 rpm and 4 cycle (thus 1/2 power strokes/stroke). Thus the equation used for i.c. engine comparison is;

$$PW = 13.75 \text{ (J/cc)} (rc / [rc - 1]) (1 - rc^{1-\gamma}) \quad (8.24)$$

For an engine like this, assuming it is suited for automotive use, the range of PW should be from 20 to 60 kW/l. Currently, for the **Table of Shock Characteristics**, I use a value of 1.38 for γ .

The next important value is the final equilibrium temperature T_2 . The equation below is for constant volume conditions. An accurate calculation would require a difficult integration due to changes in γ over the range of T_1 to T_2 , but for this paper a simple and reasonable approximation uses the average value γ_{12} and the previously used polynomial estimate for C_p . This same formula finds T_2 for constant pressure conditions by setting $\gamma_{12} = 1$.

Note that $-\Delta hd$ includes the energy changes from **1** to **d**, including dehydriding and initial transitions. The equation for T_2 includes solidification of Ti from vapor, and heat of formation of D_2 from D (released from TiD_2). It does not include dehydriding and other initial changes in $-\Delta hd$. Conceptually the equation is;

$$-\Delta hd = (\text{conversion from cal/g to J/kg}) [(M_2 \gamma_{12})^{-1} (C_p \Delta T) - (\text{heat of formation } D_2) + (J/kg) \quad (gmol/g) \quad (cal/gmol) \quad (cal/g)] \quad (8.25)$$

$$(M_{Ti}^{-1} n_{Ti}) (C_p \Delta T - \{\text{heat of condensation from vapor of Ti}\}) \\ (gmol/g) \quad (cal/gmol) \quad (cal/gmol)$$

$M_2 = M_1 = 4.03$ unless conditions get more extreme than these calculations indicate. $M_{Ti} = 47.9$, so its inverse = .0291. The numerical version is;

$$-\Delta hd = 4184 [(4.03 \gamma_{12})^{-1} (6.62\{T_2 - T_1\} + 4.05 \times 10^{-4} (T_2^2 - T_1^2) - 104,200 n_{Ti} / 4.03 + .0291 n_{Ti} (7.5\{T_2 - T_1\} - 106,000)] \quad (8.26)$$

This is easily solved for T_2 by calculator or computer. P_2 follows from gas laws: with N_1 and N_2 being the number of moles in gas form in zones 1 and 2 respectively,

$$P_2 = \frac{P_1 T_2 \rho_2 N_2}{T_1 \rho_1 N_1} \quad (8.27)$$

Since the volume and mass don't change from 1 to 2, $\rho_1 = \rho_2$. Although the Ti may not be condensed all the way to solid by zone 2, I approximate it as fully condensed. Therefore the ratio of $N_2 / N_1 = (1+nTi)$. At the temperatures and pressures typical of zone 2, there is negligible dissociation, and D from powder dehydriding has a chance to reassociate. As a result,

$$P_2 = \frac{P_1 T_2 (1+nTi)}{T_1} \quad (8.28)$$

T_p is intended to be the average peak temperature of powder particles when the energy from reactions has distributed through the particle and the pressure has reached that of the immediate environment, P_s . Knowing $-\Delta h_p$ it is possible to estimate T_p , although it is a rather wide estimate due to the variance in heat capacities with temperature and pressure, the mixture of compounds and elements in the aerosol, and the limitations of data available. However even if the accuracy is not great, a value for T_p is essential to determine the viability of the shock and the possible ranges of nTi . At the peak conditions, TiD_2 is dissociated completely and in the higher ranges of T_p ionized as well. The highest temperatures for which this equation is valid are below the ionization level due to the complex variation in enthalpy ionization causes. Since the range of greatest concern is the low end, the equation is quite useful. It is the low end that gives the limiting possible density of powder and other factors of interest in maximizing power density and in reactor design.

$-\Delta h_p$ is in units of $[J \text{ kg}^{-1}]$, and so it is necessary to distribute the energy in the equation by the proportion of mass in TiD_2 . For the two D atoms together, the mass ratio is $4.03 / 51.93 = .00776$. For Ti it is .9224. The enthalpy values i_p and i_s (the enthalpies at the peak temperature and at the spike, where the reaction starts, respectively) are interpolated from tables. In most tables the enthalpy is in $[kJ \text{ kg}^{-1}]$ and the appropriate conversion factor is in the equation. Just as with the formulas for $-\Delta h_d$ and T_2 , there is no inclusion of heats of transition. The powder starts off as solid, at T_s , but this is generally not far below the melting point of Ti; as a result the approximation of starting off as liquid is a reasonable one and worth the simplification. The C_p value for Ti as liquid is 7.5 cal mol^{-1} , and should hold between T_s and the vaporization of Ti at about 3600. Then the C_p is about 5, which holds up to T_p within the limits of the equation's utility. By using trial values of T_p and solving for i_p , one can test if the two values correspond in the tables. When they do then T_p is reasonably close.

$$\begin{aligned} -\Delta h_p &= 1000 & (.0776) & (i_p - i_s) + .9224 & (4184) & 47.9^{-1} & (C_{p,\text{Ti(l)}} [3600 - T_s] + C_{p,\text{Ti(g)}} [T_p - 3600]) \\ & [J \text{ kg}^{-1}] & [J \text{ kJ}^{-1}] & [\text{mass fraction}] & [kJ \text{ kg}^{-1}] & [\text{mass}] & [J \text{ cal}^{-1}] & [\text{mol g}^{-1}] & [\text{cal mol}^{-1}] \\ & 2 \text{ D}] & & & \text{fraction Ti}] & & & & \end{aligned} \quad (8.29)$$

$$-\Delta h_p = 77.6 (i_p - i_s) + 80.57 (7.5[3600 - T_s] + 5 [T_p - 3600]) \quad (8.30)$$

7.7.2 Sequence of Calculations

There are more variables than equations, so solutions require trial values and iterated loops, which usually converge in only a few steps to acceptable error levels for this early stage of inquiry.

Each sample case consists of set values for P_0 , n_{Ti} , and r_c . To make comparisons meaningful I use 293 as the filling temperature T_0 and 350 for T_m in all cases. ρ_0 follows at once from P_0 and n_{Ti} , and when multiplied by r_c yields ρ_1 . P_m increases over P_0 by $350/293$,

or 1.195, the ratio of T_m / T_0 . Equation 13 produces γ_1 from T_1 and nTi , which in turn is required in eq. 3 and 4 to evaluate P_1 and T_1 . (Note that for shock tubes, rc doesn't apply, $\rho_0 = \rho_1$, $P_m = P_1$, $T_m = T_1 = 350$.)

Now is the time to insert trial values for T_d and P_d . By interpolation from tables⁸⁴ and eq. 15

and 11 come γ_d , M_d , and R_d , allowing evaluation of σ_d and π_d from eq. 8 and 9. Multiplying P_1 and π_d gives a feedback value for P_d , allowing adjustment and loops as required. P_d varies slowly and convergence is very rapid.

The second loop starts here. The next variables found are D , π_s , and σ_s from eq. 10, 5, and 6 in order. Multiplying T_1 by π_s / σ_s gives T_s . Now we find T_C from eq. 1 and use the supposition that $T_s = T_C$. If they are unequal, beyond the degree of error expected, this modifies the choice of T_d and P_d .

Once $T_s = T_C$, it's possible to find all the rest of the variables. $M\#$ comes from eq. 16, which gives an idea as to the strength of the shock. ρ_d comes from the product of σ_d and ρ_1 , and is required in eq. 17 to find $-\Delta h_d$. This in turn yields $-\Delta h_p$ from eq. 18. If $-\Delta h_p$ is too low, then T_p , the peak temperature of the powder, is inadequate and the reaction is not viable, at least in the context of a C-J shock. Estimating this peak temperature is difficult, as mentioned above. Borderline cases are unlikely to produce energy densities of interest for reactors, and so approximations are useful. In general peak powder temperatures place upper limits on nTi , since high nTi values lower the peak temperature.

PW follows from eq. 23 after evaluating J/cc . This is good only for the sample engine type described above. Next comes evaluating T_2 both for CV and CP reaction chambers, from eq. 25, and P_2 from eq. 27. For both PW and the CV T_2 , to avoid integration that would add accuracy beyond the error tolerance and thus add unwarranted complication, the equations use an average value γ_{12} . In practice this is a difficult value to find due to the relatively low temperatures and pressures--tables don't generally cover this range. However γ_{12} will be close enough to 1.38 in the sample shocks that all the calculations in the table use this value.

P_2 , valid for CV chambers, represents a limiting factor. Conventional Diesel engines commonly contain P_2 of 6 MPa; generally this is too low for adequate power density in WF engines. I show values of P_2 up to about 12 MPa and hope that proper engineering will cope with the pressure. More than this, or in general P_2 values above some acceptable limit, require another feedback loop for modifying the original values defining the reaction.

7.7.3 *Interpretation of Table of Shock Characteristics*

The Table includes figures for the Ti-D reaction described in this first paper, as well as figures for Li-H, Li-Ni, and Li-Ti covered in the second paper of the series. The Table is in six sections, the first and third of which cover the Ti-D reaction.

The first section covers shock tubes, which operate without initial compression and can either be open to a tank thus approximating constant pressure conditions, or closed to have constant volume conditions. The fact that this section is about shock tubes is shown in the “type” column, where after “TiD” there is “/s”. The third section covers reactors operating with compression before the reaction, such as with piston engines, turbines, and (if possible) MHD generators.

Column 1, P_0 , lists the initial filling temperature at 273 K. Due to the heating from repeated experiments in the shock tubes and normal elevated ambient temperatures in reactors, the actual ambient temperature, or manifold temperature T_m I take to be 350 in all cases and do not list it in the Table. This results in higher starting pressures than otherwise would be the case; the starting pressure is P_1 (column 12) for shock tubes and P_m (column 9) for reactors that have compression subsequently raising the temperature to P_1 .

Columns 3, 4, and 5 denote the molar concentration of powder. Only column 5, n_{Ti} , is of interest here. I show only two values which are probably fairly close to the interesting range, .01 and .02. Much higher than .02 results in T_p being too low and the shock probably not being viable. Below .01 results in $-\Delta h_p$ being too high to be reasonable or likely; there are other effects as noted below.

Column 6 shows ρ_0 , the initial density in either the shock tube or the reactor vessel before compression. Column 7, rc , is the compression ratio when it applies, NA when it does not. When there is compression, there follows ρ_1 , the post-compression density, and P_m , the pre-compression or manifold pressure. To compute first the pressure and temperature after compression, and in all cases the following shock characteristics, we must use column 10, γ_1 . Then follow values for T_1 and P_1 which in all cases are the values immediately preceding the shock.

Columns 1-12 are either the preliminary boundary conditions or derived from them, and constitute the environment for the inquiry into shock behavior. All the following columns describe the consequences of the shock. The terms for columns until 28 have been described above along with how they are computed.

Column 28 is the final equilibrium temperature at constant pressure CPT_2 , followed by the higher value for constant volume, CVT_2 . Then comes P_2 , the constant volume final pressure, and a very rough figure for T_p .

The Table only shows shocks whose parameters are reasonably close to chemically-induced detonation shocks within the C-J limits and which have reasonable T_p and $-\Delta h_{p0}$ values. Also I didn't allow P_2 to range up into levels where reactors would be impractical or difficult to build and where shock tubes would be overly expensive. Such high-pressure regions are still of interest but may not be suited to initial experiments and applications. Per unit of energy evolved, P_2 will always be significantly higher than with chemical detonations due to the physical characteristics of D₂ or H₂ gas as compared with heavier mixtures, and the nature of WF. These result in comparatively greater P_1 levels for equivalent energy density in chemical detonations.

Chemical values for σ_d are usually quite stable and are between 1.75 and 1.8. Only the most energetic WF shocks would be above the lower level. Also, typical chemical T_S is from 1400 to 1800, and the range in the shock tube section is close to that. $-\Delta h_d$ is lower than its chemical analog by a factor of about ten, but this is due to the fact that it has a distinctly

different meaning. PWCC shows a range compatible with the 20-80 expected in standard internal combustion engines of a range of types.

Expected divergence from chemical detonations comes from two main considerations. No explosive gas mixtures can hope to be as light as D₂-TiD₂ aerosol; that low density increases the sound speed and decreases the density compression ratios σ_d and σ_s among other effects. However, the D₂-TiD₂ aerosol is still close enough to the lightest types of chemically reacting gas mixtures, such as H₂-O₂, to make comparison reasonable. This is much more difficult in the aerosols investigated in the second paper due to the use of H₂ and Li, resulting in extremely low density even when adding Ni or Ti.

There are several simple conclusions from these rather approximate figures. One is that high initial pressures and low initial temperatures make the highest power densities. Another intensifying factor is for the nTi value to be as high as T_p allows. Both results make MHD less likely, since the high density of gas and especially the high powder density makes electron mobility, and hence conductivity, relatively low even at maximum possible temperatures. A third, and most important, conclusion is that the whole idea of a self-sustaining shock wave that provides appropriate conditions for WF reactions is feasible in regards to shock dynamics, reasonably expected power densities in the reacting powder, the interaction of solid hydride with gas in conditions of high temperature and pressure, and temperatures and pressures compatible with achievable reaction chambers and existing applications. There remains the larger question of whether the reactions actually will occur....

Table of Shock Characteristics (Columns 1-15)

	1	2	3	4	5	6	7	8	9	10	11	12	13	14	15
#	Po	type	nLi	nNi	nTi	o	rc	₁	Pm	₁	T ₁	P ₁	Td	Pd	d
	atm					kg/m ³		kg/m ³	MPa		K	MPa	K	MPa	
1	5	TiD/s			.01	.9372	NA	NA	NA	1.395	350	.6054	2630	7.11	1.286
2	10	TiD/s			.01	1.874	NA	NA	NA	1.395	350	1.211	2925	16.0	1.274
3	20	TiD/s			.01	3.749	NA	NA	NA	1.395	350	2.422	3200	35.4	1.279
4	20	TiD/s			.02	4.147	NA	NA	NA	1.390	350	2.422	3525	36.1	1.269
5	20	LiH/s	.12			2.268	NA	NA	NA	1.343	350	2.422	5940	61.8	1.188
6	20	LiNi/s	.005	.005		1.936	NA	NA	NA	1.395	350	2.422	5830	76.1	1.254
7	20	LiTi/s	.005		.005	1.900	NA	NA	NA	1.395	350	2.422	4510	43.3	1.271
8	3	TiD			.01	.5623	4	2.249	.3634	1.395	605	2.512	2425	15.0	1.319
9	3	TiD			.02	.6221	4	2.488	.3634	1.389	601	2.494	2700	15.5	1.302
10	3	TiD			.01	.5623	6	3.374	.3634	1.395	710	4.421	2400	21.8	1.324
11	5	TiD			.01	.9372	4	3.749	.6054	1.395	605	4.185	2660	27.7	1.312
12	3	LiH	.01			.2588	4	1.035	.3634	1.394	604	2.508	4310	27.2	1.207
13	3	LiH	.04			.281	4	1.24	.3634	1.375	588	2.422	4650	28.7	1.195
14	3	LiH	.08			.3106	4	1.242	.3634	1.351	569	2.364	5100	30.5	1.185
15	3	LiH	.12			.3402	4	1.361	.3634	1.331	553	2.299	5490	32.3	1.180
16	3	LiNi	.005	.005		.2905	4	1.162	.3634	1.394	604.5	2.510	5110	37.0	1.227
17	3	LiNi	.015	.015		.3685	4	1.474	.3634	1.383	595	2.470	5820	35.3	1.259
18	3	LiTi	.005		.005	.2849	4	1.140	.3634	1.394	604.5	2.510	3975	20.5	1.261
19	3	LiTi	.01		.01	.3186	4	1.274	.3634	1.388	800	2.491	4175	19.5	1.304

7.8 Fusion Engine

7.8.1 Cycle

[See Fig. 7.2.] This description starts as the cool gas and largely hydrided TiD_2 exits the heat exchanger. When the engine is running the action of the pistons pump the gas through the cycle. The pressure differential opens the check valve (1) and bypasses the compressor, which switches off when 1 is open. Otherwise the compressor circulates the gas through open poppet valves on the engine and through the entire circuit to stir up the powder as required, especially before a cold start.

Next comes the cold holding tank. This completes the hydriding of the fume by allowing time at T_m and P_m . As described above, the maximum solubility of D in Ti, as in other binary metal hydrides, occurs at low temperatures, and the hydriding process does require time. However the time will be much shorter than with any bulk form of metal as the particles are so minute, and the holding tanks will not have to be very large. This cold tank is handy to use as a manifold for pipes and valves allowing gas evacuation and filling.

Next, the gas and fully hydrided fume enter the engine cylinders during the intake stroke of the standard 4-stroke cycle. (2-cycle engines would have a great disadvantage due to pre-heating of the gas, to which WF is very sensitive. As a result they are probably not very practical.) There follows compression with a low compression ratio compared to i.c. engines. At or very near top dead center, the plasma jet plug fires.

During the expansion of the power stroke there will be some blow-by past the rings. An easy way of coping with this is to include the sealed crankcase as part of the circuit. The blowby exit path shown in the figure is only one possible way of doing this, and is much simplified. Sealing the crankcase will pose pressure problems, which can be dealt with by having an even number of cylinders sharing the crankcase volume, such that the volume remains roughly the same through the cycle.

After the exhaust stroke pumps the gas out of the cylinder, it enters the hot holding tank. This is to start the hydriding process, and in very fast engines possibly finish the condensation of supersaturated Ti vapor into solid fume particles. The rate of D uptake is

rapid while the gas is hot, which this tank takes advantage of, but it cannot complete the process at high temperatures.

Next comes the heat exchanger. In any mobile engine the most likely form would be an air-cooled radiator, while in fixed applications the usual coolant water or any variety of cooling currently used in closed-cycle heat engines would be appropriate. Unfortunately there isn't a phase change, which makes the size of exchanger larger than if there were; but the relatively high P_m level will help the size be small. The details of the reaction will heavily influence the major aspects of heat exchanger design.

7.8.2 *Cylinder Design*

There will probably be a small chamber functioning something like the ignition chamber in some i.c. engines, to be a little shock tube and contain the bulk of the reaction in a volume optimized for shocks. As there is a wide variety of possible geometries and design is premature I do not illustrate any details of such chambers.

One major consideration is protection of the piston rings from the shock, since they are likely made of temperature-sensitive materials more fragile than the cast iron of i.c. engines; the lubrication difficulty is discussed below. Both the shape of the top of the cylinder and the shape of the piston head will factor into this protection, as well as the use of one or more guard rings that do not quite touch the cylinder walls.

The cylinder walls and head should not be coated with ceramics, despite the advantages of corrosion resistance and thermal efficiency. The gas would be pre-heated by the large thermal swing of the coating, which is much lessened with metal.

7.8.3 *Advantages and Difficulties*

The advantages of piston engines are many in any application where i.c. engines currently find favor over gas turbines. The technology is the most developed of any in existence due to those advantages. However there are some aspects that do not so strongly apply to WF and fusion engines and turbines; the most critical of these is the lower rc . Small

gas turbines usually resort to centrifugal compressors with an rc of about 5, significantly lowering efficiency. Piston engines have a much easier method of compression, especially since it is not strictly speed dependent, at least within normal operating range; and that range is far greater than any turbine can accommodate. WF operates well at $rc = 5$, or even below, which changes the balance considerably.

The main problem with fusion engines, which has the potential of making them impractical, is lubrication. Conventional i.c. relies on an oil film and hard, durable piston rings. cycle engines cannot use liquid film and instead rely on close machining tolerances, high-alloy steel to maintain the smooth finish, and tolerance to blow-by. This is not a very good solution, adding considerably to manufacturing costs, lowering efficiency, and making the engines temperamental, especially on cold starts. This would be a last resort for fusion engines.

There may be solutions with imaginative use of Teflon. The cylinder walls might work with a porous nickel-hard coating impregnated with Teflon, and the piston rings could be a Teflon composite. There are sealing and lubrication problems with every moving part in the gas that must find solutions, and this may be the theme whose variations do the job.

Hot D₂ at several atmospheres is seriously corrosive, and will pose design problems wherever the gas temperature is too high to use copper or aluminum alloys. There is much engineering research in the field of hydrogen corrosion and all the relevant problems have general solutions applicable to this specific situation. Cost and fabrication difficulties posed by using high alloy steel are similar to those in cycle engines, with the exception of the 's use of external heating. The internal heating of WF is a major advantage.

7.9 Fusion Turbine

7.9.1 General Idea

Existing gas turbines rely on compressors to provide high density gas to combustors, which supply a steady flow of hot gas at slightly reduced pressure to turbines. For use with WF, turbines would use reaction chambers that convert the intermittent shocks of WF into a

steady flow of hot gas similar to combustors. There would be minimal design changes from existing closed-cycle plants except that the heat is from internal reactions instead of externally applied, and the compression ratio will be relatively low. As turbine design is highly developed, this paper only mentions factors relevant to WF specifically.

I do not anticipate a steady-state shock, for instance in the throat of a nozzle, where sub-sonic aerosol jumps to sonic at the narrow point. This is not compatible with C-J detonation shocks and causes a considerable loss of pressure. Conditions in such a shock would not be severe enough, and it's hard to see how such a shock could be stable. However I am not an expert in the field and will defer to those more experienced. If a steady-state shock could be devised it would have great advantages over relying on shocks in relative motion to the reaction chamber.

7.9.2 Cycle

Figure 7.3 shows an adaptation of a Rolls-Royce Dart turboprop engine to WF⁸⁵; in practice there would be more elaborate alteration to accommodate the differences between D₂ and air, as mentioned below. If the compression ratio is as low as 4 then there could be only one stage of compression.

This description starts at the entrance of the compressor, through a scrolled volute, at the bottom of Figure 7.3. The aerosol is in the same basic condition as when entering the engine cylinder, with fully hydrided powder and as low a temperature as is practical. In small sizes, centrifugal compressors have an advantage, while large turbines have the option of axial compressors. (If powder buildup on blades is a serious problem, centrifugal compressors and radial turbines will have a big advantage in all sizes.) The shaft exit will need a very good seal, probably of double thickness, which will be a major design challenge.

The compressed gas enters reaction chambers, which generate shocks and create a steady flow of heated gas. There are a wide variety of design options; my current favorite is the can reaction chamber in its muzzle loading version, described below and shown in Figures 7.3 and 7.4. The hot compressed gas enters the turbine section and exhausts into a

diffuser, where it cools and begins the condensation and rehydriding process as with the engine. It then passes through a heat exchanger and then back to the compressor.

Some control of the reaction rate and power produced comes from adjusting the ambient pressure, by pumping into and release from a storage tank. A similar method would be included in engines as well.

7.9.3 Advantages and Difficulties

All turbines have several inherent advantages over piston engines. The major one is the basic geometry. Turbines are essentially tubes through which gas flows at a high rate, while engines force the gas through small pipes and cylinders. Gas flows through a turbine about 70 times faster than through an engine of equal volume; since the major factor in power density is how much gas reacts, this provides the turbine with maximal power density in terms of both volume and weight.

The existing designs for closed-circuit gas turbine plants using He (usually for fission nuclear power) are close to those for WF and D₂ due to similar gas characteristics. However the ambient pressure of the He systems is higher, about 20 atm or more, to decrease the size of the plant, while the WF process will probably not be able to run that high from shock temperature limitations. The major gas difference would be in the lower value for γ in D₂. One major advantage over air is the very high sound speed due to low molecular weight, which largely eliminates shock problems and allows high flow rates just as with He. In other WF designs, such as those discussed in the second paper of this series, the potential use of H₂ enhances this trait even more. Shared with the He reactors is the leakage problem, especially as D₂ is costly. There is also the problem of corrosion that He reactor designs need not consider.

Lubrication is not anywhere near as difficult as with the fusion engine, and in fact this problem alone may make the turbine the most practical application for shaft power. Maintenance is easier with turbines, as there are far fewer moving parts and the entire plant is simpler than an engine. The modest compression ratios inherent to WF are well-suited to

ease of design, manufacture, and affordability, even including smaller sizes than usually seen in gas turbines.

The difficulties are somewhat the same as with gas turbines--a small speed range and all of it very fast, impracticality in smallest sizes, and difficulty with rapidly changing loads. For automobiles and trucks and similar applications, it may be best to simply use fusion turbines as generators and have a small battery powering the wheels with electric motors. This would save the difficulties of the elaborate transmission required. Also, a free turbine design would work well. The engineering for this has already been done in attempts to adapt gas turbines to automotive use; most of that work could be used with fusion turbines for the same purpose.

There are great advantages in cost, bulk, and simplicity to the use of single-stage centrifugal compressors with aluminum impellers. These would be practical in fusion turbines up to a compression ratio of about 4.

In any application currently favoring gas or steam turbines, where the load is typically continuous, such as aircraft, marine power plants, and generators, fusion turbines would be of tremendous utility. Aircraft in particular would convert *en masse* should this technology be viable.

7.9.4 Reaction Chamber Design

The function of a turbine's reaction chambers are to provide a constant flow of hot gas at or even above the pressure of the gas flowing from the compressor. If the equilibrium T_2 is too hot for the turbine blades, the shocked gas must be mixed at least to some extent with unreacted compressed gas.

Thermal efficiency would be better in constant volume (CV) reaction chambers, as with internal combustion, and there may be a way of configuring CV reaction chambers with valves. However the outflow would be intermittent and the device would be complex. CV turbines were the subject of research in Germany from 1908 through 1930, but they proved inferior to CP turbines. This paper will deal only with constant pressure (CP) chambers.

Inherent in any open-ended, CP shock tube is that the gas comes out in short, fast bursts, followed by low pressure sucking gas back in, unless there is a fast-acting valve on the beginning end, which I call the “breech-loading” version. Such valves would have the same problems found in CV chambers.

Figure 7.4 shows one current idea, the can reactor in the muzzle-loading version. I call it a “can reactor” as it resembles in overall shape the can combustors used in many gas turbines, and “muzzle-loading” because the unreacted fresh gas sucks into the shock tubes from the open far end after most of the reacted gas has exited. Valves are difficult to apply to shock tubes, and in this case would have to act very quickly, opening even before the shock reaches the end of the tube. These valves would require complex timing and represent a system that can break down. So there’s a lot of advantage to having a simple, no-moving-parts muzzle-loading system if it can work with comparable efficiency.

For the shock tube design, the velocity of the gas before the shock should be very low relative to the walls compared to the shock speed. This is a special complication for breech-loading systems.

The gas enters at the bottom of the figure and travels up within the inner pipe up to the shroud openings. This shroud helps direct the fresh gas into the shock tubes during their low-pressure recharge phase, while helping the exiting shock to mix minimally with fresh gas (although some will entrain).

Section A shows the radial arrangement of shock tubes at full width. The numbers indicate the order of firing, such that the pressure differences between adjacent tubes is minimized and the intake of fresh gas is maximally efficient.

At the beginning of the shock tubes are plasma jet plugs and cutoff valves. The valves when closed isolate the plugs and allow easy removal and replacement, an important feature given the problems with electrode erosion that remain unsolved. The beginning shock develops first in the apex of a truncated cone or pyramid shape, gradually increasing in width as shown.

7.10 Figures

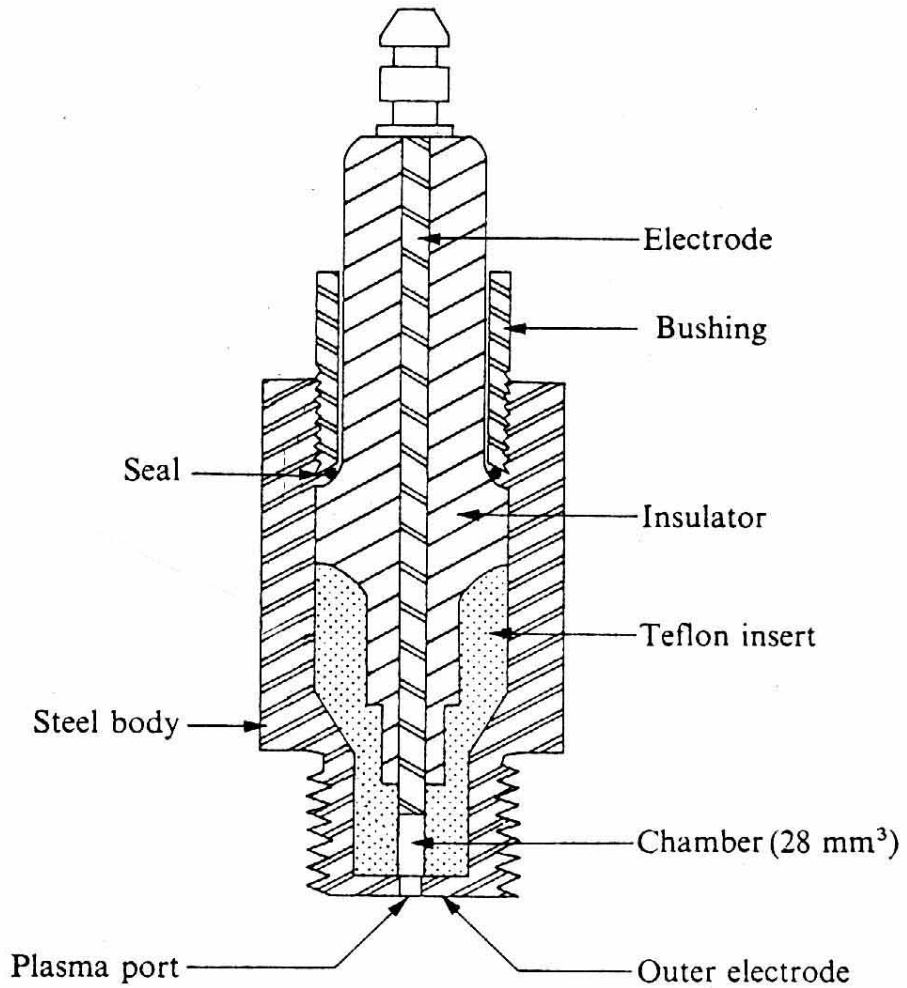


Figure 7.1: Plasma Jet Plug [from Weinberg et al. (1978)]

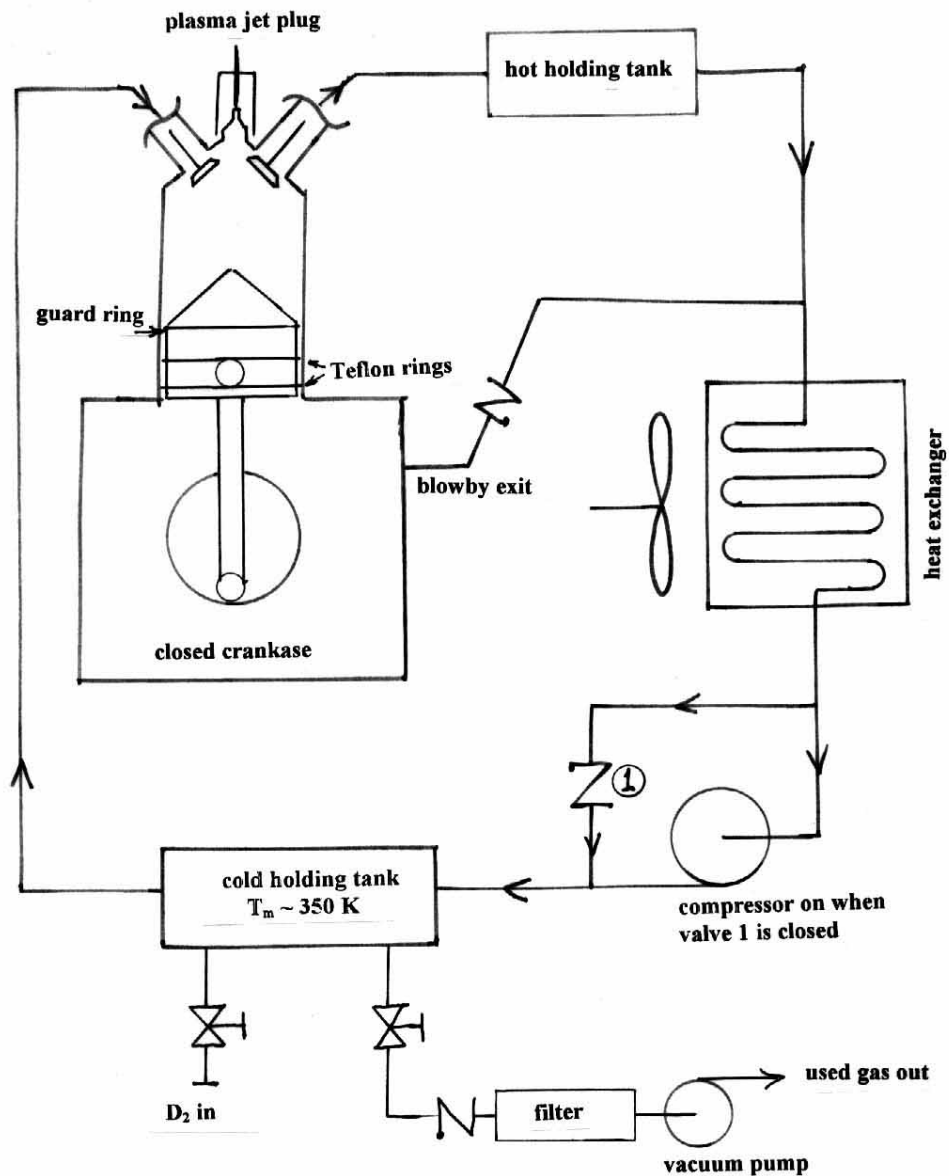


Figure 7.2: Fusion Engine Cycle Schematic

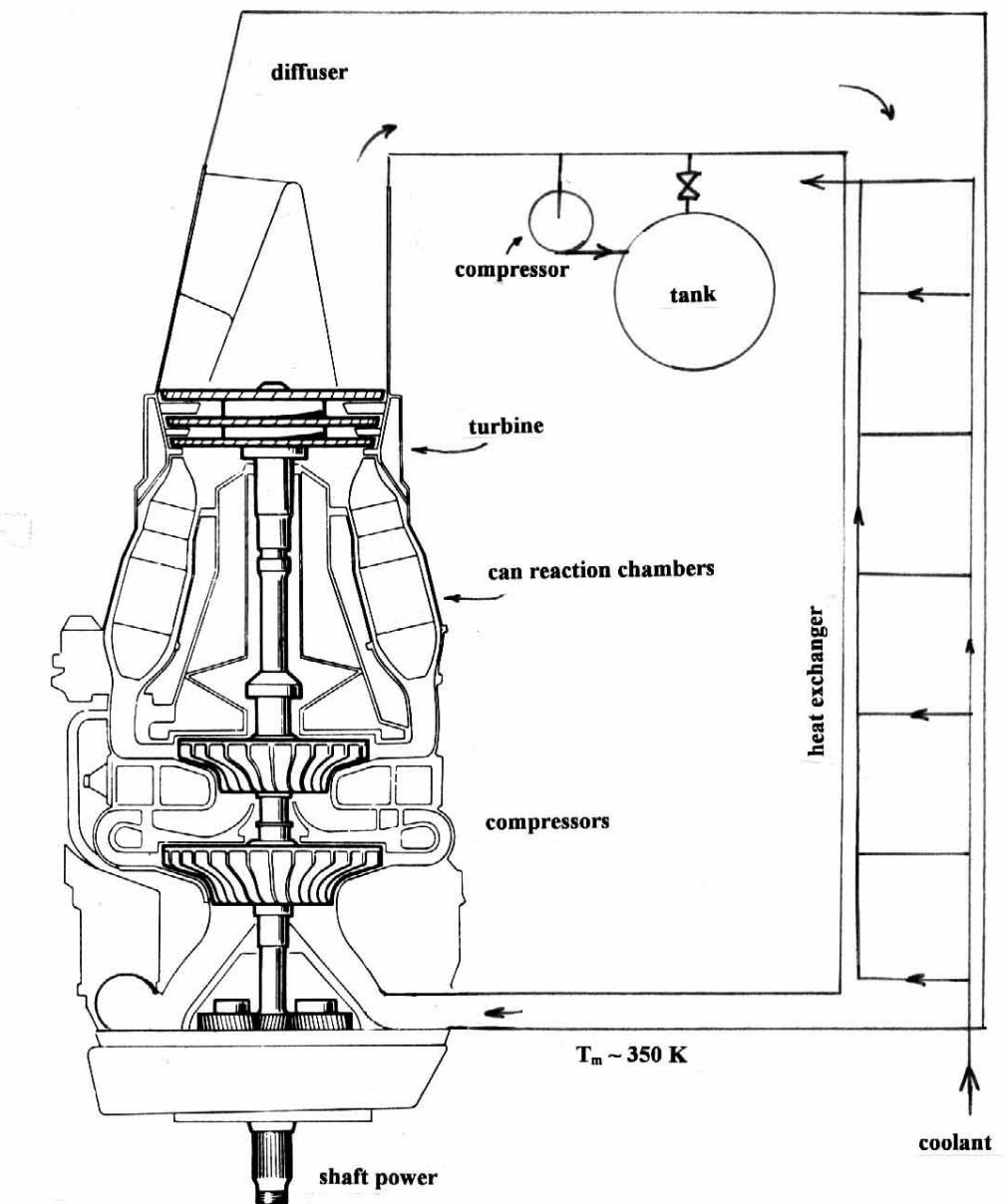


Figure 7.3: Fusion Turbine Cycle Schematic

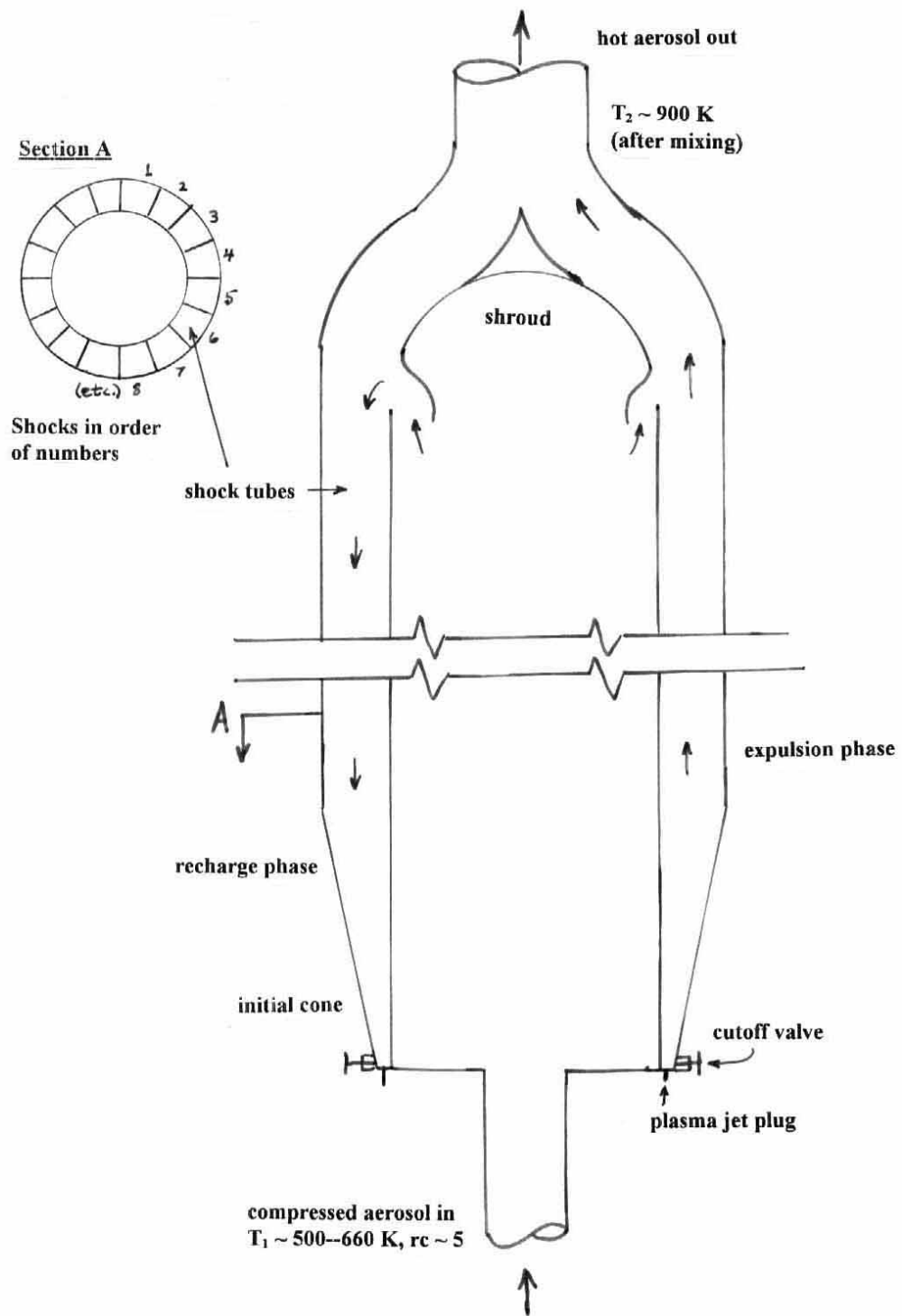


Figure 7.4: Can Reaction Chamber (muzzle loading version)

8 Appendix B: Warm Fusion II, Lithium Warm Fusion

8.1 Existing Evidence

Crystal Energy Inc. reports anomalous production of heat in a context that encourages extension of WF experimentation to powders containing lithium.⁸⁶ [*Note from 2009: Crystal Energy Inc. disappeared some years ago and one supposes the core claims they made are highly questionable, unverified, and almost certainly false. In particular, addition of lithium salts to diesel fuel aids in the combustion of soot, increasing the efficiency of the engine.*⁸⁷]

In the 1960's NASA conducted combustion experiments involving lithium compounds that generated more energy than would have been chemically possible. Following that were experiments with lithium salts added to a variety of fossil fuels in a wide range of applications including internal combustion in diesel and spark-ignition engines, as well as in boilers with external combustion.

The initial concept, continued to the present by some observers, was that the energy came from thermonuclear reactions from vapor Li and H atoms at the highest end of the energy distribution of the gas at typical flame temperatures. This would result in conventional nuclear reactions of the type $^6\text{Li} + \text{H} \rightarrow ^3\text{He} + \alpha$ and $^7\text{Li} + \text{H} \rightarrow 2 ^4\text{He} + 17.3$ Mev. (Although this is really a kind of light element fission I will call it fusion since it is in the class of light element nuclear reactions that are typically fusion, and to call it fission is confusing.) Indeed there are observations of alpha particles in about the amounts one would expect from the number of particles in the range of 12-30 KeV from the Boltzmann distribution, maybe a bit more. This is of the order of a million counts per minute within 5 cm. of a small flame, and is vastly smaller than required to account for the anomalous energy. Thus it is unlikely that conventional nuclear reactions have anything to do with the bulk of the unaccountable energy production. Cold fusion (CF) experiments typically do not produce high energy products, for reasons unknown, but do produce transmutation products and anomalous heat. The heat is in line with the observations of Crystal Energy, although they have not documented the transmuted elements. Accurate measurements of these

elements in this type of experiment would be very costly and is beyond the limited means of the experimenters to date. Closed systems such as WF and other CF experiments do not have such severe difficulties, although with the low atom count it will always be a challenge until power density is high.

Crystal Energy claims that there is a sort of chain reaction that provides enough fast hydrogen nuclei to cause the next generation of fusion reactions; maybe this has some small effect, but the argument is not convincing from the point of view of conventional physics, and doesn't explain the low alpha count. After all, were a chain reaction of this type in evidence in such a diffuse system, then putting LiH or some similar solid compound or mixture in the path of fast protons from an accelerator would result in a nuclear explosion.

While Crystal Energy argues that there is no connection between their process and CF, in fact there is much in common. One factor is that the Li-H reaction in flames is not predictable in efficacy, with experimental results varying unpredictably from zero to 30% augmentation. This is definitely a characteristic of typical CF experiments, especially as no one can say what makes the difference in energy production between any of them--indeed the same apparatus operated the same way gives different results. A second factor is the lack of sufficient high-energy products one would expect from conventional transmutation. And a third is the lack of any viable explanation for the anomalous heat from conventional physics, and the consequent difficulty in gathering interest in the field for serious inquiry. However well-observed, anomalous results devoid of convincing theory results in a severe disadvantage for the research.

8.1.1 Differences from Warm Fusion

Crystal Energy's process requires that the Li be added in a stable chemical compound (typically a nitrate) to fossil fuel. On ignition the Li vaporizes and reacts with H found in the hydrocarbon fuel. They propose a subsequent process where the 8.6 Mev alpha particles knock protons off of hydrogen compounds causing further Li-H collisions and reactions, which as noted above is hard to justify and which I do not believe to be true in terms of there

being enough reactions to make any difference. This is a process without regard to the specifics of the accompanying chemical reaction, as long as the chemical fuel includes hydrogen as a constituent element. Their process works either with detonation as in diesel engines or in constant-pressure external combustion. Oddly enough, the anomalous heat is least effective in spark-ignition engines where there is no detonation. Crystal Energy's process is always in an open system where the excess Li, which constitutes almost all of the Li, is lost with the exhaust of chemical reaction products. Considering that Li is a non-renewable resource, this is a serious flaw, only justified, as in their article, by temporary economic expediency.

WF, on the other hand, is a closed cycle that uses no chemical reactions for net energy production. No reaction products or unused fuel escape to the environment, leading to both vastly superior fuel usage efficiency and easy measurement and collection of transmuted elements. The fundamental idea in Lithium Warm Fusion (LWF) is the interaction of gas at high pressure and temperature with minute particles of solid hydride which either react itself, as with LiH, or both react and catalyze the reaction, as with LiH and Ni or LiH and TiH₂. An electrically initiated shock wave starts the process which powers itself as a detonation shock wave. There is a great advantage for solid LiH as the form of fuel over diffuse vaporized Li, as the density of H in the hydride is not much different than that of solid H. There is scant evidence for catalyst activity in CF experiments with any catalyst not in solid form, and in fact most of the theories (none of which are terribly convincing) of CF activity rely on some sort of lattice structure to cause reacting atoms to approach closely at low energies. In fact the limitations of maintaining such a lattice over time, since it is destroyed by CF reactions or by high temperatures, and the difficulties in quickly loading any bulk lattice geometry with reactants are the motivations for designing WF.

As such it is surprising to see any anomalous activity at all with diffuse vaporized Li in an atmosphere of relatively low density of H. Some of the reported observations might be true, but one must be wary in these matters.

8.2 Lithium Warm Fusion

8.2.1 Conditions Required

The conditions for LWF are the same as in *PRWF I* with the substitution of H₂ as the gas instead of D₂, and with the change in hydrides. This causes a higher sound speed and hence a faster shock wave at similar Mach numbers, as well as a higher resistance to shock formation while flowing through a reactor at high speed. Naturally there is no corresponding problem as with D₂ or H₂ contamination.

As with TDWF, T_s ≡ T_C; however, the T_C that applies must be the lowest of the two hydrides when two different types mix. This is the case with LTWF, when TiH₂ has the lesser stability and lower T_C values. Since Ni forms hydrides in negligible concentrations, in LNWF it is the LiH T_C that counts. LiH is very stable indeed, more stable than TiH₂, which leads to hot shocks. In fact, the addition of TiH₂ may be required at least in part, and perhaps essentially, to cool the shock, with a lower T_C. The effects are evident in the **Table of Shock Characteristics**. One would expect viable shocks to be similar to those seen in chemical detonations, although in all cases with LWF the gas is so much lighter than any chemical fuel that comparisons are not so easy to make. Even if hot shocks are viable in experiment, for applications the reactor design may require cooler conditions at more moderate pressures, especially in the case of constant volume reactions.

8.2.2 Reaction and Products

As stated above, the reactions would be ${}^6\text{Li} + \text{H} \rightarrow {}^3\text{He} + \alpha$ and ${}^7\text{Li} + \text{H} \rightarrow 2 {}^4\text{He} + 17.3 \text{ Mev}$, with the Be lasting on the order of 10^{-16} sec. (There is of course a family of related reactions but these are the least unlikely!) Crystal Energy reports no production of hard gamma rays or neutrons from their experiments, which would be in agreement with the above reaction. They do report some soft gamma rays at 500 kV but do not specify the intensity. The construction of any reactor would shield these rays without extra material. Experiments with LWF will include careful measurement of these gamma rays as well as alpha particles and fast protons; however the expectation is that almost all the energy

produced will go via an unknown mechanism to heating the powder and then the gas. This would be in line with other CF experiments and with those of Crystal Energy as well.

For purposes of understanding the reaction only, further trials using refined ^6Li and D would be useful. Then the reaction would be $^6\text{Li} + ^2\text{D} \rightarrow ^4\text{He} + 22.4 \text{ Mev}$, and also $^6\text{Li} + ^2\text{D} \rightarrow ^7\text{Be}^* + ^1\text{n} + 3.38 \text{ Mev}$. The ^7Be has a half-life of 53.4 days and an EC decay with .86 Mev. This is not a good idea for power generation for the obvious reasons of unnecessary cost of isotope separation and the danger of neutron production. However there is the anomaly of the lack of neutrons in other CF experiments where one would presume to find them, such as with D-D reactions--one of the several puzzles that relegate CF research to outsider status. The shock equations follow from the ones for $^7\text{Li}-\text{H}$ reactions with simple mass adjustments and are not included in this paper. (The equations in this paper are for isotopically unrefined Li.)

Li is highly reactive, and prefers a good many elements over H for forming compounds. Any powder added to the gas must be not only non-reactive with Li or LiH, it must not appreciably lessen the stability of the LiH as described in equation 28 or interfere with the hydriding of the condensed Li during and after cooling. Neither Ti nor Ni form stable bonds or alloys with Li, nor do they interfere with the Li-H reactions or form bimetallic hydrides. As a result the equations below treat the metals as autonomous.

8.2.3 Application Differences from PRWF I

Outward leakage from any reactor will be of much less consequence with H_2 than with D_2 , and as leakage is inevitable--especially with the most practical application, turbines--this is a substantial advantage of LWF. Air contamination of the aerosol would be worse with LWF as atmospheric oxygen and moisture would form compounds with the Li very quickly, but since the ambient pressure inside is always above atmospheric such contamination is relatively simple to avoid. There will have to be safeguards for such operations as changing plasma jet plugs, especially as the plugs will require frequent replacement.

Hot Li vapor will add to the already corrosive effects of the aerosol, and material choice will be strongly influenced by this problem.

It is possible that the temperatures and pressures of LWF could be adjusted by aerosol composition and initial or manifold pressures within a wide range, which could include very hot and high-pressure regions. In this case there could be reactors of especially high power density built to withstand extreme conditions, as well as more ordinary reactors built more lightly and cheaply. This potential range would be less in TDWF.

Should LWF include very high T_2 levels, then magnetohydrodynamic (MHD) generators may become practical. The hot gas would have to go through a nozzle to reduce the relatively high density and increase electron mobility; since this would cool the gas, it must start out at a sufficiently high T_2 to stay sufficiently conductive after the nozzle. (With sufficient velocity and proper geometry, the relaxation time required for electron recombination could lead to a higher conductivity after the nozzle than the temperature alone would allow.) Besides the generally higher efficiency than mechanical power extraction methods, there is the advantage of replacing turbine blades with magnetic fields when dealing with such a corrosive hot gas. In general the reactor design would be very much like a fusion turbine design with the MHD duct in the place of the turbine, except for the lower density of the gas in the duct. This would also imply lower density in the heat exchanger, leading to it having to be substantially larger than for a fusion turbine. In any case, MHD would only be practical in sizes of at least 1 MW. Any details beyond these broad statements must wait for experimental results, as MHD design is quite complex and highly dependent on many details of the gas properties.

LWF, however, may be possible to configure in a way that works in a gasdynamic laser, especially if the aerosol can be diluted and retain high enough power density. This will be the subject of further research.

8.3 C-J Detonation Shock Equations

8.3.1 Equations Unchanged from PRWF I

The basic form of equation 1, relating the pressure to T_C , is the same for LWF; however it is only *exactly* the same, with the same values for A and B, for LTWF since TiH_2 is the first to dehydride of the two hydrides. I neglect the small difference in stability between the deuteride and the hydride.

Equations 3, 4, 5, 6, 7, 8, 9, 10, 16, 17, 22, 23, and 26 are exactly the same for all WF shock calculations.

8.3.2 Equations Changed from PRWF I

For TDWF, $n\text{Ti}$ is low enough to have a minor effect; this is probably the case for LNWF and LTWF. However, $n\text{Li}$ levels are likely to be much greater in LHWF, leading to large effects for M and γ , and thus for all the other numbers. Since the major inaccuracies in these figures are in the modification of γ due to the powder, LHWF will have the least accurate equations.

Equation 1, $T_C = -A / (B - \ln P_s)$, continues to hold with different values for A and B in those cases where LiH is the hydride in question. This is the case in LHWF and LNWF. However the numerical version that I use must be modified, as (rather awkwardly) the equation I found is in terms of base 10 logarithms and pressure in millimeters of mercury. Since P_s is in pascals, the numerical version of (1) for LiH is

$$T_s = \frac{8244}{9.9258 \log(7.501 \times 10^{-3} P_s)} \quad (9.1)$$

The conceptual and numerical versions of (2) modify differently for each type of LWF. For LHWF, remembering that P_0 is in atm, $T_0 = 273$:

$$\rho_0 = P_0 \left(\text{moles m}^{-3} \text{ of ideal gas at 1 atm at } T_0 \right) \left(\text{kg mol}^{-3} \text{ of H}_2 + \text{kg mol}^{-3} \text{ of LiH} \right)$$

with the other types simply adding on kg mol⁻³ of Ni or TiH₂. The numerical versions for the three types are:

$$\text{LHWF } \rho_0 = 41.57 P_0 (2.016 \times 10^{-3} [1 - nLi] + 7.947 \times 10^{-3} nLi) \quad (9.2)$$

LNWF

$$\rho_0 = 41.57 P_0 (2.016 \times 10^{-3} [1 - nLi - nNi] + 7.947 \times 10^{-3} nLi + 58.69 \times 10^{-3} nNi) \quad (9.3)$$

LTWF

$$\rho_0 = 41.57 P_0 (2.016 \times 10^{-3} [1 - nLi - nTi] + 7.947 \times 10^{-3} nLi + 49.92 \times 10^{-3} nTi) \quad (9.4)$$

Equations for finding π_s , π_d , σ_d , and D rely on values for R_1 , M_1 , and/or M_d which are different in LWF. M_1 is the molecular weight of H₂ at T₁ and is always 2.016. R_1 thus is always $R_0 M_1^{-1} = 4124 \text{ J K}^{-1} \text{ mol}^{-1}$.

The general method for finding M_d is the same but adapted to LWF and is more complex. In zone **d**, all hydrides have dehydrated completely, and the H has not had time to reassociate. Frequently T_d will be high enough for substantial dissociation of the surrounding H₂, so M_{H2} can change appreciably, more than with TDWF. The molecular weight of all metal species must be included in the gas because, as before, it is in the form of supersaturated vapor.

The molar proportions become confusing with multiple powder types. As before, the molar proportions nLi, nNi, and nTi apply to the hydride powder in zone 1; after dehydrating and with atomic H, the proportions will change in each case differently. Following the same arguments as in PRWF I, the numerical versions of (11) are for the three types of LWF:

$$\text{LHWF } M_d = (M_{H2} [1 - nLi] + 7.947 nLi) / (1 + nLi) \quad (9.5)$$

$$\text{LNWF } M_d = (M_{H2} [1 - nLi - nNi] + 7.947 nLi + 58.69 nNi) / (1 + nLi) \quad (9.6)$$

$$\text{LTWF } M_d = (M_{H2} [1 - nLi - nTi] + 7.947 nLi + 49.92 nTi) / (1 + nLi + 2 nTi) \quad (9.7)$$

For finding various values for γ_x I must, for the moment, make the same approximations as before. Thus, I take C_p for Li to be the same as for LiH, although this certainly is not true. For LHWF, T_1 will always be less than 953 K, so LiH will be solid even at atmospheric pressure--and P_1 will almost certainly be above 1 atm. As a result $C_p = C_v$. Substituting the polynomial expression for C_p of Li for that of Ti into equation (1.13), γ_1 for LHWF is

$$\gamma_1 = \frac{(1-nTi)(6.62+0.00081T_1) + nTi(3.05+0.0086T_1)}{(1-nTi)(6.62+0.00081T_1) + nTi(3.05+0.0086T_1)} \quad (9.8)$$

For LNWF, the expression is the same except for the addition of $nNi (6 + .0018 T_1)$ to both numerator and denominator. Likewise, for LTWF it is the same as (35) except for the addition of $nTi (5.25 + .00252 T_1)$ to numerator and denominator.

Until further information comes in with regard to the effect of solid particles on the overall γ of an aerosol at high enough temperatures for the C_p of the powder to be appreciably greater than the C_v , I am approximating γ_{12} in all cases as 1.38. This is the only time γ_2 finds use in these equations. In time I will refine the values considerably.

For γ_d equations, I will show them here in terms of C_p and nX values only, since the polynomial expressions for C_p are shown above and there would be needless repetition. Also, C_{pH} , which is for dissociated hydrogen, varies a great deal and must come from tables. All the metal is in vapor form. C_p for Li vapor in the temperature and pressure likely in zone d is about 6 cal mol⁻¹; for Ti and Ni, C_p at d is 5. For all the metal vapors I take γ_d to be 1.63, and for dissociated H, $\gamma_d = 5/3$. Following the same logic as for equation (1.15), which should be a good deal more reliable than for γ_1 and γ_2 , the three new γ_d equations are:

$$\text{LHWF} \quad \gamma_d = \frac{Cp_{H_2}(1-nLi) + nLi(Cp_{Li} + Cp_H)}{\frac{Cp_{H_2}(1-nLi)}{\gamma_{H_2}} + nLi(0.61Cp_{Li} + 0.6Cp_H)} \quad (9.9)$$

$$\text{LNWF} \quad \gamma_d = \frac{Cp_{H_2}(1-nLi-nNi) + nLi(Cp_{Li} + Cp_H) + nNi Cp_{Ni}}{\frac{Cp_{H_2}(1-nLi-nNi)}{\gamma_{H_2}} + nLi(0.61Cp_{Li} + 0.6Cp_H) + 0.61Cp_{Ni}} \quad (9.10)$$

$$\text{LTWF} \quad \gamma_d = \frac{Cp_{H_2}(1-nLi-nTi) + nLi(Cp_{Li} + Cp_H) + nTi(Cp_{Ti} + 2Cp_H)}{\frac{Cp_{H_2}(1-nLi-nTi)}{\gamma_{H_2}} + nLi(0.61Cp_{Li} + 0.6Cp_H) + nTi(0.61Cp_{Ti} + 1.2Cp_H)} \quad (9.11)$$

Equation (1.18) must also change to reflect different proportions and molecular weights in finding Δhp as follows:

$$\text{LHWF} \quad \Delta hp = \Delta hd (2.016[1 - nLi] + 7.947 nLi) / 7.947 nLi \quad (9.12)$$

$$\text{LNWF} \quad \Delta hp = \frac{\Delta hd (2.016[1 - nLi - nNi] + 7.947 nLi + 58.69 nNi)}{7.947 nLi + 58.69 nNi} \quad (9.13)$$

$$\text{LTWF} \quad \Delta hp = \frac{\Delta hd (2.016[1 - nLi - nTi] + 7.947 nLi + 49.92 nTi)}{7.947 nLi + 49.92 nTi} \quad (9.14)$$

The modifications to find J/cc simplify to the following numerical versions:

$$\text{LHWF} \quad \text{J/cc} = (-\Delta hd + 127.7 \times 10^6 nLi) \rho_0 (10^{-6}) \quad (9.15)$$

$$\text{LNWF} \quad \text{J/cc} = (-\Delta hd + 127.7 \times 10^6 nLi + 6.75 \times 10^6 nNi) \rho_0 (10^{-6}) \quad (9.16)$$

$$\text{LTWF} \quad \text{J/cc} = (-\Delta hd + 127.7 \times 10^6 nLi + 117.4 \times 10^6 nTi) \rho_0 (10^{-6}) \quad (9.17)$$

To find T_2 , the previous method has to change to accommodate both different molar proportions and heats of condensation, as well as melting and boiling points for the three metals. In LTWF and LNWF, the temperatures both for constant pressure (CPT_2) and constant volume (CVT_2) are low enough with regard to P_2 , in the first case, and P_1 in the second, so that $M_2 = M_1 = 2.016$ at least to a good approximation. The metals in zone 2 are either solids or liquids, thus not modifying the molecular weight of the gas, and contribute in a simple way to T_2 by condensing either to solid, in the case of Ti and Ni, or to liquid for Li. While it is difficult to estimate γ_2 accurately, it is clear that in these cases it is not very low, and that the approximate value of 1.38 for the average γ_{12} is reasonable until better formulas are available. Therefore the equations for finding T_2 are simple adaptations of that used for TDWF where the Ti condenses to solid, and $M_2 = M_1$.

LHWF, on the other hand, reaches such high T_2 values that in many cases the Li stays in vapor form. This increases M_2 in both CVT_2 and CPT_2 calculations, and lowers γ_2 for CVT_2 . At these T_2 levels, H_2 is appreciably dissociated, especially with CP at P_1 which is far lower than P_2 , which has the effect of decreasing M_2 . Also the heat usually transferred to the gas by Li condensation no longer does so, raising T_2 in both cases. As a result there must be multiple equations and iterated loops, which at the time of this writing I have only started to deal with. The next edition will have a much more refined approach, especially with a better understanding of γ_2 . It is clear from the approximate work to date that LHWF is considerably hotter and produces higher P_2 levels than any of the other methods proposed.

Finding T_p is straightforward in adaptation of the TDWF method. One additional variable is VPLi, the melting point of Li, which varies according to pressure and must be taken from tables. Since T_p is the average peak temperature of the powder after its pressure has reached that of its environment, P_s , I use that pressure to determine VPLi. Again I make the approximation that the Cp for LiH is about the same as that for Li, which I will improve when more information is at hand. Thus the value for $Cp\Delta T$ for the Li has to split into the temperature range from T_C to VPLi, where the Cp of Li is about 7, and the rest of the way

from VPLi to T_p , where the Cp is about 6. The boiling point for nickel is about 3200 and for Ti about 3600; the Cp for Ni solid at these temperatures is about 9.2 and for vapor is about 5, while the Cp for Ti solid is 7.5 and vapor is 5.

The mass fractions for H, Li, Ni, and Ti in LNWF and LTWF are tedious. To simplify them here, \mathbf{D} stands for the denominator in the fraction; in LNWF, $\mathbf{D} = 7.95 \text{ nLi} + 58.7 \text{ nNi}$, and in LTWF, $\mathbf{D} = 7.95 \text{ nLi} + 49.9 \text{ nTi}$.

The concept of the equations is explained in *PRWF I*; below are the numerical versions for LWF.

$$\text{LHWF } -\Delta h_p = 126.8 (i_p - i_s) + 526.5 (7 [VPLi - T_s] + 6 (T_p - VPLi)) \quad (9.18)$$

$$\begin{aligned} \text{LNWF } -\Delta h_p = & (1008 \text{ nLi } \mathbf{D}^{-1}) (i_p - I_l) + (6940 \text{ nLi } \mathbf{D}^{-1}) (7 [VPLi - T_s] + 6 [T_p - VPLi]) \\ & + (58700 \text{ nNi } \mathbf{D}^{-1}) (9.2 [3200 - T_s] + 5 [T_p - 3200]) \end{aligned} \quad (9.19)$$

$$\begin{aligned} \text{LTWF } -\Delta h_p = & (1008 [nLi + 2 nTi] \mathbf{D}^{-1}) (i_p - i_s) + (6940 \text{ nLi } \mathbf{D}^{-1}) (7 [VPLi - T_s] + \\ & 6 [T_p - VPLi]) + (47900 \text{ nTi } \mathbf{D}^{-1}) (7.5 [3600 - T_s] + 5 [T_p - 3600]) \end{aligned} \quad (9.20)$$

8.4 Interpretation of Table of Shock Characteristics

8.4.1 LHWF

There is one example of shock tube LHWF, #5. I used 20 atm as a common value for several shock tube samples as it has a high energy density but low enough pressures to do experiments without excessive expenditure on equipment. An nLi of .12 was about as high as possible without T_p going too low, and as with other types of WF the energy density goes up with more powder. Even with this large powder content the density is not much more than with Ni and TiH added in much smaller amounts as seen in # 6 and 7, and is almost half that of TDWF at its highest powder density in otherwise similar conditions. Note how low γ values are, especially γ_d . T_d is the highest of any sample in the table, and P_d the second highest.

As with all LHWF, σ_d is lower than any but for LTWF--both types are considerably lower than the normal range for chemical detonations of 1.75-1.8. Both TDWF and LNWF are in or near the normal range. Since σ_d is the most stable of all the characteristic values for C-J shocks, this may indicate problems with shock viability--or maybe just that the gas is abnormally light.

D has dramatically high values for all the LWF samples due to the light molecular weight, and in #5 the value is maximal. The Mach number also is the second-highest behind #6. Due to the high stability of the ionic bond in LiH, T_C in both LHWF and LNWF is very high, and is maximal in #5. The normal range for chemical detonations is from 1400 to 1800, so this is a hot shock. J/cc is also highest in the table indicating an enormous energy release; on the other hand it also indicates that about this much energy *must* be released to make the shock, which is a heavy demand on the still-speculative reaction.

$-\Delta h_p$ is about as low as it can get before T_p is too cool. Generally $-\Delta h_p$ has to be above about 50 MJ/kg. Too many multiples above this strains credulity as to the possible energy density on the powder level of the reaction. While the T_2 and P_2 levels are not yet accurate enough for tabulation, they are almost certainly the highest in the table. T_p at about 12000 is a good level.

Next are #12-15, reactions after compression, all at initial pressure of 3 atm and a compression ratio of 4. These explore the range of nLi from .01 to .12, and show the dramatic influence of powder density.

8.4.2 LNWF

The shock tube example for LNWF is #6, again at 20 atm initial pressure. The sample nLi and nNi values are both .005, which could be considerably increased given the high T_p . Using this powder density allows comparison with TDWF, which is at a serious disadvantage in almost every respect. Later editions of this table will explore higher powder densities.

Ni is unique in the prospective powders as it does not form hydrides to any appreciable extent and thus does not alter T_S by chemical reaction. Thus the high T_C of LiH

allows high-temperature and high-pressure shocks, even higher pressure than with LTWF. #6 has the second-highest D and the highest Mach number in the table, and would be even more with greater powder density. One possibly significant factor is the relatively high σ_d value of 1.77, the highest listed and well within the chemical detonation norm. This is also true of the two reaction-chamber samples #16 and 17, and may play a role in justifying the use of Ni.

#16 and 17 are the same in initial conditions except for the variation in powder density. #16 has the same as #6, while #17 has three times as much at .015 for both nLi and nNi. This is about as high as a compression cycle allows, and has the usual beneficial effects, although more modest than usual. PWCC and J/cc are marginally higher in #17, but both T_2 values and P_2 are lower, which is unique in the table for a result from increased powder density.

8.4.3 LTWF

The effects of adding TiH_2 is quite different than those of Ni. Since TiH_2 is less stable than LiH, T_C is lower than other forms of LWF, and in the same vicinity as TDWF. #7, the shock tube example for LTWF, has less powder density than it could have, but it is not as far below its upper limit as #6. Of all the LWF examples it has the highest γ_d , and the lowest values for all parameters after column 12. The values for σ_d are so low that the viability of the shock come into question.

The reason for using LTWF would be in the hopes of enhancing the reaction through catalysis, especially if LHWF doesn't work and Ni doesn't help. If one of the two other methods works as shown, then LTWF would only be useful where there is a need for lower temperatures, pressures, and energy density than in other methods. This may be marginal as all three would occur simply by reducing P_0 in the other forms of WF.

Table 8.4 Shock Characteristics (columns 16-31)

	16	17	18	19	20	21	22	23	24	25	26	27	28	29	30	31
#	d	d	D	s	s	Ts=Tc	M#	d	hd	J/cc	PWCC	hp	CPT ₂	CVT ₂	P ₂	T _p
	m/s			K			MJ/kg			kW/l		MJ/kg	K	K	MPa	K
																x1000
engine																
1	1.71	11.7	4320	21.9	5.27	1460	4.30	1.60	5.50	6.25	NA	47.8	1235	1550	2.71	>10
2	1.73	13.2	4580	24.8	5.47	1585	4.56	3.24	6.23	13.9	NA	54.1	1325	1670	5.84	>10
3	1.73	14.6	4830	27.5	5.57	1730	4.82	6.49	6.94	30.4	NA	60.3	1415	1790	12.5	>10
4	1.74	14.9	4870	28.0	5.65	1735	4.85	7.22	6.66	37.3	NA	57.8	1380	1740	12.2	>10
5	1.54	25.5	8217	41.2	7.09	2035	6.39	3.49	21.6	83.7	NA	61.8	----	----	----	~12
6	1.77	31.4	7544	33.8	5.93	1990	7.08	3.29	30.2	59.8	NA	212	2290	2935	20.4	>>10
7	1.44	17.9	6870	27.9	5.63	1735	5.33	2.74	18.2	37.0	NA	144	1650	2100	14.6	>>10
8	1.63	5.96	4000	10.7	4.15	1565	3.03	4.84	3.40	2.57	19.3	29.5	1200	1420	5.96	>8
9	1.65	6.23	4070	11.2	4.28	1570	3.10	4.89	3.52	3.65	27.4	16.9	1360	1635	6.93	6+
10	1.60	4.94	3970	8.73	3.81	1625	2.74	4.75	4.76	3.34	27.2	43.7	1470	1745	11.0	>10
11	1.65	6.61	4220	12.0	4.34	1675	3.20	6.19	5.04	5.82	43.7	43.7	1410	1700	11.9	>10
12	1.42	10.9	6810	16.1	5.23	1855	4.06	1.47	20.3	5.59	42.0	531	1965	2435	10.2	>10
13	1.44	11.8	7010	17.6	5.55	1870	4.25	1.79	17.9	6.48	48.6	127	2050	----	----	>>10
14	1.46	12.9	7250	19.6	5.95	1880	4.49	1.77	19.6	9.25	69.4	76.6	----	----	----	~15
15	1.48	14.0	7470	21.6	6.30	1895	4.71	2.01	18.5	11.5	86.3	52.8	----	----	----	~9
16	1.76	14.7	6714	15.5	5.07	1850	4.78	2.05	23.3	6.96	52.2	163	2100	2615	10.9	>10
17	1.74	14.3	6644	15.4	4.97	1845	4.76	2.57	17.5	7.21	54.1	52.4	1840	2270	9.47	10.5
18	1.34	8.16	5860	11.7	4.48	1580	3.54	1.53	13.8	4.28	32.1	109	1600	1955	8.18	>10
19	1.31	7.83	5750	11.2	4.28	1570	3.50	1.49	12.4	4.72	35.4	55.0	1620	1980	8.35	10

9 Appendix C: Magnet Calculations

These calculations were completed in the summer of 2006 just before starting construction. I used cylindrical coordinates with the z axis along the poles of the reactor, and the polar plane separating the hemispheres. The hemispheres have current flowing in opposite directions, resulting in a cusp field with polar and rim cusps.

Using Mathematica, I calculated first the direction and magnitude of the **B** field in a plane including the poles and bisecting the hemispheres, which are displayed in a vector field plot; thus the azimuthal angles are 0 and π . (This field plot is displayed after the magnitude plots.) Then I calculated the magnitudes of **B** and displayed the results in a contour plot of iso-magnetic surfaces. This assumed a radius for the magnet spindle of 0.3315 m surrounding the pressure sphere, whose location is indicated by thick double lines. At the current indicated, the ECR oblate spheroid is well within the antenna tips and is displayed by an extra-thick contour line.

I used the off-axis formulas using elliptic integrals for a single current loop for each of 20 loops on the surface of the spindle for one hemisphere, leaving room for the polar pipe and equatorial flange and coax cable access. The program starts with the definition of these formulas. With symmetry the field is mirrored for the other hemisphere. I used one equation for each of the two coordinates of every loop's field, and added up the fields from all the loops. By putting in trial values for the current in each loop, and observing the effect on the contour plot of iso-surfaces, I could adjust each loop current to produce the desired effect. (There is an analytic method for doing this⁸⁸, but it is extremely difficult and does not produce any better result for the vastly increased work. There are also Finite Element Analysis programs available, of which mine is rather similar, but I found it easier to write my own than to try and adapt off-the-shelf code and learn how to use it.)

In this geometry, it is possible to adjust the current distribution (via coil winding density) such that there is one iso-surface that is a sphere. Between that sphere and the magnet, the surfaces become chaotic. Inside that sphere, all the surfaces become

progressively more and more oblate. As the shape of the iso-surfaces is independent of current levels, when the magnet pulse proceeds the **B** magnitudes will increase over time in this geometry, and the ECR surface will migrate from the outside to the ultimate inner surface. Thus it is necessary to place the one spherical iso-surface very close to the magnet, and allow the ECR to be oblate instead of spherical when it is well within the reactor.

The result is a magnet that is going to be complex, challenging to build, and with considerable power requirements. While I made a mock-up of the magnet spindles using acrylic hemispheres, the real magnet would require substantial spindles equipped to secure the magnets against serious forces pushing them apart. The copper winding should weigh about 90 pounds per hemisphere, assuming splitting the winding into about four parallel strands of equal length and using the most efficient gauge wire. The initial experiment calls for brief pulsed power, so cooling is not a major issue; but with frequent pulses, this could be a further complication and expense.

$$\begin{aligned}
& \left(\mu_0 = \frac{4\pi}{10^7}; Bo[i_-, a_-] := \frac{\mu_0 i}{2a}; R = 0.3315^\circ; \right) \\
& \left(\begin{array}{l} Bo[i, a] \left(\frac{\text{EllipE}\left[\frac{4r}{a\left(\left(1+\frac{r}{a}\right)^2 + \left(\frac{z}{a}\right)^2\right)}\right] \left(1 - \left(\frac{r}{a}\right)^2 - \left(\frac{z}{a}\right)^2\right)}{\left(\left(1+\frac{r}{a}\right)^2 + \left(\frac{z}{a}\right)^2\right) - \frac{4r}{a}} + \text{EllipK}\left[\frac{4r}{a\left(\left(1+\frac{r}{a}\right)^2 + \left(\frac{z}{a}\right)^2\right)}\right] \right), \\ Bz[a_-, i_-, r_-, z_-] := N\left[\frac{Bo[i, a] \left(\frac{\text{EllipE}\left[\frac{4r}{a\left(\left(1+\frac{r}{a}\right)^2 + \left(\frac{z}{a}\right)^2\right)}\right] \left(1 + \left(\frac{r}{a}\right)^2 + \left(\frac{z}{a}\right)^2\right)}{\left(\left(1+\frac{r}{a}\right)^2 + \left(\frac{z}{a}\right)^2\right) + \frac{4r}{a}} - \text{EllipK}\left[\frac{4r}{a\left(\left(1+\frac{r}{a}\right)^2 + \left(\frac{z}{a}\right)^2\right)}\right] \right)}{\pi \sqrt{\left(1 + \frac{r}{a}\right)^2 + \left(\frac{z}{a}\right)^2}} \right], \\ Br[a_-, i_-, r_-, z_-] := N\left[\frac{Bo[i, a] z \left(\frac{\text{EllipE}\left[\frac{4r}{a\left(\left(1+\frac{r}{a}\right)^2 + \left(\frac{z}{a}\right)^2\right)}\right] \left(1 + \left(\frac{r}{a}\right)^2 + \left(\frac{z}{a}\right)^2\right)}{\left(\left(1+\frac{r}{a}\right)^2 + \left(\frac{z}{a}\right)^2\right) + \frac{4r}{a}} - \text{EllipK}\left[\frac{4r}{a\left(\left(1+\frac{r}{a}\right)^2 + \left(\frac{z}{a}\right)^2\right)}\right] \right)}{r \left(\pi \sqrt{\left(1 + \frac{r}{a}\right)^2 + \left(\frac{z}{a}\right)^2} \right)} \right] \end{array} \right) \\
& \left(\begin{array}{l} Bztotal[i1_-, i2_-, i3_-, i4_-, i5_-, i6_-, i7_-, i8_-, i9_-, i10_-, i11_-, i12_-, i13_-, i14_-, i15_-, \\ i16_-, i17_-, i18_-, i19_-, i20_-, r_-, z_-] := Bz[R \sin\left[\frac{6.08^\circ \pi}{180}\right], i1, r, z + R \cos\left[\frac{6.08^\circ \pi}{180}\right]] + \\ Bz[R \sin\left[\frac{10.22^\circ \pi}{180}\right], i2, r, z + R \cos\left[\frac{10.22^\circ \pi}{180}\right]] + Bz[R \sin\left[\frac{14.39^\circ \pi}{180}\right], i3, \\ r, z + R \cos\left[\frac{14.39^\circ \pi}{180}\right]] + Bz[R \sin\left[\frac{18.49^\circ \pi}{180}\right], i4, r, z + R \cos\left[\frac{18.49^\circ \pi}{180}\right]] + \\ Bz[R \sin\left[\frac{22.63^\circ \pi}{180}\right], i5, r, z + R \cos\left[\frac{22.63^\circ \pi}{180}\right]] + Bz[R \sin\left[\frac{26.77^\circ \pi}{180}\right], i6, r, \\ z + R \cos\left[\frac{26.77^\circ \pi}{180}\right]] + Bz[R \sin\left[\frac{30.09^\circ \pi}{180}\right], i7, r, z + R \cos\left[\frac{30.09^\circ \pi}{180}\right]] + \\ Bz[R \sin\left[\frac{35.04^\circ \pi}{180}\right], i8, r, z + R \cos\left[\frac{35.04^\circ \pi}{180}\right]] + Bz[R \sin\left[\frac{39.18^\circ \pi}{180}\right], i9, r, \\ z + R \cos\left[\frac{39.18^\circ \pi}{180}\right]] + Bz[R \sin\left[\frac{43.31^\circ \pi}{180}\right], i10, r, z + R \cos\left[\frac{43.31^\circ \pi}{180}\right]] + \\ Bz[R \sin\left[\frac{47.45^\circ \pi}{180}\right], i11, r, z + R \cos\left[\frac{47.45^\circ \pi}{180}\right]] + Bz[R \sin\left[\frac{51.59^\circ \pi}{180}\right], i12, \\ r, z + R \cos\left[\frac{51.59^\circ \pi}{180}\right]] + Bz[R \sin\left[\frac{55.72^\circ \pi}{180}\right], i13, r, z + R \cos\left[\frac{55.72^\circ \pi}{180}\right]] + \\ Bz[R \sin\left[\frac{59.86^\circ \pi}{180}\right], i14, r, z + R \cos\left[\frac{59.86^\circ \pi}{180}\right]] + Bz[R \sin\left[\frac{64\pi}{180}\right], i15, r, z + R \cos\left[\frac{64\pi}{180}\right]] + \\ Bz[R \sin\left[\frac{68.14^\circ \pi}{180}\right], i16, r, z + R \cos\left[\frac{68.14^\circ \pi}{180}\right]] + \\ Bz[R \sin\left[\frac{72.27^\circ \pi}{180}\right], i17, r, z + R \cos\left[\frac{72.27^\circ \pi}{180}\right]] + Bz[R \sin\left[\frac{76.41^\circ \pi}{180}\right], i18, \\ r, z + R \cos\left[\frac{76.41^\circ \pi}{180}\right]] + Bz[R \sin\left[\frac{83.7^\circ \pi}{180}\right], i19, r, z + R \cos\left[\frac{83.7^\circ \pi}{180}\right]] + \\ Bz[R \sin\left[\frac{87.7^\circ \pi}{180}\right], i20, r, z + R \cos\left[\frac{87.7^\circ \pi}{180}\right]] + Bz[R \sin\left[\frac{87.7^\circ \pi}{180}\right], -i20, r, \end{array} \right)
\end{aligned}$$

Printed by Mathematica for Students

$$\begin{aligned}
& z - R \cos\left[\frac{87.7^\circ \pi}{180}\right] + Bz\left[R \sin\left[\frac{83.7^\circ \pi}{180}\right], -119, r, z - R \cos\left[\frac{83.7^\circ \pi}{180}\right]\right] + \\
& Bz\left[R \sin\left[\frac{76.41^\circ \pi}{180}\right], -118, r, z - R \cos\left[\frac{76.41^\circ \pi}{180}\right]\right] + Bz\left[R \sin\left[\frac{72.27^\circ \pi}{180}\right], -117, r, z - R \cos\left[\frac{72.27^\circ \pi}{180}\right]\right] + \\
& Bz\left[R \sin\left[\frac{68.14^\circ \pi}{180}\right], -116, r, z - R \cos\left[\frac{68.14^\circ \pi}{180}\right]\right] + \\
& Bz\left[R \sin\left[\frac{64^\circ \pi}{180}\right], -115, r, z - R \cos\left[\frac{64^\circ \pi}{180}\right]\right] + Bz\left[R \sin\left[\frac{59.86^\circ \pi}{180}\right], -114, r, z - R \cos\left[\frac{59.86^\circ \pi}{180}\right]\right] + \\
& Bz\left[R \sin\left[\frac{55.72^\circ \pi}{180}\right], -113, r, z - R \cos\left[\frac{55.72^\circ \pi}{180}\right]\right] + \\
& Bz\left[R \sin\left[\frac{51.59^\circ \pi}{180}\right], -112, r, z - R \cos\left[\frac{51.59^\circ \pi}{180}\right]\right] + Bz\left[R \sin\left[\frac{47.45^\circ \pi}{180}\right], -111, r, z - R \cos\left[\frac{47.45^\circ \pi}{180}\right]\right] + \\
& Bz\left[R \sin\left[\frac{43.31^\circ \pi}{180}\right], -110, r, z - R \cos\left[\frac{43.31^\circ \pi}{180}\right]\right] + \\
& Bz\left[R \sin\left[\frac{39.18^\circ \pi}{180}\right], -19, r, z - R \cos\left[\frac{39.18^\circ \pi}{180}\right]\right] + Bz\left[R \sin\left[\frac{35.04^\circ \pi}{180}\right], -18, r, z - R \cos\left[\frac{35.04^\circ \pi}{180}\right]\right] + \\
& Bz\left[R \sin\left[\frac{30.09^\circ \pi}{180}\right], -17, r, z - R \cos\left[\frac{30.09^\circ \pi}{180}\right]\right] + \\
& Bz\left[R \sin\left[\frac{26.77^\circ \pi}{180}\right], -16, r, z - R \cos\left[\frac{26.77^\circ \pi}{180}\right]\right] + Bz\left[R \sin\left[\frac{22.63^\circ \pi}{180}\right], -15, r, z - R \cos\left[\frac{22.63^\circ \pi}{180}\right]\right] + \\
& Bz\left[R \sin\left[\frac{18.49^\circ \pi}{180}\right], -14, r, z - R \cos\left[\frac{18.49^\circ \pi}{180}\right]\right] + Bz\left[R \sin\left[\frac{14.39^\circ \pi}{180}\right], -13, r, z - R \cos\left[\frac{14.39^\circ \pi}{180}\right]\right] + Bz\left[R \sin\left[\frac{10.22^\circ \pi}{180}\right], -12, r, z - R \cos\left[\frac{10.22^\circ \pi}{180}\right]\right] + \\
& Bz\left[R \sin\left[\frac{6.08^\circ \pi}{180}\right], -11, r, z - R \cos\left[\frac{6.08^\circ \pi}{180}\right]\right]; \\
& \left(\text{Brtotal}[i1_, i2_, i3_, i4_, i5_, i6_, i7_, i8_, i9_, i10_, i11_, i12_, i13_, i14_, i15_, \right. \\
& \quad \left. i16_, i17_, i18_, i19_, i20_, r_, z_] := \text{Br}\left[R \sin\left[\frac{6.08^\circ \pi}{180}\right], i1, r, z + R \cos\left[\frac{6.08^\circ \pi}{180}\right]\right] + \right. \\
& \quad \left. \text{Br}\left[R \sin\left[\frac{10.22^\circ \pi}{180}\right], i2, r, z + R \cos\left[\frac{10.22^\circ \pi}{180}\right]\right] + \text{Br}\left[R \sin\left[\frac{14.39^\circ \pi}{180}\right], i3, r, z + 0.9688^\circ R\right] + \right. \\
& \quad \left. \text{Br}\left[R \sin\left[\frac{18.49^\circ \pi}{180}\right], i4, r, z + R \cos\left[\frac{18.49^\circ \pi}{180}\right]\right] + \text{Br}\left[R \sin\left[\frac{22.63^\circ \pi}{180}\right], i5, r, z + R \cos\left[\frac{22.63^\circ \pi}{180}\right]\right] + \right. \\
& \quad \left. \text{Br}\left[R \sin\left[\frac{26.77^\circ \pi}{180}\right], i6, r, z + R \cos\left[\frac{26.77^\circ \pi}{180}\right]\right] + \text{Br}\left[R \sin\left[\frac{30.09^\circ \pi}{180}\right], i7, r, z + R \cos\left[\frac{30.09^\circ \pi}{180}\right]\right] + \right. \\
& \quad \left. \text{Br}\left[R \sin\left[\frac{35.04^\circ \pi}{180}\right], i8, r, z + R \cos\left[\frac{35.04^\circ \pi}{180}\right]\right] + \right. \\
& \quad \left. \text{Br}\left[R \sin\left[\frac{39.18^\circ \pi}{180}\right], i9, r, z + R \cos\left[\frac{39.18^\circ \pi}{180}\right]\right] + \text{Br}\left[R \sin\left[\frac{43.31^\circ \pi}{180}\right], i10, r, z + R \cos\left[\frac{43.31^\circ \pi}{180}\right]\right] + \right. \\
& \quad \left. \text{Br}\left[R \sin\left[\frac{47.45^\circ \pi}{180}\right], i11, r, z + R \cos\left[\frac{47.45^\circ \pi}{180}\right]\right] + \right. \\
& \quad \left. \text{Br}\left[R \sin\left[\frac{51.59^\circ \pi}{180}\right], i12, r, z + R \cos\left[\frac{51.59^\circ \pi}{180}\right]\right] + \text{Br}\left[R \sin\left[\frac{55.72^\circ \pi}{180}\right], i13, r, z + R \cos\left[\frac{55.72^\circ \pi}{180}\right]\right] + \right. \\
& \quad \left. \text{Br}\left[R \sin\left[\frac{59.86^\circ \pi}{180}\right], i14, r, z + R \cos\left[\frac{59.86^\circ \pi}{180}\right]\right] + \right. \\
& \quad \left. \text{Br}\left[R \sin\left[\frac{63.08^\circ \pi}{180}\right], i15, r, z + R \cos\left[\frac{63.08^\circ \pi}{180}\right]\right] \right);
\end{aligned}$$

```

Br[R Sin[ $\frac{64 \pi}{180}$ ], i15, r, z + R Cos[ $\frac{64 \pi}{180}$ ]] + Br[R Sin[ $\frac{68.14^\circ \pi}{180}$ ], i16, r, z + R Cos[ $\frac{68.14^\circ \pi}{180}$ ]] +
Br[R Sin[ $\frac{72.27^\circ \pi}{180}$ ], i17, r, z + R Cos[ $\frac{72.27^\circ \pi}{180}$ ]] + Br[R Sin[ $\frac{76.41^\circ \pi}{180}$ ], i18,
r, z + R Cos[ $\frac{76.41^\circ \pi}{180}$ ]] + Br[R Sin[ $\frac{83.7^\circ \pi}{180}$ ], i19, r, z + R Cos[ $\frac{83.7^\circ \pi}{180}$ ]] +
Br[R Sin[ $\frac{87.7^\circ \pi}{180}$ ], i20, r, z + R Cos[ $\frac{87.7^\circ \pi}{180}$ ]] + Br[R Sin[ $\frac{87.7^\circ \pi}{180}$ ], -i20, r,
z - R Cos[ $\frac{87.7^\circ \pi}{180}$ ]] + Br[R Sin[ $\frac{83.7^\circ \pi}{180}$ ], -i19, r, z - R Cos[ $\frac{83.7^\circ \pi}{180}$ ]] +
Br[R Sin[ $\frac{76.41^\circ \pi}{180}$ ], -i18, r, z - R Cos[ $\frac{76.41^\circ \pi}{180}$ ]] + Br[R Sin[ $\frac{72.27^\circ \pi}{180}$ ], -i17,
r, z - R Cos[ $\frac{72.27^\circ \pi}{180}$ ]] + Br[R Sin[ $\frac{58.14^\circ \pi}{180}$ ], -i16, r, z - R Cos[ $\frac{58.14^\circ \pi}{180}$ ]] +
Br[R Sin[ $\frac{64 \pi}{180}$ ], -i15, r, z - R Cos[ $\frac{64 \pi}{180}$ ]] + Br[R Sin[ $\frac{59.86^\circ \pi}{180}$ ], -i14, r,
z - R Cos[ $\frac{59.86^\circ \pi}{180}$ ]] + Br[R Sin[ $\frac{55.72^\circ \pi}{180}$ ], -i13, r, z - R Cos[ $\frac{55.72^\circ \pi}{180}$ ]] +
Br[R Sin[ $\frac{51.59^\circ \pi}{180}$ ], -i12, r, z - R Cos[ $\frac{51.59^\circ \pi}{180}$ ]] + Br[R Sin[ $\frac{47.45^\circ \pi}{180}$ ], -i11,
r, z - R Cos[ $\frac{47.45^\circ \pi}{180}$ ]] + Br[R Sin[ $\frac{43.31^\circ \pi}{180}$ ], -i10, r, z - R Cos[ $\frac{43.31^\circ \pi}{180}$ ]] +
Br[R Sin[ $\frac{39.18^\circ \pi}{180}$ ], -i9, r, z - R Cos[ $\frac{39.18^\circ \pi}{180}$ ]] + Br[R Sin[ $\frac{35.04^\circ \pi}{180}$ ], -i8,
r, z - R Cos[ $\frac{35.04^\circ \pi}{180}$ ]] + Br[R Sin[ $\frac{30.09^\circ \pi}{180}$ ], -i7, r, z - R Cos[ $\frac{30.09^\circ \pi}{180}$ ]] +
Br[R Sin[ $\frac{26.77^\circ \pi}{180}$ ], -i6, r, z - R Cos[ $\frac{26.77^\circ \pi}{180}$ ]] + Br[R Sin[ $\frac{22.63^\circ \pi}{180}$ ], -i5,
r, z - R Cos[ $\frac{22.63^\circ \pi}{180}$ ]] + Br[R Sin[ $\frac{18.49^\circ \pi}{180}$ ], -i4, r, z - R Cos[ $\frac{18.49^\circ \pi}{180}$ ]] +
Br[R Sin[ $\frac{14.39^\circ \pi}{180}$ ], -i3, r, z - R Cos[ $\frac{14.39^\circ \pi}{180}$ ]] + Br[R Sin[ $\frac{10.22^\circ \pi}{180}$ ], -i2,
r, z - R Cos[ $\frac{10.22^\circ \pi}{180}$ ]] + Br[R Sin[ $\frac{6.08^\circ \pi}{180}$ ], -i1, r, z - R Cos[ $\frac{6.08^\circ \pi}{180}$ ]];)

(BmagSph[i1_, i2_, i3_, i4_, i5_, i6_, i7_, i8_, i9_, i10_, i11_, i12_,
i13_, i14_, i15_, i16_, i17_, i18_, i19_, r_, z_] :=
 $\sqrt{Bztotal[i1, i2, i3, i4, i5, i6, i7, i8, i9, i10, i11, i12, i13, i14, i15,$ 
 $i16, i17, i18, i19, i20, r, z]^2 + Brtotal[i1, i2, i3, i4, i5, i6, i7, i8,$ 
 $i9, i10, i11, i12, i13, i14, i15, i16, i17, i18, i19, i20, r, z]^2});)

coiltips = Graphics[{Dashing[{0.01^\circ, 0.02^\circ}], Thickness[0.003^\circ], Circle[{0, 0}, 0.157^\circ]}];
EllipE[m_] :=  $\frac{\pi}{2} - \frac{\pi m}{8} - \frac{3\pi m^2}{128} - \frac{5\pi m^3}{512} - \frac{175\pi m^4}{32768};$ 
EllipK[m_] :=  $\frac{\pi}{2} + \frac{\pi m}{8} + \frac{9\pi m^2}{128} + \frac{25\pi m^3}{512} + \frac{1225\pi m^4}{32768};$ 
(groundplane1 =
Graphics[{Thickness[0.003^\circ], Circle[{0, 0}, 0.279^\circ]}])$ 
```

```

(magnetsphere1 = Graphics[{Thickness[0.003`], Circle[{0, 0}, 0.33`]}];
magnetsphere2 = Graphics[{Thickness[0.003`], Circle[{0, 0}, 0.3254`]}];
groundplane2 = Graphics[{Thickness[0.003`], Circle[{0, 0}, 0.288`]}];
centerdot = Graphics[{Thickness[0.005`], Circle[{0, 0}, 0.002`]}])

General::spell1 : Possible spelling error: new
symbol name "EllipK" is similar to existing symbol "EllipE". More...
General::spell1 : Possible spelling error: new
symbol name "Brtotal" is similar to existing symbol "Bztot". More...

CoilsCircles =
Graphics[{Thickness[.005], Circle[{0.037, 0.347}, 0.01], Circle[{0.062, 0.343}, 0.01],
Circle[{0.087, 0.338}, 0.01], Circle[{0.111, 0.331}, 0.01], Circle[{0.135, 0.322}, 0.01],
Circle[{0.158, 0.311}, 0.01], Circle[{0.180, 0.299}, 0.01], Circle[{0.201, 0.285}, 0.01],
Circle[{0.222, 0.270}, 0.01], Circle[{0.241, 0.253}, 0.01], Circle[{0.258, 0.235}, 0.01],
Circle[{0.275, 0.215}, 0.01], Circle[{0.290, 0.195}, 0.01], Circle[{0.303, 0.173}, 0.01],
Circle[{0.315, 0.151}, 0.01], Circle[{0.325, 0.127}, 0.01], Circle[{0.333, 0.103}, 0.01],
Circle[{0.340, 0.079}, 0.01], Circle[{0.347, 0.038}, 0.01], Circle[{0.349, 0.014}, 0.01],
Circle[{0.349, -0.014}, 0.01], Circle[{0.347, -0.038}, 0.01],
Circle[{0.340, -0.079}, 0.01], Circle[{0.333, -0.104}, 0.01],
Circle[{0.325, -0.128}, 0.01], Circle[{0.315, -0.151}, 0.01],
Circle[{0.303, -0.173}, 0.01], Circle[{0.290, -0.195}, 0.01],
Circle[{0.275, -0.215}, 0.01], Circle[{0.258, -0.235}, 0.01],
Circle[{0.241, -0.253}, 0.01], Circle[{0.222, -0.270}, 0.01],
Circle[{0.201, -0.285}, 0.01], Circle[{0.180, -0.299}, 0.01],
Circle[{0.158, -0.311}, 0.01], Circle[{0.135, -0.322}, 0.01],
Circle[{0.111, -0.331}, 0.01], Circle[{0.087, -0.338}, 0.01],
Circle[{0.062, -0.343}, 0.01], Circle[{0.037, -0.347}, 0.01]}]

Show[CoilsCircles]

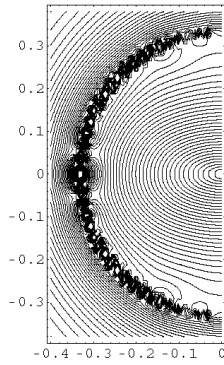

```

```
BmagSph[2800, 2400, 3600, 4300, 7400, 11000, 14000, 16000, 18000, 20000, 23000, 25000,
26000, 27000, 25000, 24000, 25000, 15000, 20000, 15000, 0.0001, 0.03] / 0.0875 // N
```

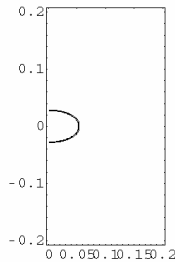
1.06858

(*other half of BmagSph plot, saves time to show only half below*)

```
gL = ContourPlot[BmagSph[2800, 2400, 3600, 4300, 7400, 11000, 14000, 16000, 18000, 20000,
23000, 25000, 26000, 27000, 25000, 24000, 25000, 15000, 20000, 15000, -r, z],
{r, -0.001^, -0.4^}, {z, 0.38^, -0.38^}, Contours -> 60,
ContourShading -> False, PlotPoints -> 60, AspectRatio -> Automatic]
```



```
gBcR = ContourPlot[BmagSph[2800, 2400, 3600, 4300, 7400, 11000, 14000, 16000, 18000, 20000,
23000, 25000, 26000, 27000, 25000, 24000, 25000, 15000, 20000, 15000, r, z] - 0.0875,
{r, .001, 0.2}, {z, 0.2, -0.2}, Contours -> 2, ContourShading -> False,
PlotPoints -> 30, AspectRatio -> Automatic, PlotRange -> {-0.005, 0.005}]
```



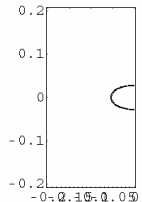
- ContourGraphics -

```

gBcL = ContourPlot[BmagSph[2800, 2400, 3600, 4300, 7400, 11000, 14000, 16000, 18000, 20000,
23000, 25000, 26000, 27000, 25000, 24000, 25000, 15000, 20000, 15000, -r, z] - 0.0875,
{r, -0.2, -.001}, {z, 0.2, -0.2}, Contours -> 2, ContourShading -> False,
PlotPoints -> 60, AspectRatio -> Automatic, PlotRange -> {-0.005, 0.005}]

General::spell1 : Possible spelling error: new
symbol name "gBcL" is similar to existing symbol "gBcR". More...

```

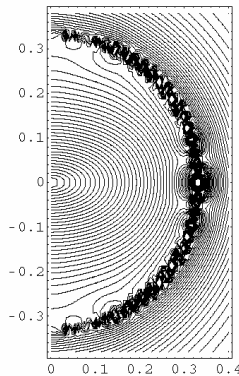


- ContourGraphics -

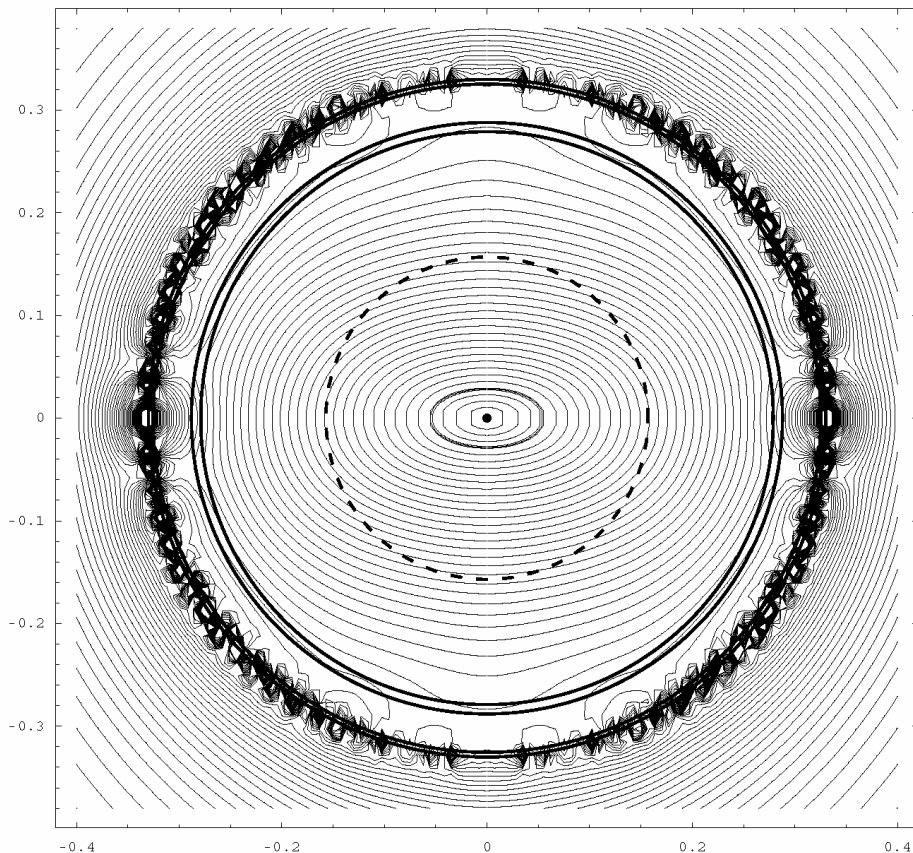
```

gR = ContourPlot[BmagSph[2800, 2400, 3600, 4300, 7400, 11000, 14000, 16000, 18000, 20000,
23000, 25000, 26000, 27000, 25000, 24000, 25000, 15000, 20000, 15000, r, z],
{r, 0.001^, 0.4^}, {z, 0.38^, -0.38^}, Contours -> 60, ContourShading -> False,
PlotPoints -> 60, AspectRatio -> Automatic]

```



```
Show[{gR, gL, gBcL, gBcR, groundplane1,
  groundplane2, magnetsphere1, magnetsphere2, coiltips, centerdot}]
(*Shows coils (counter-rotating upper and lower hemispheres),
magnitude of B field as fraction of Bc, and where B = Bc*)
```

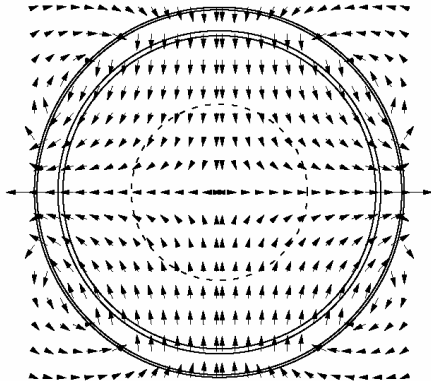


- Graphics -

(*this shows the B field throughout the chamber*)

8 | 07-14Mag13cm.nb

```
v1 = (Needs["VectorFieldPlots`"]; VectorFieldPlots`VectorFieldPlot[
{Brtotal[2800, 2400, 3600, 4300, 7400, 11000, 14000, 16000, 18000, 20000,
23000, 25000, 26000, 27000, 25000, 24000, 25000, 15000, 20000, 15000, r, z],
Bztotal[2800, 2400, 3600, 4300, 7400, 11000, 14000, 16000, 18000, 20000,
23000, 25000, 26000, 27000, 25000, 24000, 25000, 15000, 20000, 15000, r, z]}, 
{r, 0.005^, 0.33^}, {z, -0.33^, 0.33^}, ScaleFactor → 0.05^]);
v2 = (Needs["VectorFieldPlots`"]; VectorFieldPlots`VectorFieldPlot[
{-Brtotal[2800, 2400, 3600, 4300, 7400, 11000, 14000, 16000, 18000, 20000, 23000,
25000, 26000, 27000, 25000, 24000, 25000, 15000, 20000, 15000, -r, z],
Bztotal[2800, 2400, 3600, 4300, 7400, 11000, 14000, 16000, 18000, 20000,
23000, 25000, 26000, 27000, 25000, 24000, 25000, 15000, 20000, 15000, -r, z]}, 
{r, -0.005^, -0.33^}, {z, -0.33^, 0.33^}, ScaleFactor → 0.05^]);
Show[{v1, v2, groundplane1, groundplane2, magnetsphere1, magnetsphere2, coiltips, centerdot}]
```



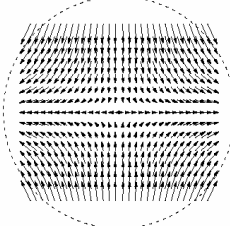
- Graphics -

(*this shows B inside the antenna tips*)

Printed by Mathematica for Students

```
v1a = (Needs["VectorFieldPlots`"]; VectorFieldPlots`VectorFieldPlot[
{Brtotal[2800, 2400, 3600, 4300, 7400, 11000, 14000, 16000, 18000, 20000,
23000, 25000, 26000, 27000, 25000, 24000, 25000, 15000, 20000, 15000, r, z],
Bztotal[2800, 2400, 3600, 4300, 7400, 11000, 14000, 16000, 18000, 20000,
23000, 25000, 26000, 27000, 25000, 24000, 25000, 15000, 20000, 15000, r, z]}, 
{r, 0.005^, 0.12^}, {z, -0.12^, 0.12^}, ScaleFactor → 0.03^]);
v2a = (Needs["VectorFieldPlots`"]; VectorFieldPlots`VectorFieldPlot[
{-Brtotal[2800, 2400, 3600, 4300, 7400, 11000, 14000, 16000, 18000, 20000, 23000,
25000, 26000, 27000, 25000, 24000, 25000, 15000, 20000, 15000, -r, z],
Bztotal[2800, 2400, 3600, 4300, 7400, 11000, 14000, 16000, 18000, 20000,
23000, 25000, 26000, 27000, 25000, 24000, 25000, 15000, 20000, 15000, -r, z]},
{r, -0.005^, -0.12^}, {z, -0.12^, 0.12^}, ScaleFactor → 0.03^]);

```

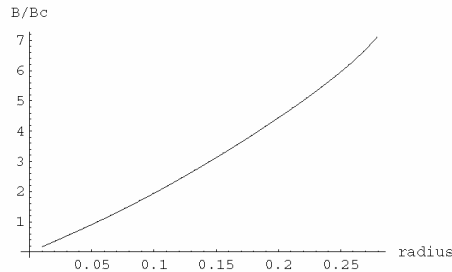


- Graphics -

```
Show[{v1a, v2a, coiltips}]
```

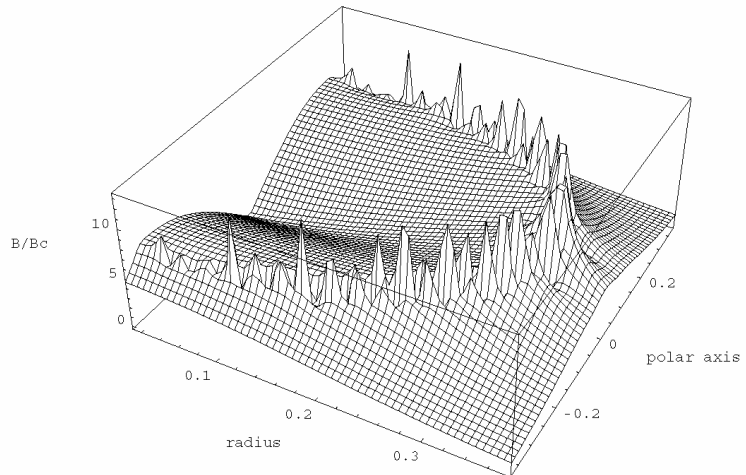
```
(*this is Xsection of B along equator*)
Plot[BmagSph[2800, 2400, 3600, 4300, 7400, 11000, 14000, 16000, 18000, 20000, 23000,
25000, 26000, 27000, 25000, 24000, 25000, 15000, 20000, 15000, r, 0]/0.0875,
{r, .01, 0.279}, AxesLabel → {radius, "B/Bc"}]
```

```
General::spell1 : Possible spelling error: new
symbol name "radius" is similar to existing symbol "Radius". More...
```



- Graphics -

```
Plot3D[ $\frac{1}{0.0875}$ BmagSph[2800, 2400, 3600, 4300, 7400, 11000, 14000, 16000, 18000, 20000,  
23000, 25000, 26000, 27000, 25000, 24000, 25000, 15000, 20000, 15000, r, z],  
{r, 0.01^, 0.38^}, {z, -0.38^, 0.38^}, PlotPoints -> 60,  
AxesLabel -> {radius, "polar axis", "B/Bc"}, ColorFunction -> (White &)]
```



- SurfaceGraphics -

```
BarChart[{2800, 2400, 3600, 4300, 7400, 11000, 14000, 16000, 18000, 20000,
          23000, 25000, 26000, 27000, 25000, 24000, 25000, 30000, 20000, 15000},
AxesLabel -> {coils, Amp - turns}, ColorOutput -> GrayLevel, PlotStyle -> {GrayLevel[0.1]}]
```

